DENSE, LONGITUDINAL SAMPLING REVEALS KEY GUT MICROBIAL COMMUNITIES ASSOCIATED WITH ALZHEIMER'S DISEASE PATHOLOGIES

By Emily Borsom

A Dissertation

Submitted in Partial Fulfillment

of the Requirements for the Degree of

Doctor of Philosophy in Biology

Northern Arizona University

December 2022

Approved:

Emily Cope Ph.D.

Carol Barnes Ph.D.

J. Gregory Caporaso Ph.D.

O'neil Guthrie Ph.D.

ABSTRACT

DENSE, LONGITUDINAL SAMPLING REVEALS KEY GUT MICROBIAL COMMUNITIES ASSOCIATED WITH ALZHEIMER'S DISEASE PATHOLOGIES

EMILY BORSOM

The gut microbiota, the aggregate of microbial cells that inhabit the gastrointestinal tract, communicates bidirectionally with the brain via immune, neural, metabolic, and endocrine pathways, known as the gut-brain axis. The gut-brain axis is suspected to contribute to the development of Alzheimer's disease (AD). *We hypothesize that specific gut microbiota compositions contribute to the development of AD pathologies and neuroinflammation via the gut-brain axis.* To characterize the gut microbiota of 3xTg-AD mice modeling plaque deposition and hyperphosphorylated tau, fecal samples were collected fortnightly from 4 to 52 weeks of age, the V4 region of the 16S rRNA gene was amplified and sequenced on the Illumina MiSeq. Data were analyzed using QIIME 2. We have identified changes in the gut microbiota and immune response that may be predictive of the development of AD pathologies. To explore the effect of modulation of the gut microbiota in mice modeling AD pathologies, we performed fecal microbiota transplants (FMT) from aged (52-64 weeks) 3xTg-AD mice, which are modeling plaques and neurofibrillary tangles, to young 3xTg-AD (n=5) or wild-type mice (n=10) with the sequencing methods described above. We observed a shift in microbiota composition of FMT-treated mice when compared to control (PBS-treated) mice with no effect on neuroinflammation. To investigate the gut microbiota composition with high resolution taxonomic assignments and include fungi, viruses, and other eukaryotic microbes, shallow shotgun metagenomic sequencing (SSMS) was run on

select samples from the initial longitudinal and subsequent FMT study. *Bacteroides, Lactobacillus,* and *Turicibacter,* identified in the studies using 16S rRNA gene sequencing, were classified at species and strain level using SSMS. Finally, a meta-analysis of the gut microbiota composition in WT mice bred at NAU compared to WT mice bred at Jackson Laboratories using our available 16S rRNA gene sequencing data was performed. Beta diversity metrics reveal mice bred at Jackson Laboratories had an adjustment period of about 6 months, before more closely resembling mice bred at NAU. Taken together, our work shows that 3xTg-AD mice harbor a unique gut microbiota composition, associated with disease pathologies, early in life, that becomes more similar to WT mice by 52 weeks of age. The microbial communities associated with later stages of modeling AD pathologies are more transferrable to other 3xTg-AD mice than WT mice, but do not alter neuroinflammation. Finally, SSMS revealed the species and strain level classification of the microbial communities of interest from the 16S rRNA gene sequencing data. Future studies investigating the role of *Bacteroides fragilis, Turicibacter H121, Lactobacillus murinis,* and *Lactobacillus animalis* in the gut microbiome of 3xTg-AD mice are warranted to uncover potential therapeutic targets in the gut microbiota-brain axis for AD.

ACKNOWLEDGEMENTS

I would like to express my deepest gratitude to the following people for supporting me unconditionally during my PhD program. It truly does take a village, and I am unbelievably thankful for mine.

To Emily Cope, my PhD advisor, words cannot express how thankful I am for your guidance and solace throughout my professional career, and for demonstrating strength, intelligence, and kindness in everything you do. There is truly no other person I would rather have by my side for my PhD program. Additionally, many thanks to my PhD committee, Carol Barnes, Greg Caporaso, and O'neil Guthrie for help in navigating my dissertation research and giving constructive feedback during committee meetings. Thanks should also go to the incredible instructors and professors that I took courses with, taught with, and sought advice from during my time at Northern Arizona University. Furthermore, I would like to thank the Arizona Alzheimer's Consortium, especially Eric Reiman, for the funding support to carry out the work described in this dissertation. I would also like to acknowledge and thank the NAU Vivarium staff, especially Kathleen Freel and Dr. Kimberley Cohen for animal care.

To all the current and past members of the Cope Lab group, thank you for your incredible hard work on my projects. To Keehoon Lee and Sierra Jaramillo, thank you for your advice and support in my first few years of graduate school as to how to be independent and lead. To the members of the Caporaso Lab group, especially Chloe Herman and Chris Keefe, thank you for your patience and guidance as I learned from you, as well as being incredible friends. A special thanks to Katie Conn, Ally Hirsch, and Gaby Orsini, for your excellent work in the early stages of my research projects while

being supportive friends. Thank you also to Melanie Palma Avila, George Testo, and Oliver Kask for your hard work on these projects.

I am also grateful for the incredible friends I met along the way in graduate school. In particular, thank you Katie Conn for being my travel buddy and reminding me that we can balance graduate school and life adventures. I would also like to acknowledge my lifelong friends. A special shoutout to Mason Weekley, Samantha Hawker, Anna Wanless, Elizabeth Fil, Molly Jepson, Regan Jepson, and Kendahl Darschewski for your support and laughs over the last 4 years.

Finally, I would like to thank my family for supporting me in my crazy idea to get a PhD. To my mom, thank you for listening to me cry just as many times as celebrating with me. Special thanks to my sister, Molly, for your extra help these past few years. To my many aunts, uncles, and cousins, thank you for continued interest in my work. Last but certainly not least, thank you to my sweet pup, Aspen, for many long walks and emotional support during the highs and lows of graduate school.

DEDICATION

My dissertation is dedicated to my family, who has been greatly affected by Alzheimer's disease, especially my mother and grandmother, Harriet.

PREFACE

This dissertation is original work by Emily Borsom. The work described here is a combination of published data (Literature Review published in Brain Science, MDPI), a manuscript in review (Chapter 1 in review with ASM Spectrum), and manuscripts in preparation for manuscript submission (Chapters 2 and 4). As a consequence of journal format, there is repetition in the work as each chapter is written to be read on its own.

Table of Contents

DENSE, LONGITUDINAL SAMPLING REVEALS KEY GUT MICROBIAL COMMUNITIES ASSOCIATED WITH ALZHEIMER'S DISEASE PATHOLOGIES i

ABSTRACT ii

ACKNOWLEDGEMENTS iv

DEDICATION vi

Chapter 1: Literature Review 1

ABSTRACT 1

REVIEW 2

Introduction 2

Methodology 6

Characterization of Alzheimer's Disease 6

Techniques for Microbiome Analysis 8

Gut microbiota-brain axis in Alzheimer's Disease 9

Enteric Nervous System: Vagus Nerve 10

Gut microbiota composition and diversity in individuals with AD 12

Gut microbiota composition and diversity in murine models of key AD pathologies 14

Potential role of the gut microbiome in neuroinflammation in AD 16

Neuroinflammation: microglial activation and the gut microbiome 17

Neuroinflammation: astrocyte activation and gut microbiome 20

Microbial Etiology Hypothesis in AD 22

Potential for microbiome-based therapeutics 25

Limitations of Current Research 29

CONCLUSIONS 30

REFERENCES 33

CHAPTER 2: Predicting neurodegenerative disease using pre-pathology gut microbiota composition: a longitudinal study in mice modeling Alzheimer's disease pathologies 61

ABSTRACT 62

INTRODUCTION 63

RESULTS 66

Inflammatory gene biomarkers in the hippocampus and colon 67

3xTg-AD mice have a distinct gut microbiota composition prior to the development of AD-associated pathologies 69

Bacterial features are differentially enriched in 3xTg-AD and WT mice over time 72

Associations between bacterial microbiota and mouse genotype over time using Linear Mixed Effects and Random Forest machine learning 72

DISCUSSION 75

METHODS 83

SUPPLEMENTAL MATERIALS 91

REFERENCES 93

CHAPTER 3: Engraftment of gut microbiota composition from aged 3xTg-AD mice modeling amyloidosis and tauopathy did not alter neuroinflammation in young 3xTg-AD mice. 103

ABSTRACT 103

IMPORTANCE 104

Introduction 104

METHODS 108

RESULTS 113

Fecal microbiota transplant (FMT) experimental design 113

Successful engraftment of the gut microbiota composition from 3xTg-AD mice into WT-FMT group 114

3xTg-AD mice shift towards FMT donor community composition at 24 weeks of age when compared to WT mice 116

Feature volatility reveals dynamic microbial communities endogenous to 3xTg-AD mice and transferable between phenotypes 118

Associations between bacterial microbiota and FMT treatment group over time using Linear Mixed Effects 120

Inflammatory gene biomarkers in the hippocampus and colon 121

DISCUSSION 122

CONCLUSIONS 126

SUPPLEMENTAL MATERIALS 127

REFERENCES 133

CHAPTER 4: Shallow shotgun metagenomic sequencing of observational and interventional studies in 3xTg-AD mice Alzheimer's disease pathologies reveals unique species- and strain- level gut microbes 142

ABSTRACT 142

INTRODUCTION 144

METHODS 145

RESULTS 149

Analysis of gut microbiota composition using SSMS in observational and interventional studies 149

Sequencing depth using 16S rRNA gene sequencing compared to SSMS 150

Non-phylogenetic alpha diversity metrics reveal 3xTg-AD mice have lower microbial diversity associated with disease pathology modeling 150

Weighted beta diversity metrics suggest highly abundant taxa are driving differences in 3xTg-AD mice compared to WT mice 153

Identifying microbial features that differentiate mouse genotype using a heatmap 155

Differential abundance analysis reveals three Ligilactoabillus species drive differences between the gut microbiota composition between 3xTg-AD and WT mice 157

Observed features decreased in all treatment groups compared to PBS treated WT mice following 16 weeks of FMT treatment. 158

Weighted beta diversity metrics suggest highly abundant taxa are driving differences between mouse genotype at 2 months and by treatment group at 6 months 160
Identifying microbial features that differentiate FMT treatment groups using a heatmap 162
Differential abundance analysis reveals three Ligilactoabillus species drive differences between the gut microbiota composition between FMT treatment groups 164
DISCUSSION 165
CONCLUSIONS 170
SUPPLEMENTAL MATERIALS 171
REFERENCES 176

CHAPTER 5: Gut microbiota adaptations to the environment of in-house bred versus vendor bred B6129F2/J mice on the gut microbiota composition in the first six months of life 182
ABSTRACT 183
INTRODUCTION 184
METHODS 186
RESULTS 188
JAX and NAU bred mice have distinct gut microbiota composition in the first 6 months of life 189
Identifying bacterial features that are differentially abundant between breeder locations 193
DISCUSSION 195
CONCLUSIONS 198
REFERENCES 199

CHAPTER 6: Conclusions 202

Chapter 1: Literature Review

ABSTRACT

The human microbiota is composed of trillions of microbial cells inhabiting the oral cavity, skin, gastrointestinal tract, airways, and reproductive organs. The gut microbiota is composed of dynamic communities of microorganisms that communicate bidirectionally with the brain via cytokines, neurotransmitters, hormones, and secondary metabolites, known as the gut microbiota-brain axis. The gut microbiota-brain axis is suspected to be involved in the development of neurological diseases, including Alzheimer's disease (AD), Parkinson's disease, and Autism Spectrum Disorder. AD is an irreversible, neurodegenerative disease of the central nervous system (CNS), characterized by amyloid-β plaques, neurofibrillary tangles, and neuroinflammation. Microglia and astrocytes, the resident immune cells of the CNS, play an integral role in AD development, as neuroinflammation is a driving factor of disease severity. The gut microbiota-brain axis is a novel target for Alzheimer's disease therapeutics to modulate critical neuroimmune and metabolic pathways. Potential therapeutics include probiotics, prebiotics, fecal microbiota transplantation, and dietary intervention. This review summarizes our current understanding of the role of the gut microbiota-brain axis and neuroinflammation in the onset and development of Alzheimer's disease, limitations of current research, and potential for gut microbiota-brain axis targeted therapies.

REVIEW

Introduction

The human microbiota, the aggregate of all bacterial, viral, fungal, and archaeal cells that inhabit the human body, consists of 1-1.5x more microbial cells than human cells (~10^{14}) [1]. The microbiome, or the collective genomes of the resident microbes, resides throughout the entire human body, including the skin, oral cavity, respiratory tracts, vaginal cavity, and the GI tract [2]. Recent studies of the human microbiome demonstrate a myriad of roles that these microbes play in host health, including host immune function [3,4], protection against pathogen colonization [5], and host metabolism [6]. Perturbations to normal gut microbiome functions are associated with a variety of diseases, including gastrointestinal, autoimmune, neurological, and metabolic diseases [7]. The GI tract houses about 70% of the human microbiota and comprises Firmicutes, Bacteroidetes, Actinobacteria, Proteobacteria, and Verrucomicrobia [8]. These microbes aid in digestion [6], vitamin synthesis [9], and development of the nervous, endocrine, and immune system [3,4]. Members of the genera *Bacteroides, Prevotella*, and *Lactobacillus* produce B vitamins which play important roles in the host immune regulation [10]. The development of the immune system is influenced by the gut microbiome, for instance, a study by Atarashi et al. demonstrated that oral inoculation of *Clostridium* strains in germ-free mice induced colonic CD4+ T regulatory cells and reduced colitis [11]. Gut microbes are able to ferment indigestible carbohydrates, producing short chain fatty acids (SCFA) as a byproduct, and thereby promote maturation of the immune system, including colonic regulatory T cells [12] and bone marrow hematopoiesis of new circulating monocytes and dendritic cells [13,14]. In

the gastrointestinal tract, dysbiosis of the microbial communities can lead to overgrowth of pathogenic bacteria and a decrease in the integrity of the intestinal barrier, allowing proinflammatory molecules to circulate throughout the bloodstream [15]. For example, *Ruminococcus gnavus,* a common gut pathogen in Crohn's disease patients, utilizes mucin as a carbon source, directly breaking down the gut mucosal barrier and producing proinflammatory cytokines, including TNF-α [16].

The endocrine, neural, metabolic, and immune mechanisms that comprise the gut microbiota-brain axis contribute significantly to overall host health [17]. For instance, decreased alpha diversity in humans is correlated with decreased systemic estrogens. Depleted systemic estrogens are linked to cognitive decline, memory loss, and reduced fine motor skills [18,19]. Another key player in the gut microbiota-brain axis is the vagus nerve, which allows for direct communication via neurotransmitters between the CNS and the enteric nervous system (ENS) [20]. As an example, the gut bacteria *Lactobacillus rhamnosus* can regulate GABA receptors in mice, therefore reducing depressive behaviors via the vagus nerve [21]. Severing the vagus nerve reversed this outcome, negating the beneficial effects of *L. rhamnosus* in mitigating depressive behavior. Additionally, secondary metabolites and cytokines produced by the host-microbial interactions in the gut can cross the intestinal barrier and travel through the blood to induce systemic inflammation [2]. One study found increased levels of the plasma cytokines IL-2, IL-1β, and IFN-γ in Ldlr-/- mice, an atherosclerosis mouse model, that were colonized with the proinflammatory gut microbiota from Casp1−/−

mice, a knockout inflammatory mouse model, via fecal microbiota transplants. These findings suggest that the dysbiotic gut microbiota of the Casp1−/− mice shifted the gut microbiota of FMT treated Ldlr-/- mice. This shift led to a decrease in short chain fatty acids (SCFA) and an increase in the NF-kB activity in immune cells, thereby increasing the production of proinflammatory cytokines [2,22].

The role of the gut microbiota-brain axis has been implicated in many neurological disorders and diseases, including multiple sclerosis, gliomas, Parkinson's disease, and Alzheimer's disease (AD) [23]. In non-AD dementia, there was a lower relative abundance of *Bacteroides* compared to the gut microbiome of cognitively non-impaired subjects, which is the opposite pattern of what is observed in the AD gut microbiome [24]. Another study analyzed and compared the fecal microbiome and metabolites of patients with and without dementia, and the gut microbiota-associated metabolite of dementia patients was distinct from non-dementia patients [25]. For example, high phenol and p-cresol were observed in patients with dementia, which induces an increase in fecal ammonia and increases the risk of dementia. Conversely, in people without dementia, high fecal lactic acid was observed which was associated with a low risk of dementia [25]. Vascular cognitive impairment (VCI), a common cause of dementia, may be mediated with metabolites produced by gut microbiota. For example, LPS and trimethylamine-N-oxide (TMAO) from gut microbiota can contribute to the increased intestinal epithelial permeability that leads to immune responses associated with VCI [26].

Several studies have demonstrated that celiac disease (CD) is associated with neurological disease development [27,28]. CD is an autoimmune disease caused by inability to digest gluten in the small intestine. Due to intestinal epithelial dysfunction caused by CD, immunotoxic gluten peptide is introduced into the circulatory system and passes through the BBB, causing neuroinflammation. CD also decreases the expression of PPAR-ɣ, which plays a role in modulating inflammation. Decreased PPAR-ɣ is associated with dysbiosis of the gut microbiome and an increase in factors related to AD development such as elevated LPS, pro-inflammatory cytokines, and bacterial metabolites. One study demonstrated that CD-induced changes in the gut microbiome and neurological disease development can be improved through a gluten-free diet (GFD). Not only did GFD reduce the amount of neuroinflammation, but it also correlated with an increase in the expression of PPAR-γ and gut microbiome health [27]. In addition, Transcranial magnetic stimulation (TMS), a non-invasive brain stimulation technique, enables early diagnosis of “hyperexcitable celiac brain” that often appears before dementia in CD patients even before any onset of clear symptoms. So that these patients can be prescribed a GFD to prevent neurodegeneration that can lead to dementia as early as possible [29,30].

In this review, we present an up-to-date, comprehensive evaluation of the field of gut microbiome research in Alzheimer’s Disease, with a unique perspective on the potential role of the gut microbiome in neuroinflammation. We also summarize a potential mechanistic pathway describing a hypothesized role for LPS in AD pathologies. As

Hippocrates once said, “All disease begins in the gut” [31]. Could this statement hold the truth, even after 2500 years? In this review, we will discuss the current understanding of the role of the gut microbiota-brain axis in AD and provide commentary on potential mechanisms for AD pathogenesis.

Methodology

Search terms to identify appropriate literature for this review using Google Scholar include, but are not limited to, “Alzheimer’s disease,” “gut microbiota,” “gut microbiota-brain axis,” in combination with “microglia,” “astrocytes,” “LPS,” “neuroinflammation.” This review provides a current, comprehensive overview of the gut microbiota brain axis in AD, with emphasis on modern molecular techniques, gut microbiota-induced neuroimmune pathways, and uncovering potential therapeutics. Primary studies that led to novel insights on the gut microbiome and AD in preclinical murine models and human AD participants were included in this literature review.

Characterization of Alzheimer’s Disease

AD was first identified by psychiatrist and neuropathologist, Alois Alzheimer, in 1906. After observing plaques and neurofibrillary tangles in the brain histology of a patient who suffered from memory loss, aggression, confusion, and paranoia, he presented his findings at the 37th Meeting of South-West German Psychiatrists. Shortly after, the disease characterized by Alzheimer was coined with the name “Alzheimer’s disease” by his colleague, Emil Kraepelin [32]. Today, Alzheimer's disease (AD) is the most

common cause of dementia, affecting 5.8 million people in the United States alone. The prevalence of Alzheimer's disease is predicted to rise to 13.8 million in the United States by 2050 [33]. Apolipoprotein E (*APOE*) genotype is recognized as the strongest genetic risk factor for the development of AD. The *APOE* protein is involved in several biochemical regulatory processes, including immunoregulation, neuroinflammation, and neuroprotection. *APOE* exists in 3 isoforms, although *APOE4* prevails as the strongest predictor of dementia. The prevailing hypothesis is the cascade hypothesis, which states that amyloid-β plaque deposition leads to intracellular neurofibrillary tangles caused by hyperphosphorylation of the protein tau and disintegration of the microtubules in neurons, resulting in loss of neuronal function [34]. These two hallmark pathologies, extracellular amyloid-β plaques and intracellular neurofibrillary tau tangles, are present in the hippocampus and prefrontal cortex, and result in loss of neuronal function and cognitive impairment [35]. Amyloid plaques form when the amyloid precursor protein (APP) is sequentially cleaved by endogenous proteases, β- protease and γ -protease.This cleavage event renders peptides ranging in length and solubility, yetAβ-42 tends to form soluble fibrils, and is the predominant species observed in the brain of severe AD patients [37,38]. Amyloidosis may begin as early as 10-20 years before cognitive decline or AD symptoms become apparent [39]. In addition to plaques and tangles, neuroinflammation is increasingly recognized as central to disease progression; current studies have identified both microglia and astrocyte induced inflammation as a key pathological feature of AD [40]. While not yet considered a core pathology for diagnosis, neuroinflammation remains a driving feature in AD pathogenesis [41].

Techniques for Microbiome Analysis

Advances in the fields of sequencing and bioinformatics allow for increasingly accurate analysis of microbial communities and their role in human health. The field of microbiome sequencing has been dominated by marker gene sequencing. For bacteria, 16S rRNA gene is a widely used marker gene, and fungi can be identified using marker sequences on the 18S rRNA gene or the ITS (internal transcribed spacer) region.Selection of the 16S rRNA gene was based on the presence of nine highly variable regions within the gene, allowing for bacterial taxonomic classification, that are flanked by conserved regions that allow for primer design [42]. The ITS regions are situated between the 18S rRNA gene and the 5.8S rRNA gene (ITS1) and the 5.8S rRNA gene and the 28S rRNA gene (ITS2). ITS1 and ITS2 have high evolutionary rates, allowing for greater taxonomic resolution than is possible with 18S rRNA gene sequencing [(Ihrmark et al. 2012)]. However, for those who are interested in species- and strain-level taxonomic resolution, shallow shotgun metagenomic sequencing (SSMS) is becoming increasingly popular. [44]. While SSMA does not provide the depth of taxonomic and functional resolution that deep shotgun metagenomic sequencing does, it is relatively low cost compared to deep shotgun metagenomics, and therefore more feasible to apply in large-scale studies [44].

Functional and mechanistic aspects of the microbiome's integral role in health or disease can be assessed by integrating a multi’omics approach including deep shotgun metagenomics, transcriptomics, and metabolomics. As discussed above, deep shotgun

metagenomic sequencing will provide strain-level and functional information encoded in the DNA content of a microbiome. In shotgun metagenomics, all of the DNA present in a sample is sequenced with minimal PCR amplification bias. This allows characterization of the species and encoded genes in a wide array of microorganisms, including fungi, bacteria, archaea, parasites, and DNA viruses. Although metagenomic sequencing can characterize the functional potential of a microbial community, this DNA-based approach is unable to determine differences in gene expression in a given environment. Transcriptomics, or RNA-seq, can be used to evaluate changes in gene expression. Finally, we can identify and quantify primary and secondary metabolites (e.g. short chain fatty acids) produced by the host and microbiota using metabolomics. Metabolomics can lead to a better understanding of microbial communication and microbial community involvement in metabolic pathways [50]. Understanding community composition is essential for microbiome studies, however, an integrated, multi-omics approach is critical to elucidate the microbial taxa and associated mechanisms essential to host health and disease.

Gut microbiota-brain axis in Alzheimer's Disease

Although amyloid plaques and tau tangles are thought to be central to AD, over 2000 clinical trials targeting plaques, tangles, neurotransmitters, and other related mechanisms have failed to successfully treat AD [51]. However, the bidirectional communication between the gastrointestinal tract and the central nervous system (CNS) via immune, endocrine, neural, and metabolic pathways, known collectively as the gut microbiota-brain axis, has recently been hypothesized to contribute to AD etiology and

pathogenesis [23,52]. The human gut microbiome influences neuroinflammation in AD through the production of proinflammatory cytokines and bacterial metabolites that can enter circulation and reach the brain to act on neuronal immune cell populations [53]. Proinflammatory cytokines involved in AD pathogenesis include IL-1β, IL-6, IL-18, TNF-α, and IFN-γ [54]. Overexpression of IL-1 has been shown to favor plaque deposition *in vivo* and *in vitro* [55], while upregulation of IL-6 is associated with hyperphosphorylation of tau, leading to neuronal degradation [55,56]. Both Aβ plaques and neurofibrillary tangles are co-localized with activated glial cells in the CNS, suggesting gliosis plays a major role in AD pathogenesis and neuroinflammation [57]. In addition to cytokines, bacterial metabolites, including trimethylamine *N*-oxide (TMAO) and SCFAs may play a role in the development of or protection against AD pathologies. TMAO, a gut microbiome-produced metabolite previously linked to cardiovascular disease [58], is increased in the cerebrospinal fluid of AD patients and is directly correlated to CSF tau biomarkers, suggesting a role in brain aging and cognitive decline [59]. On the other hand, SCFAs, particularly valeric, butyric, and propionic acid, have the potential to ameliorate amyloidosis by interfering with Aβ1-40 and Aβ1-42 peptide interactions, thereby preventing conversion to neurotoxic Aβ plaque formation [60]. We expand on each of these topics, below.

Enteric Nervous System: Vagus Nerve

The enteric nervous system (ENS) is the largest part of the autonomic nervous system, composed of over 100 trillion neurons that function independently from the CNS [61]. The neural circuits that make up the ENS control local motor function and blood flow,

fluid secretions and transports, and regulate immune and endocrine functions [62]. As a major component of the gut microbiota-brain axis, the vagus nerve directly connects the gut to the brain and spinal cord [17]. The vagus nerve mediates signaling pathways for satiety, stress, and mood via microbial and neural signaling [63]. Therefore, perturbations to the nerve disturb the gut-microbiota brain axis, leading to gastrointestinal diseases, including irritable bowel syndrome [64]. However, the vagus nerve is also able to receive input from the gut microbiota and transfer this information to the central nervous system [65]. To illustrate, enteroendocrine cells (EECs), making up 1% of gut epithelial cells, release 5-HT (serotonin precursor) in response to chemical or mechanical stimulation, which stimulates 5-HT3 receptors on the vagus nerve. Stimulation of these receptors controls physiological responses including peristalsis, gut motility, and other visceral functions [66].

In terms of treatment options, the vagus nerve remains a viable target for AD treatment. Clinical trials targeting the vagus nerve through stimulation have shown some cognitive improvement in AD patients up to one year post-treatment [67,68]. Vagus nerve stimulation (VNS) has also shown sustained, long term cognitive improvement in refractory depression patients [69]. A more recent study in transgenic APP/PS1 mice reversed morphological signs of aging and activation in 12 month mice using non-invasive vagus nerve stimulation [70]. However, the use of VNS as a therapeutic for AD is still a novel idea and requires further investigation of the mechanisms involved.

Gut microbiota composition and diversity in individuals with AD

The hypothesis that members of the gut microbiota contribute to AD onset and progression via the gut microbiota-brain axis has emerged in the past 5 years. However, few studies have been completed in the clinical setting. To our knowledge, five studies have characterized the gut microbiota composition in human AD patients compared to age-matched, non-AD controls, all showing an altered bacterial microbiota composition in AD patients. A cross sectional study of the gut microbiota composition in patients selected for their *APOE* genotype demonstrated that *APOE4* carriers had decreased abundance of butyrate producing gut bacteria, including *Clostridium*, and lower levels of fecal SCFAs compared to other *APOE* genotypes, indicating a relationship between *APOE* isoforms and gut microbiota compositions [71]. The second study conducted in AD patients demonstrated a decrease in the phyla Firmicutes and an increase in Bacteroidetes, as well as an increase in the genus *Blautia* in AD patients. They also observed decreased alpha (within sample) diversity in AD patients. Additionally, they observed correlations between CSF markers of AD and relative abundance of taxa; a significant positive correlation was demonstrated between the genus *Bacteroides* and CSF YK-40, a marker of astroglia and microglia activation. These findings suggest an increase in *Bacteroides* may be linked to increased neuroinflammation [72]. We discuss the potential mechanisms below. The other three studies demonstrate a gut microbiota composition with decreased abundance of SCFA-producing bacteria and increased abundance of proinflammatory bacteria when comparing AD patients to non-dementia,

aged matched controls [73][74][75][73] Taxa identified in the individual studies can be found in Table 1.

Alterations in the bacterial gut microbiota have been observed in AD patients, indicating a potential role for gut microbes in AD. Three of the five studies in human patients showed significant changes in the genus *Bacteroides,* although the directionality of this change, whether *Bacteroides* relative abundance increased or decreased, differed (Table 1). Future research to determine whether environmental factors independent of AD pathologies cause the observed shifts in the gut microbiome are necessary. For example, dietary changes as a person progresses through dementia, the influence of medications on the composition of the gut microbiota in AD, decreased body mass, and overall well-being should be considered as potential mediators of the gut microbiota composition and diversity. Finally, changes in the microbiota may extend beyond the gut. The post mortem brain of AD patients has a higher bacterial burden when compared to age matched controls, consisting mostly of Actinobacteria, particularly *Propionibacterium acnes* [76]. Additionally, mice infected orally with *Porphyromonas gingivalis* exhibited brain colonization associated with increased amyloidosis [77]. These findings provide intriguing evidence for translocation of microbes from the gut, suggesting that microbes have the ability to cross both a dysfunctional gut epithelial barrier and blood brain barrier. Further studies are required to determine whether microbial translocation from other body sites to the brain occurs in AD.

Gut microbiota composition and diversity in murine models of key AD pathologies

Transgenic mouse models of key AD pathologies are an essential tool in mechanistic studies and drug discovery with the potential for translational treatments in clinical trials [32]. Numerous studies have shown that transgenic murine models have unique gut microbiota compositions when compared to the gut microbiota compositions of wild-type mice of the same genetic background, or compared to transgenic mice with the wild-type allele [35,78,79]. Parikh and colleagues assessed changes in the gut microbiota composition of 5xFAD mice, a transgenic familial model of plaque deposition, that were homozygous for *APOE2* , *APOE3* , or *APOE4*. Significant changes observed in the gut microbiota between genotypes regardless of 5xFAD mutations suggests a relationship between the gut microbiota composition and *APOE* isoforms [80].In a study by Chen and colleagues, transgenic APP/PS1 mice, a model bearing the mutations in transgenes for APP and PSEN1 resulting in Aβ plaque deposition, demonstrated altered microbiota preceding amyloidosis and microgliosis, suggesting a role of the gut microbiota in AD pathogenesis (Table 1, [78]). In 5xFAD mice, which express human APP and PSEN1 transgenes with five AD-linked mutations, leading to rapid development of amyloidosis, an increase in the phylum *Firmicutes* and a decrease in the phylum *Bacteroidetes* was observed at 9 weeks. More specifically, *Clostridium leptum* was increased in 5xFAD mice, a common gut bacteria associated with gut inflammation [79]. When raised germ-free, APP/PS1 mice exhibited significantly reduced amyloidosis and microgliosis, suggesting that in absence of the gut microbiota,

AD pathologies are less severe and supports the hypothesis that the gut microbiota plays a critical role in AD pathologies [81].

To better understand the mechanisms behind these alterations in the gut microbiota composition of transgenic models of AD pathologies, including amyloid deposition and neurofibrillary tangles, manipulation of the gut microbiota allows for uncovering potential processes involved in AD development. Manipulation of the gut microbiota through prebiotics, probiotics, and fecal microbiota transplants are potential therapeutic options for AD and have been explored in preclinical murine models of AD pathologies (Table 2). Bonfili and colleagues administered SLAB51, a mixture of nine live bacterial strains, to 3xTg-AD mice, a transgenic model exhibiting Aβ plaques and tau tangles. SLAB51 treated mice reduced proinflammatory cytokine production (IL1β, IFNɣ, and TNFα) and cerebral Aβ, while simultaneously increasing SCFA production and cognitive function. However, there were no significant changes in microbial taxa, but rather an overall shift of the gut microbiota following SLAB51 treatment [82]. Another study employed the prebiotic, fructooligosaccharides (FOS), to modulate the gut microbiota in APP/PS1 mice. FOS treated mice exhibited decreased Aβ deposition, increased cognitive function and synaptic plasticity, and reversed altered gut microbiota in APP/PS1 mice to more closely resemble wildtype mice [83]. A study on the impact of high-fat diet in 3xTg-AD mice showed increased *Rikenellaceae* and *Lachnospiraceae* and decreased Bifidobacteriaceae and *Lactobacillaceae* in the colon when compared to normal fed 3xTg-AD mice [84]. Wang and colleagues treated 5xFAD mice with sodium oligomannate (GV-971), an algae-based drug, which remodeled the gut microbiota, and

reduced M1 microglia activation and neuroinflammation. These findings suggest gut microbiota derived metabolites including the amino acids phenylalanine and isoleucine invoke neuroinflammation. In the same study, 5xFAD mice were co-housed with wildtype mice from birth to 7 months. The results showed the gut microbiota of the 5xFAD and wildtype had shifted to resemble each other, and co-housed wild type mice had increased infiltrating Th1 cells in the brain, indicating the role of the gut microbiota composition in changes immune cell expression and neuroinflammation [35]. FMT treatment of APP/PS1 with wildtype mouse feces alleviated cognitive decline, Aβ accumulation, and Tau hyperphosphorylation through reversing alterations in the gut microbiota of APP/PS1 mice. To illustrate, before the treatment, APP/PS1 mice were enriched with Proteobacteria and Verrucomicrobia, however, post-treatment, the abundance of *Proteobacteria* and Verrucomicrobia had decreased, while Bacteroidetes increased [85].

Potential role of the gut microbiome in neuroinflammation in AD

Neuroinflammation has recently been recognized as a key feature of AD. Neuroinflammation is the body's combined biochemical and cellular responses of all resident glial cells to injury or infection of the nervous system and neurodegenerative diseases [86]. To prevent damage to the CNS, resident immune cells recognize any disturbances to homeostasis of the brain and respond with production of cytokines and chemokines to mediate tissue damage [87]. In healthy adults, aging leads to changes in the immune system, resulting in what is often termed "inflammaging", or chronic, low-grade inflammation due to aging [88]. Microglia increase responsiveness to

inflammatory stimuli with aging, while astrocytes act to preserve neuroinflammation [89]. The main driver of age-related neuroinflammation in Alzheimer's patients is reactive gliosis, or the activation of the glial cells of the CNS to prevent and repair tissue damage [90]. Age-related changes in microglial activation result in changes in gene expression, rendering dysmorphic microglia with morphological alterations, including abnormalities in cytoplasm and fragmented processes [91]. These changes may be related to the gut microbiome. A study in germ-free mice demonstrated increased abundance of *Desulfovibrio,* a gut bacteria associated with intestinal inflammation, after transfer of an aged mouse gut microbiota [92]. These findings suggest unique gut microbiota compositions in aging mice may be associated with chronic, low grade inflammation.

While neuroinflammation is initially a reparative mechanism to prevent damage, the neuroinflammatory response in AD patients shifts from neuroprotective to neurotoxic, damaging tissue in the CNS [57]. Neuroinflammation remains constant, with consistently high levels of cytokines and chemokines, and increased neuronal cell death [93]. This chronic inflammation is associated with shorter and fewer microglial processes, reducing mobility, thereby inhibiting their ability to survey and monitor their environment [70,94]. The cytokines produced by microgliosis and astrogliosis worsen tauopathy and drive sustained neuroinflammation [95].

Neuroinflammation: microglial activation and the gut microbiome

Many diseases of the CNS that are linked to the gut microbiome, such as AD, Parkinson's Disease, Multiple Sclerosis, and Autism Spectrum Disorder, simultaneously

involve dysfunctional microglia [96]. Microglia are the main immune cell in the brain, colonizing the brain early in development, and maintaining homeostasis during aging [97]. As the specialized macrophages of the CNS, microglia function as phagocytes to clear bacteria, cellular debris, and Aβ peptides [98,99]. Microglia work to monitor their microenvironment through constant extension and retraction of their highly motile processes [100]. The acute neuroinflammatory response induced by Aβ peptides is a self limiting, neuroprotective immune response [78]. However, aging microglia are ineffective at phagocytosing the neurotoxic Aβ plaques present in AD [101]. Instead, microglia are activated by aggregated Aβ plaques, driving a chronic neuroinflammatory response[39].

Microglia receive input from not only the brain but also the gastrointestinal tract via the vagus nerve [63]. When the vagus nerve senses a change in inflammation and proinflammatory cytokine production in the gastrointestinal tract, afferent fibers relay this information to the brain and influence neuroinflammation [65]. However, electrical stimulation of the vagus nerve attenuates neuroinflammation induced by peripheral LPS (lipopolysaccharide), a component of the Gram-negative bacterial cell envelope that can be released upon cell lysis. In one study, C57BL/6 mice were challenged with peripheral LPS and subjected to vagus nerve stimulation (VNS). VNS in the presence of LPS resulted in an increase of IL-6, IL-1β, and TNFα [102]. A study by Huffman and colleagues challenged C57BL6/J mice with *Escherichia coli* derived LPS to induce neuroinflammation. Percutaneous VNS stimulation reduced neuroinflammation, restored LPS-induced cognitive decline, and modulated microglial activity. [103]. Another study

using external, non-invasive VNS in 12 month old APP/PS1 transgenic AD mice illustrated a shift from neurodestructive to neuroprotective microglia phenotypes[70]. Taken together, these studies demonstrate that LPS is a potent stimulator of microglia via the vagus nerve, and vagal nerve stimulation may reverse neurotoxic microgliosis.

Microglia polarization is determined by a complex group of activation processes by different stimuli in the CNS, resulting in microglia polarization [104]. When an injury is present, microglia are capable of cytotoxic response and immune regulation, to resolve the damages [105]. Differentiated microglia polarize to two main phenotypes; pro-inflammatory or M1, and neuroprotective or M2 [106]. Microglia phenotype is based on their activation pathways that communicate via environmental signals to alter gene expression and cellular metabolism [107]. Classical activation by lipopolysaccharide (LPS) and IFN-γ polarize microglia cells to an M1 state, inducing production of pro-inflammatory cytokines, including TNFα, IL-1β, IL-12 [108,109] Alternative activation by IL-4 and IL-13 polarize microglial cells to an M2 state, inducing production of anti-inflammatory cytokines, including IL-4, IL-13, IL-10, and TGF-β [108]. Thus, microbial signals may be critical in M1/M2 polarization and therefore neurological health.

Microglia and the gut microbiota communicate via the gut microbiota-brain axis, regulating immune homeostasis. Wang and colleagues demonstrated M1 polarized neuroinflammation in 5xFAD mice is a result of abnormal production of amino acids, including phenylalanine and isoleucine, by the gut microbiota. Increased M1 activation as a result of crosstalk with Th1 cells infiltrating the CNS induced pathological

neuroinflammation and cognitive decline [35]. Gut microbiota alterations may also affect microglia activation by controlling maturation and function. In this study, adult germ-free mice, lacking microbiota signaling, have distinct microglia with changes in density and morphology [63]. Furthermore, a study on critical hypertension indicated the influence of microglia dysfunction and neuroinflammation on the microbial communities in the gut. In this study, inhibition of microglia activation led to changes in the phylum Proteobacteria, suggesting that microglia activity plays a role in modulating the gut microbiota composition [110].

Neuroinflammation: astrocyte activation and gut microbiome

Astrocytes are specialized resident glial cells in the CNS, and responsible for protection, support of neurons, and overall homeostasis [111]. When damage occurs to the CNS, astrocytes drive an inflammatory process called astrogliosis [112]. Astrocytes function in Aβ clearance and blood brain barrier (BBB) integrity maintenance through production of cytokines and chemokines, including IL-1, IL-6, and TNF-α, to signal a pro-inflammatory innate immune response [35,113,114]. Making up about 50% of human brain mass, astrocytes play critical roles in neurodegenerative disorders and cognitive decline, including AD [115].

Neuroinflammation in AD is exacerbated by dysfunction of astrocytes, resulting in decreased BBB integrity and recruitment of immune cells from the blood. Astrocyte dysfunction can lead to deposition of Aβ peptides in the brain and results in endothelial cell damage and leakage of the blood brain barrier [116]. In one study, patients with

mild cognitive impairment and early AD underwent dynamic contrast material–enhanced magnetic resonance (MR) imaging to analyze BBB leakage, demonstrating cognitive decline is directly related to severe leakage [117]. Furthermore, cytokines are able to both cross the blood brain barrier and damage the blood brain barrier by increasing permeability without entering the brain [118]. IL-1β, IL-6, and TNF-α have been shown to modify functional activity of the BBB and can be selectively transported across the BBB [119]. Aβ adhesion to microglia induces proinflammatory gene expression, producing IL-1β and TNF-α, thereby activating astrogliosis and amplifying the neuroinflammatory response. Increased proinflammatory cytokine production and neuroinflammation eventually lead to tau hyperphosphorylation and neuronal loss [120,121]. Recent studies have shown that gut microbiome impacts the function of astrocytes. The microbial product, LPS, potentiates the production of inflammatory mediators from astrocytes, leading to neurodegeneration [122]. LPS has been used in many studies to induce microgliosis, astrogliosis, and neuronal apoptosis[123],[124],[125]. Increases in the relative abundance of *Nitriliruptor, Youngiibacter, Burkholderia,* and *Desulfovibrio,* in children with an autism spectrum disorder, correlate with astrocyte activation [126]. Additionally, SCFA production by the gut microbiota may inhibit astrocyte activation. A study by Liu and colleagues demonstrated acetate, propionate, and butyrate, common SCFAs produced by the gut microbiota, suppress LPS and proinflammatory cytokine production through inhibition of the NF-kB pathway *in vitro [127]*. However, increased *Lachnospiraceae, Ruminococcaceae, and Prevotellaceae* in the GI tract of NLRP3-deficient mice ameliorated astrocyte dysfunction and reduced depressive-like behaviors [128]. These

findings suggest astrocytes may be a potential therapeutic target for neurological disorders, including AD, associated with astrocyte activation and dysfunction.

Microbial Etiology Hypothesis in AD

Changes in gut microbiota composition and diversity during aging can drive age-associated inflammation; recent studies in *Drosophila [129]* and in murine models [130,131] suggest that alterations to the gut microbiota in late life drive increased intestinal permeability and increased systemic inflammatory markers. Since neuroinflammation is a key feature of Alzheimer's Disease (AD), understanding the aging gut microbiome is critical to understanding AD progression. Mechanistically, bacteria in the GI tract can produce a significant amount of amyloids (aggregated, insoluble proteins exhibiting β-pleated sheet structures) can contribute to Aβ plaque formation and increase the risk for AD development [132–134]. Microbiome-derived functional amyloids have been described in the multiple microbial taxa, including *Saccharomyces cerevisiae,* and broadly in the family *Enterobacteriaceae. Escherichia coli* extracellular amyloids known as curli fibers help to facilitate attachment to surfaces and protection against host defenses [135–138]. Both curli fibers from *E. coli* and sup35 from *S. cerevisiae* were capable of enhancing amyloid aggregation and amyloidosis in a murine model of experimental amyloidosis, indicating that microbial-derived amyloids may have prion-like properties [139]. In another study, amyloids derived from three species of Gram negative bacteria (*E. coli, Salmonella typhimurium,* and *Citrobacter koseri* could induce polymerization of amyloid aggregates across species *in vitro*, again demonstrating the potential for microbiome-derived amyloids to contribute to

amyloidosis in AD [140]. Microbial amyloids may also enhance the immune response to endogenous amyloids, contributing to neuroinflammation. Microbial amyloids are sensed by Toll-like receptor 2 (TLR2), which can induce expression of many of the neuropathological features observed in AD, discussed above. Curli from *S. typhimurium* was sufficient to induce IL-17A, IL-22, and IL-6 in the intestinal epithelium, and these responses were blunted in TLR-2 deficient mice [141]. However, these findings must be placed into the context of a healthy or dysbiotic microbiome; another study found that commensal-derived amyloids may help to maintain the epithelial barrier and induce anti-inflammatory IL-10 expression in the gut [142]. The altered microbiome composition observed in human and preclinical models may lead to impaired epithelial barrier, allowing microbiome-derived amyloids to translocate, cross-seed with endogenous peptides, or activate a neuropathological immune response.

The endotoxin hypothesis of neurodegeneration states that the endotoxin, or LPS, found in the outer membrane in all Gram-negative bacteria, crosses the blood brain barrier to induce neuroinflammation and neurodegeneration. The proposed pathway begins with a gastrointestinal infection, or perhaps an increase in absolute abundance of a Gram-negative gut microbes, results in increased circulating endotoxins, which cross the BBB, leading to chronic neuroinflammation and finally, neurodegeneration [143,144]. Dysbiosis of the gut microbiota resulting in enrichment of Gram-negative bacteria in the gut microbiota is associated with increased LPS-driven inflammation [145]. Notably, *Bacteroides fragilis*, a known LPS-producing gut bacteria, is

hypothesized to contribute to inflammatory signaling in AD patients via the NF-kB pathway [146].

Peripheral LPS may contribute to neuroinflammation and Aβ plaque deposition in the brain (summarized in Fig. 1). LPS in the gut activates the enteric nervous system, and can stimulate production of the proinflammatory cytokines TNFα, IL-1β, and IL-6, which are secreted in the gut and can travel to the periphery [147]. More specifically, activation of the ENS leads to TNFα induced inhibition and production of IL-6 in the GI tract or ENS cells *in vitro*, a known inflammatory cytokine in AD [148]. Inflammation of the gastrointestinal tract increased intestinal permeability to recruit immune cells from circulation, however also allowing inflammatory bacterial components to cross the barrier into the peripheral circulatory system, eliciting systemic inflammation [93]. Pathogenic microbial metabolites, proinflammatory cytokines and other molecules produced by the gut microbiota, including LPS, are associated with neuronal death and neuroinflammation [149]. TLR-4, a known LPS receptor, is localized on microglia, astrocytes, and neurons, and plays a role in both cell survival and death [150]. The activation of TLR-4 on microglia and other neural cells leads to activation of the NF-kB pathway, thereby increasing the production of cytokines and Aβ deposition. Additionally, TLR-4 is expressed in vagal afferent fibers, which allow the vagus nerve to sense LPS and activate the brain [65]. In rats, IP injection of LPS resulted in increased expression of IL-6, IL-1β, and TNF-a in the brain, and LPS co-associated Aβ plaque deposition [151]. The role of LPS in the development of AD is reviewed in [152].

A considerable amount of research points towards an infectious etiology of AD. Inflammation is an essential process in healing damaged tissue and fighting off infection, however, chronic inflammation leads to permanent damage. Studies have noted bacteria, viruses, protozoa, and fungi as potential agents in systemic infections related to AD [153]. Injection of *Helicobacter pylori,* an opportunistic pathogen of the GI tract, induced memory impairment and Aβ plaque deposition through increased gene expression of presenilin-1 in rats and *in vitro*. In the same study, injection of *Escherichia coli,* another common gut pathogen, demonstrated no change in cognitive impairment or plaque deposition [154]. Furthermore, in another study, different regions of the brain in AD patients, including the frontal cortex and hippocampus, had evidence of *Candida spp.* cells and hyphae, while control patients showed no signs of fungal cells or hyphae, providing intriguing evidence for existing fungal infections in AD brains [155]. Moreover, there is evidence to suggest fungal infections in the brain can be accompanied by bacterial infections, demonstrating polymicrobial infections of the brain in AD may contribute to pathogenesis and neuroinflammation [156]. Taken together, these studies suggest translocation of microbes into the brain and chronic microbial infection may play a role in neuroinflammation and AD neuropathologies.

Potential for microbiome-based therapeutics

The gut microbiota-brain axis remains a target for future therapeutics for AD. Immunotherapy [157] and gut microbiota-targeted therapy [17] are among the many potential therapeutic targets for AD. Immunotherapy targets include the anti-Aβ and anti-tau target antibodies, Aβ vaccines, and cytokine inhibition [157–159]. Passive

immunization of naturally occurring autoantibodies injected into APPSwe mice, a single transgenic model for amyloidosis, reduced toxic Aβ oligomers, and improved cognitive function [160]. 3xTg-AD mice immunized with active, full length DNA Aβ42 demonstrated reduced plaque deposition and tauopathy [161]. LPS-treated 3xTg-AD mice injected with TNF inhibitor XENP345, a TNF cytokine inhibitor, reduced accumulation of 6E10 immunoactive protein, which contains amyloid precursor protein fragments, therefore preventing pre-amyloidosis pathologies [162]. Neuroimmune therapeutics targeting reduction of Aβ plaques and neurofibrillary tangles continue to evolve as understanding of disease pathologies becomes more clear. Due to the complexities involved in disease progression, combinatorial immunotherapy may hold promise to a future of immunotherapeutics for AD [163].

Potential gut microbiota target therapies include prebiotic/probiotic supplementation and fecal microbiota transplantation to restore gut microbiota to a diverse, healthy microenvironment [164]. In 3xTg-AD mice, oral probiotic supplementation reduced Aβ burden and hyperphosphorylated tau aggregates through gut microbiota manipulation [165]. A study using E4FAD mice, a model for late onset AD, demonstrated that supplementation with the prebiotic inulin increased SCFA's and reduced neuroinflammation [166]. Early probiotic trials in patients with AD or mild cognitive impairment remain promising with results showing improved cognitive function, suggesting the involvement of the gut microbiota brain axis [167],[168]. Despite the numerous studies on transgenic mice modeling AD pathologies, few translational studies in AD patients have been published. A case study of an 82 year old man with

AD followed the patient over a six month period following an FMT treatment for a *Clostridioides difficile* infection. The patient showed significant improvement on his Mini-Mental State Examination, and scored in the normal cognition range at two and six months post treatment. However, this was a case study, and a clinical trial of the effects of FMT on AD patients through modulation of the gut microbiota-brain axis is warranted [169].

Another method of gut microbiota targeted therapy is through dietary intervention. Numerous epidemiological evidence has demonstrated a link between diet, gut microbiota, and human health [170–172]. However, only recently have the mechanisms linking diet and human health been uncovered. Diet and lifestyle are closely related to cardiovascular and metabolic diseases, which are connected to neurological disorders. For example, insulin resistance and high plasma homocysteine levels, which are indicators of metabolic syndrome (Mets), play a major role in cerebral physiology and morphology, amyloid-β deposition, and neurological plaque accumulation [173]. In addition, several studies have demonstrated that healthy diet patterns such as Mediterranean diet (MeDi), dietary approach to stop hypertension (DASH), and Mediterranean-DASH diet intervention for neurodegenerative delay (MIND) are effective in reducing dementia and AD risk [174–177]. Brain glucose uptake is impaired in AD, possibly due to a loss of synapses and neuronal dysfunction [178]. If deprived of glucose, the primary energy source, the brain can switch to utilization of ketones (specifically β-hydroxybutyrate [β-HB] and acetoacetate [AcAc]; [179,180]). Interestingly, brain ketone uptake remains normal in AD patients [181,182]. Thus, several studies and

review articles have assessed the potentially beneficial effect of a ketogenic diet in AD [183–186]. Indeed, a systematic review of randomized clinical trials evaluating ketogenic and non-ketogenic dietary interventions in participants with mild cognitive impairment (MCI) and AD showed promising results from the studies included, despite heterogeneity in study design, dietary compliance, and participants [187].

The gut microbiome is greatly affected by these dietary interventions. Changes in the composition of the intestinal microbiota caused by diet affect the various metabolites they produce, and these changes can regulate the host immune response in a beneficial way and maintain the health of the nervous system. For example, a ketogenic diet increased relative abundances of potentially beneficial bacteria (*Akkermansia* and *Lactobacillus*) compared to mice fed a control diet. This correlated with enhanced neurovascular function, and amyloid-β clearance which was associated with reduction in mTOR expression and increased endothelial nitric oxide synthase (eNOS) protein expression [188]. In a study of patients with mild cognitive impairment, gut microbiota composition is associated with cognitive impairment. A modified Mediterranean-ketogenic diet (MMKD) regulated gut microbiome composition and production of metabolites such as SCFA, which were associated with improvement of AD symptoms [189,190]. These studies suggest the modification of gut microbiome through dietary intervention can be a strong candidate for future AD therapy. Future studies focused on the gut microbiota-brain axis as a therapeutic utilizing a multi-omics approach, which is crucial for uncovering the role of the gut microbiota-brain axis in AD and the development of therapeutics.

Limitations of Current Research

Current research on the gut microbiota-brain axis in Alzheimer's disease is based mostly on compositional microbiome data using 16S rRNA marker gene sequencing. Few studies have evaluated the role of fungal microbiota in the gut, though recent work has demonstrated a critical role of fungal communities in health and development of peripheral organs through sensing of fungi by gut-resident immune cells, such as mononuclear phagocytes [191]. While this approach has laid the foundation for the field, the use of transcriptomics, metagenomics, and metabolomics will be necessary to uncover the complex set of mechanisms involved in the gut microbiota-brain axis. There are a limited number of studies in human AD patients, as highlighted by the minimal studies cited in this review, and the studies in human AD to date have been observational. Thus, we cannot yet determine the directionality of the observed changes in the gut microbiota in AD, e.g., whether gut microbiome dysbiosis is due to altered diet, medication use, or stress in individuals with AD. However, preclinical murine models of AD pathologies demonstrate altered gut microbiota prior to emergence of amyloidosis, tauopathy, or neuroinflammation, which provides some, but limited, evidence that changes in the gut microbiome may contribute to AD progression. Future longitudinal, cross-sectional, and interventional studies in AD patients are warranted to study key changes in the gut microbiota composition, mechanistic pathways, and possible therapeutics.

In a broader sense, treatment of disease through modification of the gut microbiome is extremely challenging due to the myriad of factors that shape microbiome composition and function. Development of the gut microbiome begins at birth, and rapidly changes during the first three years of life [192]. The gut microbiome is influenced by host genetics, mode of delivery, diets, surrounding environment, and lifestyles of individuals, and even psychological factors such as stress and anxiety [193–196]. For this reason, it is difficult to accurately distinguish which gut microbiota contributes to the onset or progression of Alzheimer's disease, and even if such gut microbiota is found, it is difficult to modify and maintain changes to the gut microbiome. Patients with Alzheimer's Disease experience a range of dietary, medical, and stress-related changes as dementia progresses, which may influence the composition of the gut microbiome independent of disease pathologies. For future studies, it is important to have accurate understandings of how modifying the gut microbiome can contribute to health status of AD patients, and to determine how to maintain a healthy microbiome using a combination of rationally-developed probiotics (live microorganisms that confer a health benefit), prebiotics (nondigestible dietary ingredients that promote the growth of beneficial microorganisms), or dietary interventions.

CONCLUSIONS

Thus far, we have summarized the role of the gut microbiota-brain axis as an integral part of disease pathogenesis. However, this complex system employs a myriad of mechanisms working together in the development of AD. While there are many moving factors in AD pathophysiology, identifying key pathways and mechanisms involved in

progression is crucial in order to develop novel therapeutic targets. Growing evidence supports bidirectional communication between the CNS and the gut microbiota; studies demonstrate that the microbiota shapes AD pathologies and neuroinflammation, and AD pathogenesis modulates the gut microbiota composition. The gut microbiota-brain axis modulates key processes, including immune cell maturation, SCFA, LPS, and cytokine production, permeability of the gut epithelium and BBB, and gut microbiota diversity. Gut microbiota production of SCFA is reduced in AD thereby inducing the NF-kB pathway and increasing production of proinflammatory cytokines, including IL-1β, IL-6, and TNFα [197]. These cytokines are able to modulate the BBB permeability and translocate to the brain [119]. Once in the brain, proinflammatory cytokines potentiate Aβ deposition, tau hyperphosphorylation, microgliosis, and astrogliosis, increasing the severity of AD pathologies. Further studies are warranted to identify the directionality of observed changes in the microbiota, mechanisms, and therapeutic strategies with these novel targets. In particular, focus on elucidating the interactions between the gut microbiota communities and cytokines and their role in neuroinflammation and disease pathologies will lead to a better understanding of disease mechanisms. Studies with a multi-omics approach in both animal models, carefully selected human cohorts, and *in vitro* mechanistic studies will uncover the underlying mechanisms of the gut microbiota-brain axis and its impact on AD, dementia, and other neurological diseases. Focus on neuroinflammation and cytokines in the gut microbiota-brain axis will elucidate the role of chronic inflammation in AD and other inflammatory diseases.

Figure 1. Proposed mechanism of LPS-induced neuropathologies in AD. AD-associated microbiome composition has increased abundance of lipopolysaccharide (LPS) producing bacteria, including *Bacteroides*. LPS stimulates enteric microglia to produce IL-1β, IL-6, and TNF-α, which induces the NF-kB pathway, therefore upregulating expression of proinflammatory cytokines. Similarly, LPS stimulates the vagus nerve, activating microglia in the brain, thereby promoting neuroinflammation. LPS is able to translocate from the GI tract to the circulatory system and stimulate astrocytes. The reduction in blood brain barrier (BBB) integrity allows LPS to cross the BBB and further promote inflammation in the brain.

Table 1. Alterations in gut microbiota composition in humans and transgenic mice without intervention.

Species	Increased abundance	Decreased abundance	Citation
Human	*g.Blautia, g.Alistipes, g.Bacteroides*	*g.Turicibacter, g.Clostridium, g.Dialister*	Vogt et. al[72]
Human	*g.Gammaproteobacteria*, *g.Enterobacteriales* and *g.Enterobacteriacea*	*g.Ruminococcus g.Clostridiaceae, g.Lachnospiraceae*	Liu et. al[73]
Human	*g.Ruminococcus, g.Subdoligranulum*	*g.Lachnospiraceaeg, g.Lachnoclostridium, g.Bacteroides*	Zhuang[74]
Human	*g.Bacteroides, g.Alistipes,*	*g.Butyrivibrio*, *g.Eubacterium,*	Haran et.

	g.Odoribacter	*g.Lachnoclostridium,*	al[75]
APP/PS 1	*g.Desulfovibrio, g.Akkermansia, g.Lachnospiraceae, g.Ruminococcus*	*g.Alistiples, g.Lachnospiraceae*	Chen et. al[78]

Table 2. Alterations in gut microbiota composition in transgenic mice after the intervention.

Species	Increased abundance	Decreased abundance	Intervention	Citation
3xTg-AD	*g.Bifidobacterium*	*o.Campylobacterales*	SLAB51 probiotic	Bonfili et. al[82]
APP/PS 1	*g.Lactobacillus*	*g.Helicobacter*	FOS supplement	Sun et. al[83]
3xTg-AD	*f Rikenellaceae, f.Lachnospiraceae, f.Enterococcaceae and f.S24.7*	*g.Bifidobacterium, g.Lactobacillus*	Fatty diet	Sanguinetti et. al[84]

REFERENCES

1. Thursby, E.; Juge, N. Introduction to the human gut microbiota. *Biochemical*

Journal 2017, *474*, 1823–1836.

2. Jandhyala, S.M. Role of the normal gut microbiota. *World Journal of Gastroenterology* 2015, *21*, 8787.

3. Barcel´o-Coblijn, G.; Amedei, A. *The Interplay of Microbiome and Immune Response in Health and Diseases*; MDPI, 2019; ISBN 9783039216468.

4. Dinan, T.G.; Cryan, J.F. The Microbiome-Gut-Brain Axis in Health and Disease. *Gastroenterol. Clin. North Am.* **2017**, *46*, 77–89.

5. Ubeda, C.; Djukovic, A.; Isaac, S. Roles of the intestinal microbiota in pathogen protection. *Clinical & Translational Immunology* 2017, *6*, e128.

6. Oliphant, K.; Allen-Vercoe, E. Macronutrient metabolism by the human gut microbiome: major fermentation by-products and their impact on host health. *Microbiome* 2019, *7*.

7. Kho, Z.Y.; Lal, S.K. The Human Gut Microbiome – A Potential Controller of Wellness and Disease. *Frontiers in Microbiology* 2018, *9*.

8. Tap, J.; Mondot, S.; Levenez, F.; Pelletier, E.; Caron, C.; Furet, J.-P.; Ugarte, E.; Muñoz-Tamayo, R.; Paslier, D.L.E.; Nalin, R.; et al. Towards the human intestinal microbiota phylogenetic core. *Environ. Microbiol.* **2009**, *11*, 2574–2584.

9. Soto-Martin, E.C.; Warnke, I.; Farquharson, F.M.; Christodoulou, M.; Horgan, G.; Derrien, M.; Faurie, J.-M.; Flint, H.J.; Duncan, S.H.; Louis, P. Vitamin Biosynthesis by Human Gut Butyrate-Producing Bacteria and Cross-Feeding in Synthetic Microbial Communities. *MBio* **2020**, *11*, doi:10.1128/mBio.00886-20.

10. Yoshii, K.; Hosomi, K.; Sawane, K.; Kunisawa, J. Metabolism of Dietary and Microbial Vitamin B Family in the Regulation of Host Immunity. *Front Nutr* **2019**,

6, 48.

11. Atarashi, K.; Tanoue, T.; Shima, T.; Imaoka, A.; Kuwahara, T.; Momose, Y.; Cheng, G.; Yamasaki, S.; Saito, T.; Ohba, Y.; et al. Induction of Colonic Regulatory T Cells by Indigenous Clostridium Species. *Science* **2011**, *331*, 337.

12. Makki, K.; Deehan, E.C.; Walter, J.; Bäckhed, F. The Impact of Dietary Fiber on Gut Microbiota in Host Health and Disease. *Cell Host Microbe* **2018**, *23*, 705–715.

13. Trompette, A.; Gollwitzer, E.S.; Yadava, K.; Sichelstiel, A.K.; Sprenger, N.; Ngom-Bru, C.; Blanchard, C.; Junt, T.; Nicod, L.P.; Harris, N.L.; et al. Gut microbiota metabolism of dietary fiber influences allergic airway disease and hematopoiesis. *Nat. Med.* **2014**, *20*, 159–166.

14. Trompette, A.; Gollwitzer, E.S.; Pattaroni, C.; Lopez-Mejia, I.C.; Riva, E.; Pernot, J.; Ubags, N.; Fajas, L.; Nicod, L.P.; Marsland, B.J. Dietary Fiber Confers Protection against Flu by Shaping Ly6c− Patrolling Monocyte Hematopoiesis and CD8 T Cell Metabolism. *Immunity* 2018, *48*, 992–1005.e8.

15. Yu, L.C.-H. Microbiota dysbiosis and barrier dysfunction in inflammatory bowel disease and colorectal cancers: exploring a common ground hypothesis. *Journal of Biomedical Science* 2018, *25*.

16. Henke, M.T.; Kenny, D.J.; Cassilly, C.D.; Vlamakis, H.; Xavier, R.J.; Clardy, J. Ruminococcus gnavus, a member of the human gut microbiome associated with Crohn’s disease, produces an inflammatory polysaccharide. *Proceedings of the National Academy of Sciences* 2019, *116*, 12672–12677.

17. Kowalski, K.; Mulak, A. Brain-Gut-Microbiota Axis in Alzheimer’s Disease.

J. Neurogastroenterol. Motil. **2019**, *25*, 48–60.

18. Baker, J.M.; Al-Nakkash, L.; Herbst-Kralovetz, M.M. Estrogen–gut microbiome axis: Physiological and clinical implications. *Maturitas* 2017, *103*, 45–53.

19. Flores, R.; Shi, J.; Fuhrman, B.; Xu, X.; Veenstra, T.D.; Gail, M.H.; Gajer, P.; Ravel, J.; Goedert, J.J. Fecal microbial determinants of fecal and systemic estrogens and estrogen metabolites: a cross-sectional study. *J. Transl. Med.* **2012**, *10*, 253.

20. Fülling, C.; Dinan, T.G.; Cryan, J.F. Gut Microbe to Brain Signaling: What Happens in Vagus…. *Neuron* **2019**, *101*, 998–1002.

21. Bravo, J.A.; Forsythe, P.; Chew, M.V.; Escaravage, E.; Savignac, H.M.; Dinan, T.G.; Bienenstock, J.; Cryan, J.F. Ingestion of Lactobacillus strain regulates emotional behavior and central GABA receptor expression in a mouse via the vagus nerve. *Proceedings of the National Academy of Sciences* 2011, *108*, 16050–16055.

22. Brandsma, E.; Kloosterhuis, N.J.; Koster, M.; Dekker, D.C.; Gijbels, M.J.J.; van der Velden, S.; Ríos-Morales, M.; van Faassen, M.J.R.; Loreti, M.G.; de Bruin, A.; et al. A Proinflammatory Gut Microbiota Increases Systemic Inflammation and Accelerates Atherosclerosis. *Circ. Res.* **2019**, *124*, 94–100.

23. Ma, Q.; Xing, C.; Long, W.; Wang, H.Y.; Liu, Q.; Wang, R.-F. Impact of microbiota on central nervous system and neurological diseases: the gut-brain axis. *J. Neuroinflammation* **2019**, *16*, 53.

24. Alkasir, R.; Li, J.; Li, X.; Jin, M.; Zhu, B. Human gut microbiota: the links with dementia development. *Protein Cell* **2017**, *8*, 90–102.

25. Saji, N.; Murotani, K.; Hisada, T.; Kunihiro, T.; Tsuduki, T.; Sugimoto, T.; Kimura, A.; Niida, S.; Toba, K.; Sakurai, T. Relationship between dementia and gut microbiome-associated metabolites: a cross-sectional study in Japan. *Sci. Rep.* **2020**, *10*, 8088.

26. Li, S.; Shao, Y.; Li, K.; HuangFu, C.; Wang, W.; Liu, Z.; Cai, Z.; Zhao, B. Vascular Cognitive Impairment and the Gut Microbiota. *J. Alzheimers. Dis.* **2018**, *63*, 1209–1222.

27. Daulatzai, M.A. Non-celiac gluten sensitivity triggers gut dysbiosis, neuroinflammation, gut-brain axis dysfunction, and vulnerability for dementia. *CNS Neurol. Disord. Drug Targets* **2015**, *14*, 110–131.

28. Mohan, M.; Okeoma, C.M.; Sestak, K. Dietary Gluten and Neurodegeneration: A Case for Preclinical Studies. *Int. J. Mol. Sci.* **2020**, *21*, doi:10.3390/ijms21155407.

29. Pennisi, M.; Bramanti, A.; Cantone, M.; Pennisi, G.; Bella, R.; Lanza, G. Neurophysiology of the “Celiac Brain”: Disentangling Gut-Brain Connections. *Front. Neurosci.* **2017**, *11*, 498.

30. Lanza, G.; Bella, R.; Cantone, M.; Pennisi, G.; Ferri, R.; Pennisi, M. Cognitive Impairment and Celiac Disease: Is Transcranial Magnetic Stimulation a Trait d’Union between Gut and Brain? *Int. J. Mol. Sci.* **2018**, *19*, doi:10.3390/ijms19082243.

31. Lyon, L. “All disease begins in the gut”: was Hippocrates right? *Brain* 2018, *141*, e20–e20.

32. Hippius, H.; Neundörfer, G. The discovery of Alzheimer’s disease.

Dialogues Clin. Neurosci. **2003**, *5*, 101–108.

33. 2020 Alzheimer's disease facts and figures. *Alzheimers. Dement.* **2020**, doi:10.1002/alz.12068.

34. Lewis, T.J.; Trempe, C.L. The Amyloid Cascade Hypothesis. *The End of Alzheimer's* 2017, 26–50.

35. Wang, X.; Sun, G.; Feng, T.; Zhang, J.; Huang, X.; Wang, T.; Xie, Z.; Chu, X.; Yang, J.; Wang, H.; et al. Sodium oligomannate therapeutically remodels gut microbiota and suppresses gut bacterial amino acids-shaped neuroinflammation to inhibit Alzheimer's disease progression. *Cell Res.* **2019**, *29*, 787–803.

36. Paul Murphy, M.; LeVine, H.; III Alzheimer's Disease and the β-Amyloid Peptide. *J. Alzheimers. Dis.* **2010**, *19*, 311.

37. Bitan, G.; Kirkitadze, M.D.; Lomakin, A.; Vollers, S.S.; Benedek, G.B.; Teplow, D.B. Amyloid beta -protein (Abeta) assembly: Abeta 40 and Abeta 42 oligomerize through distinct pathways. *Proc. Natl. Acad. Sci. U. S. A.* **2003**, *100*, 330–335.

38. Selkoe, D.J. Alzheimer's disease: genes, proteins, and therapy. *Physiol. Rev.* **2001**, *81*, 741–766.

39. Sochocka, M.; Donskow-Łysoniewska, K.; Diniz, B.S.; Kurpas, D.; Brzozowska, E.; Leszek, J. The Gut Microbiome Alterations and Inflammation-Driven Pathogenesis of Alzheimer's Disease—a Critical Review. *Molecular Neurobiology* 2019, *56*, 1841–1851.

40. Hashemiaghdam, A.; Mroczek, M. Microglia heterogeneity and neurodegeneration: The emerging paradigm of the role of immunity in Alzheimer's

disease. *J. Neuroimmunol.* **2020**, *341*, 577185.

41. Kinney, J.W.; Bemiller, S.M.; Murtishaw, A.S.; Leisgang, A.M.; Salazar, A.M.; Lamb, B.T. Inflammation as a central mechanism in Alzheimer's disease. *Alzheimers. Dement.* **2018**, *4*, 575–590.

42. Jill E. Clarridge, I.I.I. Impact of 16S rRNA Gene Sequence Analysis for Identification of Bacteria on Clinical Microbiology and Infectious Diseases. *Clin. Microbiol. Rev.* **2004**, *17*, 840.

43. Ihrmark, K.; Bödeker, I.T.M.; Cruz-Martinez, K.; Friberg, H.; Kubartova, A.; Schenck, J.; Strid, Y.; Stenlid, J.; Brandström-Durling, M.; Clemmensen, K.E.; et al. New primers to amplify the fungal ITS2 region--evaluation by 454-sequencing of artificial and natural communities. *FEMS Microbiol. Ecol.* **2012**, *82*, 666–677.

44. Hillmann, B.; Al-Ghalith, G.A.; Shields-Cutler, R.R.; Zhu, Q.; Gohl, D.M.; Beckman, K.B.; Knight, R.; Knights, D. Evaluating the Information Content of Shallow Shotgun Metagenomics. *mSystems* **2018**, *3*, doi:10.1128/mSystems.00069-18.

45. Li, D.; Liu, C.-M.; Luo, R.; Sadakane, K.; Lam, T.-W. MEGAHIT: an ultra-fast single-node solution for large and complex metagenomics assembly via succinct de Bruijn graph. *Bioinformatics* **2015**, *31*, 1674–1676.

46. Bankevich, A.; Nurk, S.; Antipov, D.; Gurevich, A.A.; Dvorkin, M.; Kulikov, A.S.; Lesin, V.M.; Nikolenko, S.I.; Pham, S.; Prjibelski, A.D.; et al. SPAdes: a new genome assembly algorithm and its applications to single-cell sequencing. *J. Comput. Biol.* **2012**, *19*, 455–477.

47. Segata, N.; Boernigen, D.; Tickle, T.L.; Morgan, X.C.; Garrett, W.S.;

Huttenhower, C. Computational meta'omics for microbial community studies. *Mol. Syst. Biol.* **2013**, *9*, 666.

48. Franzosa, E.A.; McIver, L.J.; Rahnavard, G.; Thompson, L.R.; Schirmer, M.; Weingart, G.; Lipson, K.S.; Knight, R.; Caporaso, J.G.; Segata, N.; et al. Species-level functional profiling of metagenomes and metatranscriptomes. *Nat. Methods* **2018**, *15*, 962–968.

49. Wood, D.E.; Salzberg, S.L. Kraken: ultrafast metagenomic sequence classification using exact alignments. *Genome Biol.* **2014**, *15*, R46.

50. Aguiar-Pulido, V.; Huang, W.; Suarez-Ulloa, V.; Cickovski, T.; Mathee, K.; Narasimhan, G. Metagenomics, Metatranscriptomics, and Metabolomics Approaches for Microbiome Analysis. *Evol. Bioinform. Online* **2016**, *12*, 5.

51. Liu, P.-P.; Xie, Y.; Meng, X.-Y.; Kang, J.-S. Author Correction: History and progress of hypotheses and clinical trials for Alzheimer's disease. *Signal Transduction and Targeted Therapy* 2019, *4*.

52. Sun, M.; Ma, K.; Wen, J.; Wang, G.; Zhang, C.; Li, Q.; Bao, X.; Wang, H. A Review of the Brain-Gut-Microbiome Axis and the Potential Role of Microbiota in Alzheimer's Disease. *Journal of Alzheimer's Disease* 2020, *73*, 849–865.

53. Giau, V.; Wu, S.; Jamerlan, A.; An, S.; Kim, S.; Hulme, J. Gut Microbiota and Their Neuroinflammatory Implications in Alzheimer's Disease. *Nutrients* 2018, *10*, 1765.

54. Domingues, C.; da Cruz e Silva, O.A.B.; Henriques, A.G. Impact of Cytokines and Chemokines on Alzheimer's Disease Neuropathological Hallmarks. *Current Alzheimer Research* 2017, *14*.

55. Sheng, J.G.; Ito, K.; Skinner, R.D.; Mrak, R.E.; Rovnaghi, C.R.; Van Eldik, L.J.; Griffin, W.S. In vivo and in vitro evidence supporting a role for the inflammatory cytokine interleukin-1 as a driving force in Alzheimer pathogenesis. *Neurobiol. Aging* **1996**, *17*, 761–766.

56. Quintanilla, R.A.; Orellana, D.I.; González-Billault, C.; Maccioni, R.B. Interleukin-6 induces Alzheimer-type phosphorylation of tau protein by deregulating the cdk5/p35 pathway. *Exp. Cell Res.* **2004**, *295*, 245–257.

57. Steardo, L.; Bronzuoli, M.R.; Iacomino, A.; Esposito, G.; Steardo, L.; Scuderi, C. Does neuroinflammation turn on the flame in Alzheimer's disease? Focus on astrocytes. *Frontiers in Neuroscience* 2015, *9*.

58. Koeth, R.A.; Wang, Z.; Levison, B.S.; Buffa, J.A.; Org, E.; Sheehy, B.T.; Britt, E.B.; Fu, X.; Wu, Y.; Li, L.; et al. Intestinal microbiota metabolism of L-carnitine, a nutrient in red meat, promotes atherosclerosis. *Nat. Med.* **2013**, *19*, 576–585.

59. Vogt, N.M.; Romano, K.A.; Darst, B.F.; Engelman, C.D.; Johnson, S.C.; Carlsson, C.M.; Asthana, S.; Blennow, K.; Zetterberg, H.; Bendlin, B.B.; et al. The gut microbiota-derived metabolite trimethylamine N-oxide is elevated in Alzheimer's disease. *Alzheimer's Research & Therapy* 2018, *10*.

60. Ho, L.; Ono, K.; Tsuji, M.; Mazzola, P.; Singh, R.; Pasinetti, G.M. Protective roles of intestinal microbiota derived short chain fatty acids in Alzheimer's disease-type beta-amyloid neuropathological mechanisms. *Expert Review of Neurotherapeutics* 2018, *18*, 83–90.

61. Rao, M.; Gershon, M.D. The bowel and beyond: the enteric nervous

system in neurological disorders. *Nat. Rev. Gastroenterol. Hepatol.* **2016**, *13*, 517–528.

62. Costa, M.; Brookes, S.J.; Hennig, G.W. Anatomy and physiology of the enteric nervous system. *Gut* **2000**, *47 Suppl 4*, iv15–9; discussion iv26.

63. Abdel-Haq, R.; Schlachetzki, J.C.M.; Glass, C.K.; Mazmanian, S.K. Microbiome–microglia connections via the gut–brain axis. *Journal of Experimental Medicine* 2019, *216*, 41–59.

64. Bonaz, B.; Sinniger, V.; Pellissier, S. The Vagus Nerve in the Neuro-Immune Axis: Implications in the Pathology of the Gastrointestinal Tract. *Front. Immunol.* **2017**, *8*, 1452.

65. Bonaz, B.; Bazin, T.; Pellissier, S. The Vagus Nerve at the Interface of the Microbiota-Gut-Brain Axis. *Front. Neurosci.* **2018**, *12*, 49.

66. Browning, K.N. Role of central vagal 5-HT3 receptors in gastrointestinal physiology and pathophysiology. *Front. Neurosci.* **2015**, *9*, doi:10.3389/fnins.2015.00413.

67. Merrill, C.A.; Jonsson, M.A.G.; Minthon, L.; Ejnell, H.; C-son Silander, H.; Blennow, K.; Karlsson, M.; Nordlund, A.; Rolstad, S.; Warkentin, S.; et al. Vagus nerve stimulation in patients with Alzheimer's disease: Additional follow-up results of a pilot study through 1 year. *J. Clin. Psychiatry* **2006**, *67*, 1171–1178.

68. Sjögren, M.J.C.; Hellström, P.T.O.; Jonsson, M.A.G.; Runnerstam, M.; Silander, H.C.-S.; Ben-Menachem, E. Cognition-enhancing effect of vagus nerve stimulation in patients with Alzheimer's disease: a pilot study. *J. Clin. Psychiatry* **2002**, *63*, 972–980.

69. Desbeaumes Jodoin, V.; Richer, F.; Miron, J.-P.; Fournier-Gosselin, M.-P.; Lespérance, P. Long-term Sustained Cognitive Benefits of Vagus Nerve Stimulation in Refractory Depression. *J. ECT* **2018**, *34*, 283–290.

70. Kaczmarczyk, R.; Tejera, D.; Simon, B.J.; Heneka, M.T. Microglia modulation through external vagus nerve stimulation in a murine model of Alzheimer's disease. *Journal of Neurochemistry* 2018, *146*, 76–85.

71. Tran, T.T.T.; Corsini, S.; Kellingray, L.; Hegarty, C.; Le Gall, G.; Narbad, A.; Müller, M.; Tejera, N.; O'Toole, P.W.; Minihane, A.-M.; et al. APOE genotype influences the gut microbiome structure and function in humans and mice: relevance for Alzheimer's disease pathophysiology. *The FASEB Journal* 2019, *33*, 8221–8231.

72. Vogt, N.M.; Kerby, R.L.; Dill-McFarland, K.A.; Harding, S.J.; Merluzzi, A.P.; Johnson, S.C.; Carlsson, C.M.; Asthana, S.; Zetterberg, H.; Blennow, K.; et al. Gut microbiome alterations in Alzheimer's disease. *Sci. Rep.* **2017**, *7*, 13537.

73. Liu, P.; Wu, L.; Peng, G.; Han, Y.; Tang, R.; Ge, J.; Zhang, L.; Jia, L.; Yue, S.; Zhou, K.; et al. Altered microbiomes distinguish Alzheimer's disease from amnestic mild cognitive impairment and health in a Chinese cohort. *Brain, Behavior, and Immunity* 2019, *80*, 633–643.

74. Zhuang, Z.-Q.; Shen, L.-L.; Li, W.-W.; Fu, X.; Zeng, F.; Gui, L.; Lü, Y.; Cai, M.; Zhu, C.; Tan, Y.-L.; et al. Gut Microbiota is Altered in Patients with Alzheimer's Disease. *J. Alzheimers. Dis.* **2018**, *63*, 1337–1346.

75. Haran, J.P.; Bhattarai, S.K.; Foley, S.E.; Dutta, P.; Ward, D.V.; Bucci, V.; McCormick, B.A. Alzheimer's Disease Microbiome Is Associated with Dysregulation

of the Anti-Inflammatory P-Glycoprotein Pathway. *mBio* 2019, *10*.

76. Emery, D.C.; Shoemark, D.K.; Batstone, T.E.; Waterfall, C.M.; Coghill, J.A.; Cerajewska, T.L.; Davies, M.; West, N.X.; Allen, S.J. 16S rRNA Next Generation Sequencing Analysis Shows Bacteria in Alzheimer's Post-Mortem Brain. *Frontiers in Aging Neuroscience* 2017, *9*.

77. Dominy, S.S.; Lynch, C.; Ermini, F.; Benedyk, M.; Marczyk, A.; Konradi, A.; Nguyen, M.; Haditsch, U.; Raha, D.; Griffin, C.; et al. in Alzheimer's disease brains: Evidence for disease causation and treatment with small-molecule inhibitors. *Sci Adv* **2019**, *5*, eaau3333.

78. Chen, Y.; Fang, L.; Chen, S.; Zhou, H.; Fan, Y.; Lin, L.; Li, J.; Xu, J.; Chen, Y.; Ma, Y.; et al. Gut Microbiome Alterations Precede Cerebral Amyloidosis and Microglial Pathology in a Mouse Model of Alzheimer's Disease. *BioMed Research International* 2020, *2020*, 1–15.

79. Brandscheid, C.; Schuck, F.; Reinhardt, S.; Schäfer, K.-H.; Pietrzik, C.U.; Grimm, M.; Hartmann, T.; Schwiertz, A.; Endres, K. Altered Gut Microbiome Composition and Tryptic Activity of the 5xFAD Alzheimer's Mouse Model. *Journal of Alzheimer's Disease* 2017, *56*, 775–788.

80. Parikh, I.J.; Estus, J.L.; Zajac, D.J.; Malik, M.; Maldonado Weng, J.; Tai, L.M.; Chlipala, G.E.; LaDu, M.J.; Green, S.J.; Estus, S. Murine Gut Microbiome Association With APOE Alleles. *Front. Immunol.* **2020**, *11*, doi:10.3389/fimmu.2020.00200.

81. Harach, T.; Marungruang, N.; Duthilleul, N.; Cheatham, V.; Mc Coy, K.D.; Frisoni, G.; Neher, J.J.; Fåk, F.; Jucker, M.; Lasser, T.; et al. Erratum: Reduction of

Abeta amyloid pathology in APPPS1 transgenic mice in the absence of gut microbiota. *Sci. Rep.* **2017**, *7*, 46856.

82. Bonfili, L.; Cecarini, V.; Berardi, S.; Scarpona, S.; Suchodolski, J.S.; Nasuti, C.; Fiorini, D.; Boarelli, M.C.; Rossi, G.; Eleuteri, A.M. Microbiota modulation counteracts Alzheimer's disease progression influencing neuronal proteolysis and gut hormones plasma levels. *Scientific Reports* 2017, *7*.

83. Sun, J.; Liu, S.; Ling, Z.; Wang, F.; Ling, Y.; Gong, T.; Fang, N.; Ye, S.; Si, J.; Liu, J. Fructooligosaccharides Ameliorating Cognitive Deficits and Neurodegeneration in APP/PS1 Transgenic Mice through Modulating Gut Microbiota. *J. Agric. Food Chem.* **2019**, *67*, 3006–3017.

84. Sanguinetti, E.; Collado, M.C.; Marrachelli, V.G.; Monleon, D.; Selma-Royo, M.; Pardo-Tendero, M.M.; Burchielli, S.; Iozzo, P. Microbiome-metabolome signatures in mice genetically prone to develop dementia, fed a normal or fatty diet. *Scientific Reports* 2018, *8*.

85. Sun, J.; Xu, J.; Ling, Y.; Wang, F.; Gong, T.; Yang, C.; Ye, S.; Ye, K.; Wei, D.; Song, Z.; et al. Fecal microbiota transplantation alleviated Alzheimer's disease-like pathogenesis in APP/PS1 transgenic mice. *Translational Psychiatry* 2019, *9*.

86. Chen, W.-W.; Zhang, X.; Huang, W.-J. Role of neuroinflammation in neurodegenerative diseases (Review). *Molecular Medicine Reports* 2016, *13*, 3391–3396.

87. Guo, W.; Wang, H.; Watanabe, M.; Shimizu, K.; Zou, S.; LaGraize, S.C.; Wei, F.; Dubner, R.; Ren, K. Glial-cytokine-neuronal interactions underlying the mechanisms of persistent pain. *J. Neurosci.* **2007**, *27*, 6006–6018.

88. Ferrucci, L.; Fabbri, E. Inflammageing: chronic inflammation in ageing, cardiovascular disease, and frailty. *Nat. Rev. Cardiol.* **2018**, *15*, 505–522.

89. Pan, J.; Ma, N.; Yu, B.; Zhang, W.; Wan, J. Transcriptomic profiling of microglia and astrocytes throughout aging. *J. Neuroinflammation* **2020**, *17*, 97.

90. Salas, I.H.; Burgado, J.; Allen, N.J. Glia: victims or villains of the aging brain? *Neurobiol. Dis.* **2020**, *143*, 105008.

91. Streit, W.J.; Sammons, N.W.; Kuhns, A.J.; Larry Sparks, D. Dystrophic microglia in the aging human brain. *Glia* 2004, *45*, 208–212.

92. Fransen, F.; van Beek, A.A.; Borghuis, T.; Aidy, S.E.; Hugenholtz, F.; van der Gaast-de Jongh, C.; Savelkoul, H.F.J.; De Jonge, M.I.; Boekschoten, M.V.; Smidt, H.; et al. Aged Gut Microbiota Contributes to Systemical Inflammaging after Transfer to Germ-Free Mice. *Front. Immunol.* **2017**, *8*, 1385.

93. Cerovic, M.; Forloni, G.; Balducci, C. Neuroinflammation and the Gut Microbiota: Possible Alternative Therapeutic Targets to Counteract Alzheimer's Disease? *Frontiers in Aging Neuroscience* 2019, *11*.

94. Arcuri, C.; Mecca, C.; Bianchi, R.; Giambanco, I.; Donato, R. The Pathophysiological Role of Microglia in Dynamic Surveillance, Phagocytosis and Structural Remodeling of the Developing CNS. *Front. Mol. Neurosci.* **2017**, *10*, 191.

95. Leyns, C.E.G.; Holtzman, D.M. Glial contributions to neurodegeneration in tauopathies. *Mol. Neurodegener.* **2017**, *12*, 50.

96. Wang, Y.; Wang, Z.; Wang, Y.; Li, F.; Jia, J.; Song, X.; Qin, S.; Wang, R.; Jin, F.; Kitazato, K.; et al. The Gut-Microglia Connection: Implications for Central Nervous System Diseases. *Front. Immunol.* **2018**, *9*, 2325.

97. Hemonnot, A.-L.; Hua, J.; Ulmann, L.; Hirbec, H. Microglia in Alzheimer Disease: Well-Known Targets and New Opportunities. *Front. Aging Neurosci.* **2019**, *11*, 233.

98. Lai, A.Y.; McLaurin, J. Clearance of amyloid-β peptides by microglia and macrophages: the issue of what, when and where. *Future Neurology* 2012, *7*, 165–176.

99. Mandrekar-Colucci, S.; Landreth, G.E. Microglia and Inflammation in Alzheimers Disease. *CNS & Neurological Disorders - Drug Targets* 2010, *9*, 156–167.

100. Hristovska, I.; Pascual, O. Deciphering Resting Microglial Morphology and Process Motility from a Synaptic Prospect. *Front. Integr. Neurosci.* **2015**, *9*, 73.

101. Streit, W.J.; Mrak, R.E.; Griffin, W.S.T. Microglia and neuroinflammation: a pathological perspective. *J. Neuroinflammation* **2004**, *1*, 14.

102. Meneses, G.; Bautista, M.; Florentino, A.; Díaz, G.; Acero, G.; Besedovsky, H.; Meneses, D.; Fleury, A.; Del Rey, A.; Gevorkian, G.; et al. Electric stimulation of the vagus nerve reduced mouse neuroinflammation induced by lipopolysaccharide. *J. Inflamm.* **2016**, *13*, 33.

103. Huffman, W.J.; Subramaniyan, S.; Rodriguiz, R.M.; Wetsel, W.C.; Grill, W.M.; Terrando, N. Modulation of neuroinflammation and memory dysfunction using percutaneous vagus nerve stimulation in mice. *Brain Stimul.* **2019**, *12*, 19–29.

104. Yao, K.; Zu, H.-B. Microglial polarization: novel therapeutic mechanism against Alzheimer's disease. *Inflammopharmacology* 2020, *28*, 95–110.

105. Chhor, V.; Le Charpentier, T.; Lebon, S.; Oré, M.-V.; Celador, I.L.;

Josserand, J.; Degos, V.; Jacotot, E.; Hagberg, H.; Sävman, K.; et al. Characterization of phenotype markers and neuronotoxic potential of polarised primary microglia in vitro. *Brain Behav. Immun.* **2013**, *32*, 70–85.

106. Zhang, L.; Wang, Y.; Xiayu, X.; Shi, C.; Chen, W.; Song, N.; Fu, X.; Zhou, R.; Xu, Y.-F.; Huang, L.; et al. Altered Gut Microbiota in a Mouse Model of Alzheimer's Disease. *Journal of Alzheimer's Disease* 2017, *60*, 1241–1257.

107. Amici, S.A.; Dong, J.; Guerau-de-Arellano, M. Molecular Mechanisms Modulating the Phenotype of Macrophages and Microglia. *Front. Immunol.* **2017**, *8*, 1520.

108. Tang, Y.; Le, W. Differential Roles of M1 and M2 Microglia in Neurodegenerative Diseases. *Mol. Neurobiol.* **2016**, *53*, 1181–1194.

109. Bachiller, S.; Jiménez-Ferrer, I.; Paulus, A.; Yang, Y.; Swanberg, M.; Deierborg, T.; Boza-Serrano, A. Microglia in Neurological Diseases: A Road Map to Brain-Disease Dependent-Inflammatory Response. *Frontiers in Cellular Neuroscience* 2018, *12*.

110. Sharma, R.K.; Yang, T.; Oliveira, A.C.; Lobaton, G.O.; Aquino, V.; Kim, S.; Richards, E.M.; Pepine, C.J.; Sumners, C.; Raizada, M.K. Microglial Cells Impact Gut Microbiota and Gut Pathology in Angiotensin II-Induced Hypertension. *Circ. Res.* **2019**, *124*, 727–736.

111. Siracusa, R.; Fusco, R.; Cuzzocrea, S. Astrocytes: Role and Functions in Brain Pathologies. *Front. Pharmacol.* **2019**, *10*, 1114.

112. Sofroniew, M.V.; Vinters, H.V. Astrocytes: biology and pathology. *Acta Neuropathologica* 2010, *119*, 7–35.

113. González-Reyes, R.E.; Nava-Mesa, M.O.; Vargas-Sánchez, K.; Ariza-Salamanca, D.; Mora-Muñoz, L. Involvement of Astrocytes in Alzheimer's Disease from a Neuroinflammatory and Oxidative Stress Perspective. *Frontiers in Molecular Neuroscience* 2017, *10*.

114. Michinaga, S.; Koyama, Y. Dual Roles of Astrocyte-Derived Factors in Regulation of Blood-Brain Barrier Function after Brain Damage. *Int. J. Mol. Sci.* **2019**, *20*, doi:10.3390/ijms20030571.

115. Csipo, T.; Lipecz, A.; Ashpole, N.M.; Balasubramanian, P.; Tarantini, S. Astrocyte senescence contributes to cognitive decline. *GeroScience* **2020**, *42*, 51.

116. Zenaro, E.; Piacentino, G.; Constantin, G. The blood-brain barrier in Alzheimer's disease. *Neurobiol. Dis.* **2017**, *107*, 41–56.

117. van de Haar, H.J.; Burgmans, S.; Jansen, J.F.A.; van Osch, M.J.P.; van Buchem, M.A.; Muller, M.; Hofman, P.A.M.; Verhey, F.R.J.; Backes, W.H. Blood-Brain Barrier Leakage in Patients with Early Alzheimer Disease. *Radiology* **2017**, *282*, 615.

118. Yarlagadda, A.; Alfson, E.; Clayton, A.H. The blood brain barrier and the role of cytokines in neuropsychiatry. *Psychiatry* **2009**, *6*, 18–22.

119. Pan, W.; Stone, K.P.; Hsuchou, H.; Manda, V.K.; Zhang, Y.; Kastin, A.J. Cytokine Signaling Modulates Blood-Brain Barrier Function. *Curr. Pharm. Des.* **2011**, *17*, 3729.

120. Hyvärinen, T.; Hagman, S.; Ristola, M.; Sukki, L.; Veijula, K.; Kreutzer, J.; Kallio, P.; Narkilahti, S. Co-stimulation with IL-1β and TNF-α induces an inflammatory reactive astrocyte phenotype with neurosupportive characteristics in a

human pluripotent stem cell model system. *Scientific Reports* 2019, *9*.

121. Wang, W.-Y.; Tan, M.-S.; Yu, J.-T.; Tan, L. Role of pro-inflammatory cytokines released from microglia in Alzheimer's disease. *Annals of Translational Medicine* **2015**, *3*, doi:10.3978/j.issn.2305-5839.2015.03.49.

122. Fakhoury, M. Microglia and Astrocytes in Alzheimer's Disease: Implications for Therapy. *Curr. Neuropharmacol.* **2018**, *16*, 508–518.

123. Consonni, A.; Morara, S.; Codazzi, F.; Grohovaz, F.; Zacchetti, D. Inhibition of lipopolysaccharide-induced microglia activation by calcitonin gene related peptide and adrenomedullin. *Mol. Cell. Neurosci.* **2011**, *48*, 151–160.

124. You, L.-H.; Yan, C.-Z.; Zheng, B.-J.; Ci, Y.-Z.; Chang, S.-Y.; Yu, P.; Gao, G.-F.; Li, H.-Y.; Dong, T.-Y.; Chang, Y.-Z. Astrocyte hepcidin is a key factor in LPS-induced neuronal apoptosis. *Cell Death Dis.* **2017**, *8*, e2676.

125. Ryu, K.-Y.; Lee, H.-J.; Woo, H.; Kang, R.-J.; Han, K.-M.; Park, H.; Lee, S.M.; Lee, J.-Y.; Jeong, Y.J.; Nam, H.-W.; et al. Dasatinib regulates LPS-induced microglial and astrocytic neuroinflammatory responses by inhibiting AKT/STAT3 signaling. *J. Neuroinflammation* **2019**, *16*, 190.

126. Specificity of gut microbiota in children with autism spectrum disorder in Slovakia and its correlation with astrocytes activity marker and specific behavioural patterns. *Physiol. Behav.* **2020**, *214*, 112745.

127. Liu, T.; Li, J.; Liu, Y.; Xiao, N.; Suo, H.; Xie, K.; Yang, C.; Wu, C. Short-Chain Fatty Acids Suppress Lipopolysaccharide-Induced Production of Nitric Oxide and Proinflammatory Cytokines Through Inhibition of NF-κB Pathway in RAW264.7 Cells. *Inflammation* **2012**, *35*, 1676–1684.

128. Zhang, Y.; Huang, R.; Cheng, M.; Wang, L.; Chao, J.; Li, J.; Zheng, P.; Xie, P.; Zhang, Z.; Yao, H. Gut microbiota from NLRP3-deficient mice ameliorates depressive-like behaviors by regulating astrocyte dysfunction via circHIPK2. *Microbiome* **2019**, *7*, 116.

129. Clark, R.I.; Salazar, A.; Yamada, R.; Fitz-Gibbon, S.; Morselli, M.; Alcaraz, J.; Rana, A.; Rera, M.; Pellegrini, M.; Ja, W.W.; et al. Distinct Shifts in Microbiota Composition during Drosophila Aging Impair Intestinal Function and Drive Mortality. *Cell Rep.* **2015**, *12*, 1656–1667.

130. Conley, M.N.; Wong, C.P.; Duyck, K.M.; Hord, N.; Ho, E.; Sharpton, T.J. Aging and serum MCP-1 are associated with gut microbiome composition in a murine model. *PeerJ* 2016, *4*, e1854.

131. Thevaranjan, N.; Puchta, A.; Schulz, C.; Naidoo, A.; Szamosi, J.C.; Verschoor, C.P.; Loukov, D.; Schenck, L.P.; Jury, J.; Foley, K.P.; et al. Age-Associated Microbial Dysbiosis Promotes Intestinal Permeability, Systemic Inflammation, and Macrophage Dysfunction. *Cell Host Microbe* **2017**, *21*, 455–466.e4.

132. Qin, L.; Wu, X.; Block, M.L.; Liu, Y.; Breese, G.R.; Hong, J.-S.; Knapp, D.J.; Crews, F.T. Systemic LPS causes chronic neuroinflammation and progressive neurodegeneration. *Glia* **2007**, *55*, 453–462.

133. Friedland, R.P.; Chapman, M.R. The role of microbial amyloid in neurodegeneration. *PLoS Pathog.* **2017**, *13*, e1006654.

134. Minter, M.R.; Zhang, C.; Leone, V.; Ringus, D.L.; Zhang, X.; Oyler-Castrillo, P.; Musch, M.W.; Liao, F.; Ward, J.F.; Holtzman, D.M.; et al. Antibiotic-

induced perturbations in gut microbial diversity influences neuro-inflammation and amyloidosis in a murine model of Alzheimer's disease. *Sci. Rep.* **2016**, *6*, 30028.

135. Wang, X.; Zhou, Y.; Ren, J.-J.; Hammer, N.D.; Chapman, M.R. Gatekeeper residues in the major curlin subunit modulate bacterial amyloid fiber biogenesis. *Proc. Natl. Acad. Sci. U. S. A.* **2010**, *107*, 163–168.

136. Chapman, M. P2-024: Protein misfolding done right: The biogenesis of bacterial amyloid fibers. *Alzheimer's & Dementia* 2006, *2*, S239–S239.

137. Andreasen, M.; Meisl, G.; Taylor, J.D.; Michaels, T.C.T.; Levin, A.; Otzen, D.E.; Chapman, M.R.; Dobson, C.M.; Matthews, S.J.; Knowles, T.P.J. Physical Determinants of Amyloid Assembly in Biofilm Formation. *MBio* **2019**, *10*, doi:10.1128/mBio.02279-18.

138. Biesecker, S.G.; Nicastro, L.K.; Wilson, R.P.; Tükel, Ç. The Functional Amyloid Curli Protects Escherichia coli against Complement-Mediated Bactericidal Activity. *Biomolecules* **2018**, *8*, doi:10.3390/biom8010005.

139. Lundmark, K.; Westermark, G.T.; Olsén, A.; Westermark, P. Protein fibrils in nature can enhance amyloid protein A amyloidosis in mice: Cross-seeding as a disease mechanism. *Proc. Natl. Acad. Sci. U. S. A.* **2005**, *102*, 6098–6102.

140. Zhou, Y.; Smith, D.; Leong, B.J.; Brännström, K.; Almqvist, F.; Chapman, M.R. Promiscuous cross-seeding between bacterial amyloids promotes interspecies biofilms. *J. Biol. Chem.* **2012**, *287*, 35092–35103.

141. Nishimori, J.H.; Newman, T.N.; Oppong, G.O.; Rapsinski, G.J.; Yen, J.-H.; Biesecker, S.G.; Wilson, R.P.; Butler, B.P.; Winter, M.G.; Tsolis, R.M.; et al. Microbial amyloids induce interleukin 17A (IL-17A) and IL-22 responses via Toll-like

receptor 2 activation in the intestinal mucosa. *Infect. Immun.* **2012**, *80*, 4398–4408.

142. Oppong, G.O.; Rapsinski, G.J.; Tursi, S.A.; Biesecker, S.G.; Klein-Szanto, A.J.; Goulian, M.; McCauley, C.; Healy, C.; Wilson, R.P.; Tükel, C. Biofilm-associated bacterial amyloids dampen inflammation in the gut: oral treatment with curli fibres reduces the severity of hapten-induced colitis in mice. *NPJ Biofilms Microbiomes* **2015**, *1*, doi:10.1038/npjbiofilms.2015.19.

143. Brown, G.C. The endotoxin hypothesis of neurodegeneration. *J. Neuroinflammation* **2019**, *16*, 180.

144. Banks, W.A.; Gray, A.M.; Erickson, M.A.; Salameh, T.S.; Damodarasamy, M.; Sheibani, N.; Meabon, J.S.; Wing, E.E.; Morofuji, Y.; Cook, D.G.; et al. Lipopolysaccharide-induced blood-brain barrier disruption: roles of cyclooxygenase, oxidative stress, neuroinflammation, and elements of the neurovascular unit. *J. Neuroinflammation* **2015**, *12*, 223.

145. Salguero, M.V.; Al-Obaide, M.A.I.; Singh, R.; Siepmann, T.; Vasylyeva, T.L. Dysbiosis of Gram-negative gut microbiota and the associated serum lipopolysaccharide exacerbates inflammation in type 2 diabetic patients with chronic kidney disease. *Exp. Ther. Med.* **2019**, *18*, 3461–3469.

146. Lukiw, W.J. Bacteroides fragilis Lipopolysaccharide and Inflammatory Signaling in Alzheimer's Disease. *Frontiers in Microbiology* 2016, *7*.

147. Daulatzai, M.A. Chronic functional bowel syndrome enhances gut-brain axis dysfunction, neuroinflammation, cognitive impairment, and vulnerability to dementia. *Neurochem. Res.* **2014**, *39*, 624–644.

148. Coquenlorge, S.; Duchalais, E.; Chevalier, J.; Cossais, F.; Rolli-

Derkinderen, M.; Neunlist, M. Modulation of lipopolysaccharide-induced neuronal response by activation of the enteric nervous system. *J. Neuroinflammation* **2014**, *11*, 202.

149. Maguire, M.; Maguire, G. Gut dysbiosis, leaky gut, and intestinal epithelial proliferation in neurological disorders: towards the development of a new therapeutic using amino acids, prebiotics, probiotics, and postbiotics. *Rev. Neurosci.* **2019**, *30*, 179–201.

150. Fiebich, B.L.; Batista, C.R.A.; Saliba, S.W.; Yousif, N.M.; de Oliveira, A.C.P. Role of Microglia TLRs in Neurodegeneration. *Front. Cell. Neurosci.* **2018**, *12*, 329.

151. Wang, L.-M.; Wu, Q.; Kirk, R.A.; Horn, K.P.; Ebada Salem, A.H.; Hoffman, J.M.; Yap, J.T.; Sonnen, J.A.; Towner, R.A.; Bozza, F.A.; et al. Lipopolysaccharide endotoxemia induces amyloid-β and p-tau formation in the rat brain. *Am. J. Nucl. Med. Mol. Imaging* **2018**, *8*, 86–99.

152. Zhan, X.; Stamova, B.; Sharp, F.R. Lipopolysaccharide Associates with Amyloid Plaques, Neurons and Oligodendrocytes in Alzheimer's Disease Brain: A Review. *Frontiers in Aging Neuroscience* 2018, *10*.

153. Sochocka, M.; Zwolińska, K.; Leszek, J. The Infectious Etiology of Alzheimer's Disease. *Curr. Neuropharmacol.* **2017**, *15*, 996.

154. Wang, X.-L.; Zeng, J.; Feng, J.; Tian, Y.-T.; Liu, Y.-J.; Qiu, M.; Yan, X.; Yang, Y.; Xiong, Y.; Zhang, Z.-H.; et al. Helicobacter pylori filtrate impairs spatial learning and memory in rats and increases β-amyloid by enhancing expression of presenilin-2. *Front. Aging Neurosci.* **2014**, *6*, 66.

155. Pisa, D.; Alonso, R.; Rábano, A.; Rodal, I.; Carrasco, L. Different Brain Regions are Infected with Fungi in Alzheimer's Disease. *Sci. Rep.* **2015**, *5*, 1–13.

156. Pisa, D.; Alonso, R.; Fernández-Fernández, A.M.; Rábano, A.; Carrasco, L. Polymicrobial Infections In Brain Tissue From Alzheimer's Disease Patients. *Sci. Rep.* **2017**, *7*, 1–14.

157. Bittar, A.; Sengupta, U.; Kayed, R. Prospects for strain-specific immunotherapy in Alzheimer's disease and tauopathies. *npj Vaccines* 2018, *3*.

158. Morgan, D. Immunotherapy for Alzheimer's Disease. *J. Intern. Med.* **2011**, *269*, 54.

159. Cytokine Inhibition for Treatment of Alzheimer's Disease Available online: http://www.medscape.com/viewarticle/530141 (accessed on Aug 28, 2020).

160. Mengel, D.; Röskam, S.; Neff, F.; Balakrishnan, K.; Deuster, O.; Gold, M.; Oertel, W.H.; Bacher, M.; Bach, J.-P.; Dodel, R. Naturally occurring autoantibodies interfere with β-amyloid metabolism and improve cognition in a transgenic mouse model of Alzheimer's disease 24 h after single treatment. *Translational Psychiatry* 2013, *3*, e236–e236.

161. Rosenberg, R.N.; Fu, M.; Lambracht-Washington, D. Active full-length DNA Aβ42 immunization in 3xTg-AD mice reduces not only amyloid deposition but also tau pathology. *Alzheimer's Research & Therapy* 2018, *10*.

162. McAlpine, F.E.; Lee, J.-K.; Harms, A.S.; Ruhn, K.A.; Blurton-Jones, M.; Hong, J.; Das, P.; Golde, T.E.; LaFerla, F.M.; Oddo, S.; et al. Inhibition of soluble TNF signaling in a mouse model of Alzheimer's disease prevents pre-plaque amyloid-associated neuropathology. *Neurobiology of Disease* 2009, *34*, 163–177.

163. Overk, C.; Masliah, E. Could changing the course of Alzheimer's disease pathology with immunotherapy prevent dementia? *Brain* 2019, *142*, 1853–1855.

164. Bostanciklioğlu, M. The role of gut microbiota in pathogenesis of Alzheimer's disease. *Journal of Applied Microbiology* 2019, *127*, 954–967.

165. Bonfili, L.; Cecarini, V.; Gogoi, O.; Berardi, S.; Scarpona, S.; Angeletti, M.; Rossi, G.; Eleuteri, A.M. Gut microbiota manipulation through probiotics oral administration restores glucose homeostasis in a mouse model of Alzheimer's disease. *Neurobiology of Aging* 2020, *87*, 35–43.

166. Hoffman, J.D.; Yanckello, L.M.; Chlipala, G.; Hammond, T.C.; McCulloch, S.D.; Parikh, I.; Sun, S.; Morganti, J.M.; Green, S.J.; Lin, A.-L. Dietary inulin alters the gut microbiome, enhances systemic metabolism and reduces neuroinflammation in an APOE4 mouse model. *PLOS ONE* 2019, *14*, e0221828.

167. Tamtaji, O.R.; Heidari-Soureshjani, R.; Mirhosseini, N.; Kouchaki, E.; Bahmani, F.; Aghadavod, E.; Tajabadi-Ebrahimi, M.; Asemi, Z. Probiotic and selenium co-supplementation, and the effects on clinical, metabolic and genetic status in Alzheimer's disease: A randomized, double-blind, controlled trial. *Clin. Nutr.* **2019**, *38*, 2569–2575.

168. Kobayashi, Y.; Kinoshita, T.; Matsumoto, A.; Yoshino, K.; Saito, I.; Xiao, J.-Z. Bifidobacterium Breve A1 Supplementation Improved Cognitive Decline in Older Adults with Mild Cognitive Impairment: An Open-Label, Single-Arm Study. *J Prev Alzheimers Dis* **2019**, *6*, 70–75.

169. Hazan, S. Rapid improvement in Alzheimer's disease symptoms following fecal microbiota transplantation: a case report. *Journal of International Medical*

Research 2020, *48*, 030006052092593.

170. Pistollato, F.; Battino, M. Role of plant-based diets in the prevention and regression of metabolic syndrome and neurodegenerative diseases. *Trends Food Sci. Technol.* **2014**, *40*, 62–81.

171. Mariotti, F. *Vegetarian and Plant-Based Diets in Health and Disease Prevention*; Academic Press, 2017; ISBN 9780128039694.

172. Anastasiou, C.A.; Yannakoulia, M.; Kosmidis, M.H.; Dardiotis, E.; Hadjigeorgiou, G.M.; Sakka, P.; Arampatzi, X.; Bougea, A.; Labropoulos, I.; Scarmeas, N. Mediterranean diet and cognitive health: Initial results from the Hellenic Longitudinal Investigation of Ageing and Diet. *PLoS One* **2017**, *12*, e0182048.

173. Pistollato, F.; Iglesias, R.C.; Ruiz, R.; Aparicio, S.; Crespo, J.; Lopez, L.D.; Manna, P.P.; Giampieri, F.; Battino, M. Nutritional patterns associated with the maintenance of neurocognitive functions and the risk of dementia and Alzheimer's disease: A focus on human studies. *Pharmacol. Res.* **2018**, *131*, 32–43.

174. Scarmeas, N.; Stern, Y.; Mayeux, R.; Manly, J.J.; Schupf, N.; Luchsinger, J.A. Mediterranean diet and mild cognitive impairment. *Arch. Neurol.* **2009**, *66*, 216–225.

175. Farooqui, T.; Farooqui, A.A. *Role of the Mediterranean Diet in the Brain and Neurodegenerative Diseases*; Academic Press, 2017; ISBN 9780128119600.

176. Tangney, C.C.; Li, H.; Wang, Y.; Barnes, L.; Schneider, J.A.; Bennett, D.A.; Morris, M.C. Relation of DASH- and Mediterranean-like dietary patterns to cognitive decline in older persons. *Neurology* 2014, *83*, 1410–1416.

177. McEvoy, C.T.; Guyer, H.; Langa, K.M.; Yaffe, K. Neuroprotective Diets Are Associated with Better Cognitive Function: The Health and Retirement Study. *J. Am. Geriatr. Soc.* **2017**, *65*, 1857–1862.

178. Terry, R.D.; Masliah, E.; Salmon, D.P.; Butters, N.; DeTeresa, R.; Hill, R.; Hansen, L.A.; Katzman, R. Physical basis of cognitive alterations in Alzheimer's disease: synapse loss is the major correlate of cognitive impairment. *Ann. Neurol.* **1991**, *30*, 572–580.

179. Cunnane, S.C.; Courchesne-Loyer, A.; St-Pierre, V.; Vandenberghe, C.; Pierotti, T.; Fortier, M.; Croteau, E.; Castellano, C.-A. Can ketones compensate for deteriorating brain glucose uptake during aging? Implications for the risk and treatment of Alzheimer's disease. *Ann. N. Y. Acad. Sci.* **2016**, *1367*, 12–20.

180. Owen, O.E.; Morgan, A.P.; Kemp, H.G.; Sullivan, J.M.; Herrera, M.G.; Cahill, G.F., Jr Brain metabolism during fasting. *J. Clin. Invest.* **1967**, *46*, 1589–1595.

181. Castellano, C.-A.; Nugent, S.; Paquet, N.; Tremblay, S.; Bocti, C.; Lacombe, G.; Imbeault, H.; Turcotte, É.; Fulop, T.; Cunnane, S.C. Lower brain 18F-fluorodeoxyglucose uptake but normal 11C-acetoacetate metabolism in mild Alzheimer's disease dementia. *J. Alzheimers. Dis.* **2015**, *43*, 1343–1353.

182. Ogawa, M.; Fukuyama, H.; Ouchi, Y.; Yamauchi, H.; Kimura, J. Altered energy metabolism in Alzheimer's disease. *J. Neurol. Sci.* **1996**, *139*, 78–82.

183. Henderson, S.T. Ketone bodies as a therapeutic for Alzheimer's disease. *Neurotherapeutics* **2008**, *5*, 470–480.

184. Kashiwaya, Y.; Bergman, C.; Lee, J.-H.; Wan, R.; King, M.T.; Mughal,

M.R.; Okun, E.; Clarke, K.; Mattson, M.P.; Veech, R.L. A ketone ester diet exhibits anxiolytic and cognition-sparing properties, and lessens amyloid and tau pathologies in a mouse model of Alzheimer's disease. *Neurobiol. Aging* **2013**, *34*, 1530–1539.

185. Włodarek, D. Role of Ketogenic Diets in Neurodegenerative Diseases (Alzheimer's Disease and Parkinson's Disease). *Nutrients* **2019**, *11*, doi:10.3390/nu11010169.

186. Murray, A.J.; Knight, N.S.; Cole, M.A.; Cochlin, L.E.; Carter, E.; Tchabanenko, K.; Pichulik, T.; Gulston, M.K.; Atherton, H.J.; Schroeder, M.A.; et al. Novel ketone diet enhances physical and cognitive performance. *FASEB J.* **2016**, *30*, 4021–4032.

187. Grammatikopoulou, M.G.; Goulis, D.G.; Gkiouras, K.; Theodoridis, X.; Gkouskou, K.K.; Evangeliou, A.; Dardiotis, E.; Bogdanos, D.P. To Keto or Not to Keto? A Systematic Review of Randomized Controlled Trials Assessing the Effects of Ketogenic Therapy on Alzheimer Disease. *Adv. Nutr.* **2020**, doi:10.1093/advances/nmaa073.

188. Ma, D.; Wang, A.C.; Parikh, I.; Green, S.J.; Hoffman, J.D.; Chlipala, G.; Murphy, M.P.; Sokola, B.S.; Bauer, B.; Hartz, A.M.S.; et al. Ketogenic diet enhances neurovascular function with altered gut microbiome in young healthy mice. *Sci. Rep.* **2018**, *8*, 6670.

189. Nagpal, R.; Neth, B.J.; Wang, S.; Craft, S.; Yadav, H. Modified Mediterranean-ketogenic diet modulates gut microbiome and short-chain fatty acids in association with Alzheimer's disease markers in subjects with mild cognitive

impairment. *EBioMedicine* **2019**, *47*, 529–542.

190. Neth, B.J.; Mintz, A.; Whitlow, C.; Jung, Y.; Solingapuram Sai, K.; Register, T.C.; Kellar, D.; Lockhart, S.N.; Hoscheidt, S.; Maldjian, J.; et al. Modified ketogenic diet is associated with improved cerebrospinal fluid biomarker profile, cerebral perfusion, and cerebral ketone body uptake in older adults at risk for Alzheimer's disease: a pilot study. *Neurobiol. Aging* **2020**, *86*, 54–63.

191. Li, X.; Leonardi, I.; Semon, A.; Doron, I.; Gao, I.H.; Putzel, G.G.; Kim, Y.; Kabata, H.; Artis, D.; Fiers, W.D.; et al. Response to Fungal Dysbiosis by Gut-Resident CX3CR1 Mononuclear Phagocytes Aggravates Allergic Airway Disease. *Cell Host Microbe* 2018, *24*, 847–856.e4.

192. Yatsunenko, T.; Rey, F.E.; Manary, M.J.; Trehan, I.; Dominguez-Bello, M.G.; Contreras, M.; Magris, M.; Hidalgo, G.; Baldassano, R.N.; Anokhin, A.P.; et al. Human gut microbiome viewed across age and geography. *Nature* **2012**, *486*, 222–227.

193. Rutayisire, E.; Huang, K.; Liu, Y.; Tao, F. The mode of delivery affects the diversity and colonization pattern of the gut microbiota during the first year of infants' life: a systematic review. *BMC Gastroenterol.* **2016**, *16*, 86.

194. Moise, A.M.R. *The Gut Microbiome: Exploring the Connection between Microbes, Diet, and Health*; ABC-CLIO, 2017; ISBN 9781440842658.

195. Lach, G.; Schellekens, H.; Dinan, T.G.; Cryan, J.F. Anxiety, Depression, and the Microbiome: A Role for Gut Peptides. *Neurotherapeutics* **2018**, *15*, 36–59.

196. Hasan, N.; Yang, H. Factors affecting the composition of the gut microbiota, and its modulation. *PeerJ* **2019**, *7*, e7502.

197. Kim, C.H.; Park, J.; Kim, M. Gut Microbiota-Derived Short-Chain Fatty Acids, T Cells, and Inflammation. *Immune Netw.* **2014**, *14*, 277.

CHAPTER 2: Predicting neurodegenerative disease using pre-pathology gut microbiota composition: a longitudinal study in mice modeling Alzheimer's disease pathologies

ABSTRACT

The gut microbiota-brain axis is suspected to contribute to the development of Alzheimer's Disease (AD), a neurodegenerative disease characterized by amyloid-β plaque deposition, neurofibrillary tangles, and neuroinflammation. To evaluate the role of the gut microbiota-brain axis in AD, we characterized the gut microbiota of triple transgenic (3xTg-AD) mice modeling amyloidosis and tauopathy, and wild type (WT) genetic controls (B6129F2/J) throughout development of AD pathologies. Fecal samples were collected fortnightly from 4 to 52 weeks, and the V4 region of the 16S rRNA gene was amplified and sequenced on an Illumina MiSeq. RNA was extracted from the colon and hippocampus, converted to cDNA, and used to measure immune gene expression using a RT-qPCR array. Bacterial taxonomy was classified using Greengenes. Diversity metrics were calculated using QIIME 2, and a Random Forest classifier was applied to predict bacterial features that are important in predicting mouse genotype. Gut microbiota were compositionally distinct early in life between 3xTg-AD mice and WT mice (Jaccard distance, PERMANOVA 8 weeks, p=0.001, 24 weeks, p=0.039, and 52 weeks, p=0.058). Using a Random Forest classifier, we demonstrate that mouse genotype was correctly predicted 95-100% using the fecal microbiome composition at the time point prior to development of disease pathologies. Finally, we demonstrate that *Bacteroides* species relative abundance increased over time in 3xTg-AD mice. Other taxa, such as *Turicibacter* and *Akkermansia,* increased in relative abundance in young 3xTg-AD mice, but decreased as mice reached 24 weeks of age. Only *Lactobacillus salivarius* was increased in relative abundance in WT mice compared to 3xTg-AD mice, potentially indicating a protective role for this taxon. Taken

together, we demonstrated that changes in features of the gut microbiota composition at pre-pathology timepoints are predictive of development of AD pathologies.

INTRODUCTION

The human microbiota, the aggregate of all bacterial, viral, fungal, and archaeal cells that inhabit the human body, consists of 1-1.5x more microbial cells than human cells (~10^{14}).[1] Niche-specific microbiota reside virtually across entire human body, including the skin, oral cavity, respiratory tracts, vaginal cavity, and the GI tract.[2] The gut microbiota, which makes up approximately 70% of the total microbial burden in the body,[3] contributes to a myriad of roles, including host immune regulation,[4] macronutrient metabolism,[5] and maintenance of overall health.[6] In healthy individuals, the gut microbiota tends to be highly diverse.[7] However, perturbations to the healthy gut microbiota caused by disease, aging, diet, or other environmental factors can lead to alterations in the composition or function of these communities. Alterations in a healthy gut microbiota are are associated with inflammation and chronic noncommunicable diseases such as obesity,[8] diabetes,[9] asthma,[10] and inflammatory bowel disease.[11,12,13] Recent studies of gut microbiota-associated effects of host health are beginning to demonstrate effects on extragastric organs, including neurological health and disease.[14–16]

The gut microbiota-brain axis is the bidirectional communication between the gut and brain through immune, nervous, metabolic, and endocrine signaling.[17] These collective mechanisms regulate a number of physiological processes, including gut motility and

permeability,[18] local and systemic inflammation,[19] and normal brain function.[20] Major perturbations to the gut microbiota-brain axis signaling is associated with diseases affecting the gastrointestinal tract, including Crohn's disease[21] and irritable bowel syndrome,[22] as well as the brain, including Parkinson's disease,[23] Alzheimer's disease (AD),[24] autism spectrum disorder,[25] and multiple sclerosis.[26]

Alzheimer's disease (AD) is an irreversible, neurodegenerative disease characterized by deposition of amyloid-β plaques and formation of neurofibrillary tangles in the brain, resulting in irreversible, progressive memory loss. Patients with AD experience cognitive decline, often accompanied with anger, depression, and personality changes. Unfortunately, once symptoms become apparent, the individual will continue to decline until they are unable to perform daily tasks and communicate, and the disease is ultimately fatal.[27] AD rates are rapidly increasing as our elderly population grows, with projections that cases will more than triple in the next 30 years.[28] With no cure, and few therapies available to slow the progression, understanding disease pathogenesis is critical in the timely development of effective therapies. Currently, the main targets of AD therapies are neurotransmitter receptors, secretase inhibitors, modulation of amyloidosis and tauopathy, and immunotherapy.[29] The Aβ-cascade hypothesis, which proposes neurotoxic Aβ plaques are the causative agent of AD, leading to the formation of neurofibrillary tangles, vascular damage, and dementia, has more recently been brought into question with increasing evidence against the long standing hypothesis.[30] Neuroinflammation has become a key research focus for AD, as it contributes to an increased rate of disease progression and severity.[31]

Neuroinflammation in AD is characterized by a complex set of pathways, including dysfunctional microglia and astrocytes. Microglia are the resident macrophages of the central nervous system, while astrocytes function to support neuronal synaptic function and maintain the integrity of the blood brain barrier (BBB).[32,33] Microglia clear soluble amyloid-β via macropinocytosis, however, in the insoluble, fibrillary form, microglia are unable to clear amyloid-β deposits at the rate they are forming, leading to accumulation of amyloid-β plaques.[34] The chronic neuroinflammation in AD is further characterized by pro-inflammatory biochemical processes, including the release of proinflammatory cytokines, mainly IL-1β, TNF-α, and IL-6.[35] With mounting evidence of the role of neuroinflammation in AD pathogenesis, identifying shifts in inflammatory biomarkers during disease progression is increasingly important for identifying mechanistic pathways in the gut microbiota-brain axis.

In this study, we characterized the gut microbiota fortnightly through 52 weeks of age in 3xTg-AD mice with mutations (APP(Swe), PSEN1(M146V), and MAPT(P301L)) associated with familial AD modeling amyloid-β plaques and hyperphosphorylated tau and their genetic background (B6129F2/J; wild type [WT]). The APP(Swe) mutation in the amyloid precursor protein increases total amyloid-β, while the PSEN1(M146V) mutation of the cleavage enzyme induces abnormal APP processing, resulting in increased Aβ plaque accumulation[36]. The third mutation of MAPT(P301L) accelerates the formation of neurofibrillary tangles.[37] In this preclinical model, cognitive deficits develop at 4 months, preceding plaque accumulation at 6 months, gliosis at 7 months,

and hyperphosphorylated tau at 12 months.[38,39] To our knowledge, this is the first study of its kind to characterize the gut microbiota composition of a transgenic AD murine model at 25 time points to identify key temporal patterns in the gut bacterial microbiome. Additionally, we compared changes in the gut microbiota composition to gene expression of key markers of inflammation using reverse transcriptase quantitative PCR (RT-qPCR). We hypothesized that alterations in the gut microbiome would correspond with key timepoints associated with emergence of amyloid-β plaques, hyperphosphorylated tau, and neuroinflammation.

RESULTS

Longitudinal analysis of gut microbiota composition and inflammatory gene expression in 3xTg-AD mice.

To explore shifts in gut microbial communities during disease progression, we used 16S rRNA gene sequencing to characterize fortnightly fecal samples from 4 weeks (post-weaning) to 52 weeks (amyloid-*β* plaques and hyperphosphorylated tau modeled) of age. Our cohort consisted of 57 3xTg-AD mice and 31 Wild Type (WT) mice, sacrificed at 8, 24, and 52 weeks (Fig. 1, n=88 mice, n=1,717 total fecal samples at 25 time points). Gene expression of AD-associated inflammatory biomarkers was assessed at 8, 24, and 52 weeks of age.

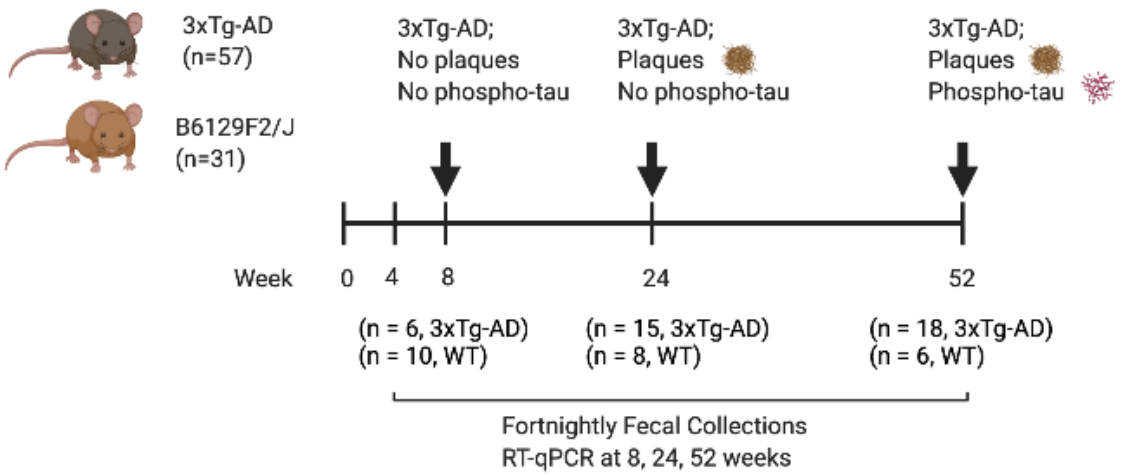

Figure 1. Longitudinal study design. Fecal sample collections from 3xTg-AD and WT mice began at 4 weeks of age and continued fortnightly until sacrifice at 8 weeks (pre-pathologies), 24 weeks (amyloidosis), and 52 weeks (amyloidosis and tauopathy). Image created using Biorender.com.

Inflammatory gene biomarkers in the hippocampus and colon

To assess severity of the inflammatory response in the colon and hippocampus of 3xTg-AD mice, we used a custom reverse transcriptase qPCR assay to evaluate 24 genes for AD-associated inflammatory biomarkers. Based on previous characterization of pathologies in the brain of 3xTg-AD mice, the hippocampus was selected for neuroinflammatory marker analysis.[40] Of the 19 genes assessed, seven were T_H1/T_H17 markers, three were astrogliosis markers, eight were microgliosis markers, one was a LPS-induced inflammation marker, and five were controls/housekeeping genes (Table S1). Fold change was calculated for hippocampus and colon samples from 8, 24, and 52 week old 3xTg-AD and WT mice using the $2^{-\Delta\Delta C_T}$ method. In the colon, gene expression of GFAP (astrogliosis marker) was increased in 3xTg-AD mice at 24 weeks

compared to 52 weeks (p=0.009, Mann-Whitney Fig. 2A), and *IL-6* was increased in 3xTg-AD mice at 52 weeks compared to WT mice at 52 weeks (p=0.049, Mann-Whitney, Fig. 2B). In the hippocampus, GFAP was increased in 52 week 3xTg-AD mice compared to 52 week WT mice (p=0.015, Mann-Whitney, Fig. 2C). Gene expression of Mrc1 (microgliosis marker) was also increased in the hippocampus of 3xTg-AD mice at 24 weeks compared to 52 weeks (p= 0.004 , Mann-Whitney, Fig. 2D).

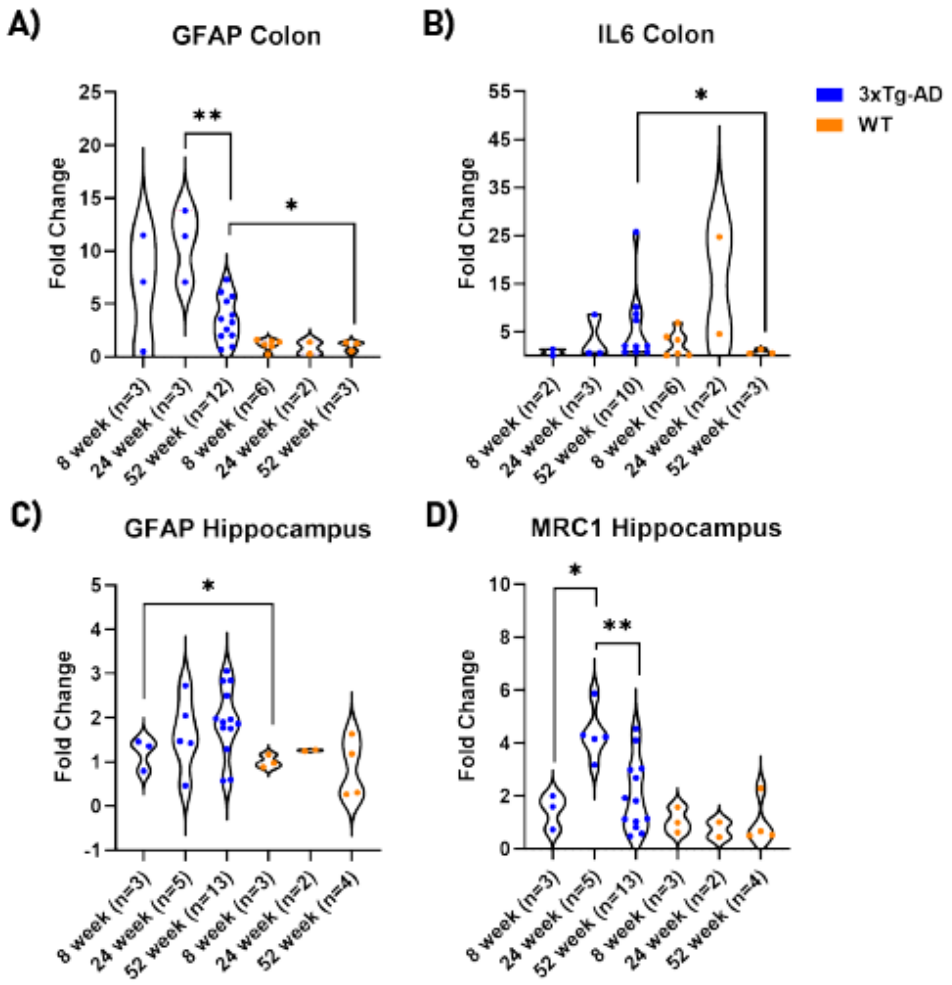

Figure 2. Relative gene expression of GFAP and IL-6 in the colon and GFAP and MRC1 in the hippocampus. Hippocampus and colon from 3xTg-AD and WT mice were collected at 8, 24, and 52 weeks. A) Gene expression of GFAP (astrogliosis marker) is significantly increased at 24 week 3xTg-AD mice compared to 52 week 3xTg-AD mice (p=0.009, Mann-Whitney) and increased in 52 week 3xTg-AD mice compared to 52

week WT mice (p=0.0484, Mann-Whitney). B) Gene expression of IL-6 is significantly increased in 52 week 3xTg-AD mice compared to 52 week WT mice (p=0.015, Mann-Whitney). C) Gene expression of GFAP (astrogliosis marker) is significantly increased at 52 week 3xTg-AD mice compared to 52 week WT (p=0.049, Mann-Whitney). D) Gene expression of Mrc1 (microgliosis marker) is significantly increased at 24 week 3xTg-AD mice compared to 52 week (p= 0.004 , Mann-Whitney) and 8 week 3xTg-AD mice (p= 0.0357, Mann-Whitney).

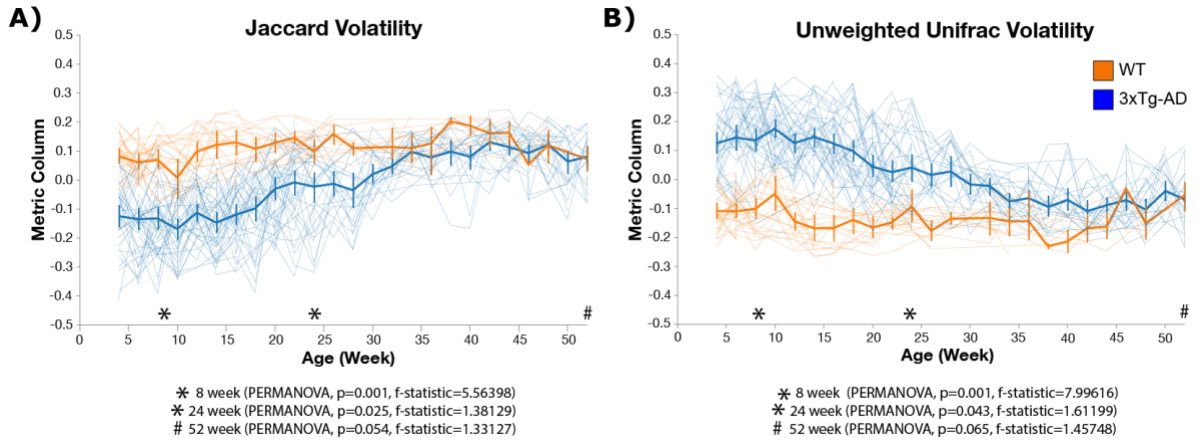

Figure 3. Volatility analysis of 3xTg-AD and WT mice from 4 to 52 weeks demonstrate distinct gut microbiota compositions in early life in 3xTg-AD mice compared to WT mice . A) Volatility plot of PCoA Axis 1 of the Jaccard dissimilarity index. This demonstrates differences in the gut microbiota until 32 weeks of age by strain. Thick lines represent the average change in the gut microbiota on PC1 over time in 3xTg-AD and WT mice, and thin lines represent changes in the gut microbiota on PC1 over time in individual mice. B) Volatility plot of PCoA Axis 1 of Unweighted Unifrac distance metric. This demonstrates differences in the gut microbiota until 42 weeks of age by strain. Thick lines represent the average change in the gut microbiota on PC1 over time in 3xTg-AD and WT mice, and thin lines represent changes in the gut microbiota on PC1 over time in individual mice.

3xTg-AD mice have a distinct gut microbiota composition prior to the development of AD-associated pathologies

Beta diversity (between-sample) metrics were used to identify compositional differences in the bacterial gut microbiota between 3xTg-AD and WT mice over time. We applied Jaccard and Unweighted Unifrac, which are unweighted (qualitative) beta diversity

metrics, and Bray-Curtis and Weighted Unifrac, which are weighted (quantitative) beta diversity metrics to our samples. Volatility analysis demonstrates a distinct gut microbiota composition for the first 30 weeks of age using Jaccard diversity (Fig. 3A) and 40 weeks using Unweighted Unifrac (Fig. 3B) in 3xTg-AD mice when compared to WT mice. As mice age, the composition of the gut microbiota becomes more similar between the strains of mice (Fig. 3, n=88 mice, n=1717 total fecal samples at 25 time points). To analyze the differences in composition at 8 weeks (baseline), 24 weeks (when amyloid plaques are present), and 52 weeks (amyloid plaques and hyperphosphorylated tau are present), a PCoA of Jaccard and Unweighted Unifrac distances were generated with PCoA 1 plotted against time, highlighting the key three timepoints. The gut microbiota composition was statistically distinct, using Jaccard and Unweighted Unifrac metrics, between 3xTg-AD and WT mice in early life, shown at 8 and 24 weeks. However, the gut microbiota composition became more similar at later time points, demonstrated at 52 weeks of age (Fig. S2A, (PERMANOVA, p=0.054, f-statistic=1.33127) and S2B, (PERMANOVA, p=0.065, f-statistic=1.45748)). Weighted beta diversity metrics show a similar, though less robust, pattern at the baseline and 24 week timepoints. Volatility analysis and PCoA of the Bray-Curtis dissimilarity metric demonstrates distinct gut microbiota compositions between 3xTg-AD and WT mice at 8 (PERMANOVA, p=0.001, f-statistic=10.1743) and 24 (PERMANOVA, p=0.016, f-statistic=1.98555) weeks of age, but not at 52 (PERMANOVA, p=0.508, f-statistic=0.90456) weeks of age (Fig. S3A, Fig. S3C). A PCoA of the Weighted Unifrac distance metric also demonstrates distinct gut microbiota compositions between 3xTg-AD and WT mice at 8 (PERMANOVA, p=0.03, f-statistic=3.10426), but not at 24

(PERMANOVA, p=0.566, f-statistic=0.717805) and 52 (PERMANOVA, p=0.066) weeks of age (Fig. S3B, Fig. S3D). Taken together, these results indicate qualitative (not weighted by abundance of taxa) metrics suggesting the strongest drivers of different microbial communities are the less abundant taxa in the murine gut microbiota.

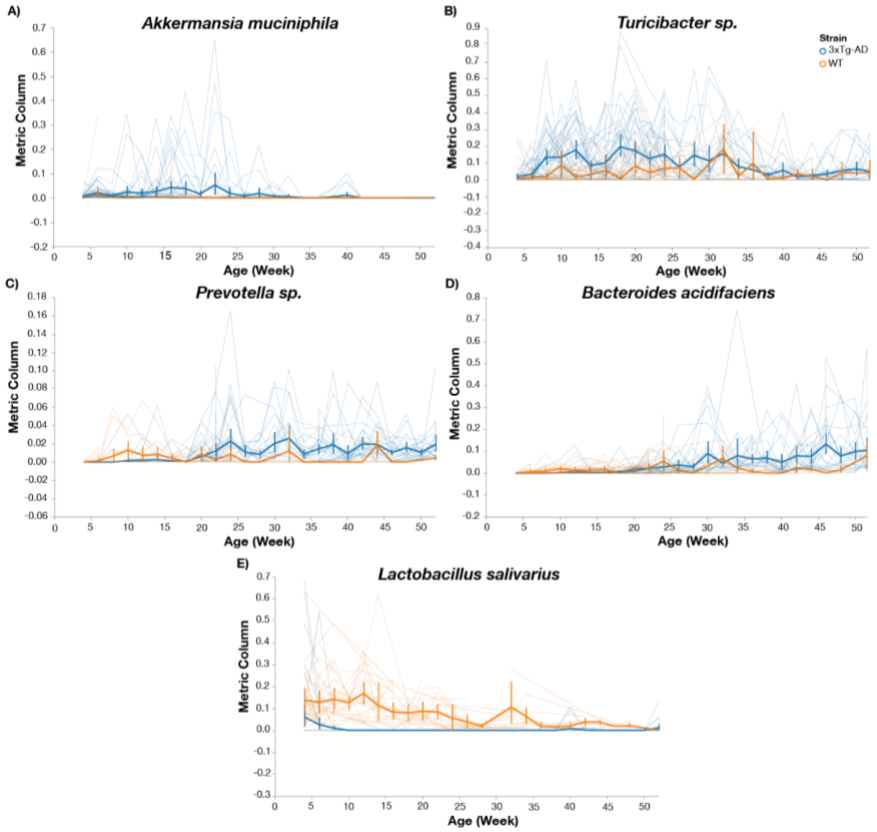

Figure 4. Feature volatility at species level. A) Feature volatility chart of *Akkermansia muciniphila* demonstrates presence early in life in 3xTg-AD mice while depleted in WT mice. B) Feature volatility chart of *Turicibacter sp.* demonstrates an increase in relative abundance in 3xTg-AD mice early in life compared to WT that decreases over time in both mouse strains. C) Feature volatility chart of *Prevotella sp.* demonstrates increasing abundance in 3xTg-AD mice after 20 weeks of age while relatively stable in WT mice. D) Feature volatility chart of *Bacteroides acidifaciens* demonstrates a stable increase in relative abundance in 3xTg-AD mice after 25 weeks of age. E) Feature volatility chart of *Lactobacillus salivarius* shows a depletion in 3xTg-AD mice compared to WT mice.

Bacterial features are differentially enriched in 3xTg-AD and WT mice over time

To identify the ASVs that are driving the differences in gut microbiota composition between 3xTg-AD and WT mice, feature volatility plots were produced using the QIIME 2 plug-in, q2-longitudinal. We identified five features collapsed at the species level. The longitudinal feature analysis demonstrates a temporal trend of increasing relative abundance of the genera *Akkermansia muciniphila* and *Turicibacter sp.* early in life while *Prevotella sp. and Bacteroides acidifaciens* increase after 24 weeks of age in 3xTg-AD mice. Further, the longitudinal feature analysis identified *Lactobacillus salivarius* as an ASV that is depleted in 3xTg-AD mice.

Differential abundance analysis of ASVs, using analysis of composition of microbiomes (ANCOM) run within individual weeks only to avoid the sample dependency issues inherent in longitudinal studies, revealed differential abundance of 59 ASVs between WT and 3xTg-AD mice at 8 weeks of age (Supplementary Table S2). At 8 weeks of age, *Akkermansia* (W=56) and *Turicibacter* (W=56) were differentially abundant ASVs enriched in 3xTg-AD mice, while *Bacteroides* (W=57), *Sutterella* (W=53), *Anaerostipes* (W=53) were enriched in WT mice. There were no differentially abundant taxa at 24 weeks, but at 52 weeks 23 taxa were differentially abundant (Supplementary Table S2).

Associations between bacterial microbiota and mouse genotype over time using Linear Mixed Effects and Random Forest machine learning

We applied a Linear Mixed Effects (LME) model to determine the relationship of genotype (as a fixed effect) on gut microbiome diversity and *Bacteroides acidifaciens*

abundance over time, leveraging the repeated measures for each mouse. When we performed pairwise comparisons at each timepoint, Faith's Phylogenetic Diversity, an alpha diversity metric, was not significantly different in 3xTg-AD mice at 8 weeks compared to WT mice at 8 weeks ($p = 0.098$, Wilcoxon Rank Sum), 3xTg-AD mice at 24 weeks compared to WT mice at 24 weeks ($p = 0.63$, Wilcoxon Rank Sum), and 3xTg-AD mice at 52 weeks compared to WT mice at 52 weeks (p-value = 0.17, Wilcoxon Rank Sum (Figure S1)). However, when we leveraged LME to analyze the effect of genotype on alpha diversity, Faith's PDl was significantly higher in the WT mice compared to the 3xTg-AD mice at baseline ($p < 0.001$), and was consistently higher over time ($p < 0.001$). To evaluate the effect of genotype on microbial composition over time, we used LME on the first principle coordinate axis (PC1) from a PCoA generated from the Jaccard dissimilarity metric. Gut microbial composition of 3xTg-AD mice was significantly distinct at baseline ($p < 0.001$) and there were significant differences over time ($p < 0.001$). Genotype did interact with time in modulating the gut microbiome, suggesting a possible impact of genotype on microbiome development ($p < 0.001$). Gut microbiome composition changed more drastically in 3xTg-AD mice from the baseline sample when compared to WT mice; the WT gut microbiome remained relatively stable over time. Finally, we wanted to determine whether there was a relationship between *Bacteroides acidifaciens* and genotype over time, since volatility analysis and ANCOM both demonstrated that this genus was enriched in 3xTg-AD mice. We applied LME to the relative abundance of *Bacteroides acidifaciens* using genotype as a fixed effect. We demonstrate that *B. acidifaciens* abundance was significantly different at baseline ($p < 0.001$) between 3xTg-AD and WT mice. Further, we demonstrate differences in *B.*

acidifaciens abundance by genotype ($p = 0.049$), and that there was a significant interaction between genotype and time ($p < 0.001$). These results demonstrate robust genotype-dependent changes in the gut microbiome over time.

We next used a Random Forest machine learning classifier to predict mouse genotype based on the bacterial features present in fecal samples. The Random Forest classifier was trained using 5 cross-fold cross validation on 80% of the samples and was then applied to the remaining 20% of samples to determine which taxa were most important in predicting mouse strain based on features of importance it identified in the training set. Feature tables were collapsed at genus level, species level, and combined with the feature table of ASV's prior to running Random Forest. We applied the Random Forest classifier on independent samples from the 8 week time point on all n=57 mice to determine if gut microbiota features accurately predict genotype, regardless of age. This time point was selected because it is prior to the onset of AD pathologies, and because there is an adequate sample size to perform Random Forest analysis. At 8 weeks of age, Random Forest accurately predicted 3xTg-AD mice 88.9% of the time, and WT mice 100% of the time, improving accuracy over baseline 1.4 fold (Table 1). Baseline accuracy is calculated by assuming every sample will be predicted as the metadata group with the largest n. Critically, these results demonstrate accurate prediction of genotype using a pre-pathology timepoint.

Table 1: Random Forest Sample Classifier Performed on 8 week old 3xTg-AD and WT mice.

Strain	Ages	Accuracy	Baseline Ratio	Accuracy Ratio
3xTg-AD	8 weeks	0.889	0.643	1.444
WT	8 weeks	1.000	0.643	1.444

DISCUSSION

Despite numerous studies investigating how the gut microbiota is altered in AD, both in human and murine models, few studies have extensively sampled longitudinally to identify the dynamic gut microbiota signatures in 3xTg-AD mice. Previous studies have shown that 3xTg-AD mice have a distinct bacterial signature compared to age-matched controls.[41–43] However, there are only two studies to our knowledge that investigate gut microbiota in 3xTg-AD mice at more than one time point; the authors evaluated the gut microbiome at two[42,44] and four[42,44] time points. In one study, the gut microbiota of 3xTg-AD and WT mice were assessed at 8, 12, 18, and 24 weeks.[44] They too demonstrate compositional differences that were highlighted at the 8 week timepoint, but the specific taxa that were depleted in the 3xTg-AD mice differed from our study. In the second study, the gut microbiota of 3xTg-AD and WT mice were assessed at 16 weeks and 24 weeks. They similarly demonstrate alterations in the gut microbiome prior to development of pathologies, but did not report taxonomic changes to the genus level.[42] Here, we assessed the temporal dynamics by dense longitudinal sampling of microbial communities in the gut of 3xTg-AD mice over the course of a year to better understand compositional changes that correlate with disease pathologies. Our study characterizes gut microbiota composition at 25 time points (n=1,717 total samples), with

multiple time points corresponding to pre-pathology development, plaque deposition, and one time point corresponding to plaque deposition and hyperphosphorylated tau. Several bacteria, including *Bacteroides acidifaciens*, *Prevotella sp.*, *Akkermansia muciniphila*, *Turicibacter sp*., and *Lactobacillus salivarius*, differed in relative abundance between 3xTg-AD and WT mice temporally. *Turicibacter sp*. and *Akkermansia muciniphila* were enriched in the gut microbiota in 3xTg-AD mice at early time points, preceding pathology development, while *Bacteroides acidifaciens and Prevotella sp.* were enriched in the gut microbiota of 3xTg-AD mice at later time points. Critically, these features in the gut microbiota were used to successfully predict strain of mice early on in life, showing potential for unique signatures in the gut microbiota composition to be used as a predictor of AD prior to pathology development.

Previous studies support that perturbations to the gut microbiota composition alter host immune responses, thereby shifting towards a proinflammatory environment in the colon and hippocampus.[45] To quantify changes in the inflammatory profile of 3xTg-AD mice, we assessed the expression of relevant neuroinflammatory and inflammatory genes at each body site. Significant increases in *TNF-α, IL-6, IL-1β, IFN-γ* gene expression via RT-qPCR on brain tissue have been observed in 3xTg-AD mice at 16 months of age.[46] In our study, we found significant upregulation of *IL-6* gene expression in the colon of 52 week 3xTg-AD mice when compared to 52 week WT mice, but no changes in *TNF-α, IL-1β, IFN-γ* were observed at 52 weeks of age. We also observed significant upregulation of glial fibrillary acidic protein (GFAP), a marker of astrogliosis, in the hippocampus and colon of 3xTg-AD mice at 52 weeks when compared to 52

week WT mice. Enteric glial cells (EGCs) are resident to the enteric nervous system, which aids in regulation of the gastrointestinal tract via modulation of immune and endocrine function.[47] EGCs resemble astrocytes in the brain in their morphology, ability to secrete cytokines, and their expression of glial fibrillary acidic protein. Increased gene expression of GFAP in the colon of rats 4 hours after intravenous LPS injection suggests that GFAP upregulation is a result of acute exposure to a systemic inflammatory environment.[47] Interestingly, GFAP has also been identified as a blood biomarker in AD patients and correlates with cognitive impairment.[48] These findings support our hypothesis that the GI tract and the brain are communicating via transport of chemical mediators in the bloodstream. Finally, MRC1 (also known as CD206) was elevated in the hippocampus at 24 weeks of age in 3xTg-AD mice, indicating microgliosis. We hypothesize that the upregulation of MRC1 at 24 weeks of age is associated with increased phagocytosis in response to the deposition of amyloid-β, which is documented at 6 months of age.[49]

In this study, we demonstrate distinct microbial compositions in 3xTg-AD mice prior to the development of AD pathologies. As mice aged, the gut microbiota of 3xTg-AD and WT mice became more similar. Unweighted metrics (Jaccard and Unweighted Unifrac) demonstrated significant differences at 8 and 24 weeks, but not at 52 weeks of age. We did observe significant differences using weighted beta diversity metrics (Bray Curtis and Weighted UniFrac) which account for abundance of observed features at 8 weeks, but not at 24 and 52 weeks. This indicates that lower abundance bacterial microbiota features are strong drivers of changes in gut microbiota composition. Similar findings of

compositional differences early in life were reported in female 3xTg-AD mice at 3 and 5 months of age when compared to B6129SF1/J mice.[42] Early-life gut microbiota composition perturbations in mice have been associated with aging-associated health and disease, including neurodegenerative diseases like AD.[50] Our findings indicate compositional differences in microbial communities, driven by rare taxa early in life, are present prior to amyloidosis and tauopathy development.

Alpha diversity is frequently used as a marker of disease status, and is decreased in several diseases associated with the gut-microbiota brain axis, including depression,[51] Autism Spectrum Disorder,[52] Parkinson's disease,[53] and in some studies, AD.[16,54] In humans, alpha diversity was reported to be decreased in elders with AD compared to age-matched healthy participants.[16] When we analyzed alpha diversity metrics by subsampling our data to include one mouse at each timepoint, we did not find significant differences. These findings align well with other studies that have been performed in mice. In one, no differences in alpha diversity were reported when comparing 3 and 5 month 3xTg-AD female mice[42] and in another, no differences in alpha diversity were reported in 8, 12, 18, and 24 week old 3xTg-AD male mice compared to age-matched WT mice.[44] However, when we leveraged dense longitudinal sampling using LME, we demonstrate that genotype has an effect on Faith's PD, where WT mice have a higher alpha diversity than 3xTg-AD mice. These findings suggest lower alpha diversity in 3xTg-AD mice may be a predictor of disease status when assessed during onset and progression of AD pathologies.

To identify key features of the gut microbiota composition that differentiate 3xTg-AD mice from WT mice, we used a Random Forest machine learning classifier on a feature table of the fecal microbiota. Our analysis demonstrated successful discrimination between 3xTg-AD and WT mice using gut microbiota compositions from 4 to 52 weeks of age, but prediction accuracy was improved when we included only samples from pre-pathology timepoints. We selected samples at 2 months of age (6 and 8 weeks) and 6 months of age (22 and 24 weeks) to increase sample size due to loss of samples during the sample classifier training. Several of the features that were most important for predicting strain were also significant in our other analyses, including *Lactobacillus sp., Lactobacillus salivarius, and Bacteroides sp*. The predictive power of these models indicates unique bacterial communities early in life and throughout life in 3xTg-AD mice modeling AD disease pathologies. Interestingly, Haran and colleagues were able to discriminate between elders with AD and elders with different types of dementia using a random forest model using strain-level features of the gut microbiome generated using shallow shotgun metagenomic sequencing.[55] Both *B. fragilis* and *B. vulgatus* were important features in classifying participants in their study. *Bacteroides* were also enriched in 3xTg-AD mice in our study. These findings suggest certain microbes identified in the cohort with AD in this study, including *Bacteroides sp.*, may play a mechanistic role in the key pathologies of AD. We are performing additional studies to evaluate the role of *Bacteroides* in AD progression.

We observed concordance in feature importance across our Random Forest classifier, longitudinal volatility analysis, and differential abundance testing (ANCOM). Analysis of

feature volatility revealed taxa at the bacterial genus- and species- level resolution that are predictive of age within each strain. *Akkermansia muciniphila*, a mucin-degrading bacteria associated with intestinal inflammation in mice, is present in 3xTg-AD early in life, but not in WT mice.[56] *Turicibacter sp.*, shown to be involved in intestinal serotonin production, is increased in 3xTg-AD mice early in life compared to WT mice.[57] *Prevotella sp.*, associated with reduction in short chain fatty acid production and intestinal inflammation in mice,[58] was increased later in life of 3xTg-AD mice. *Lactobacillus salivarius*, a bacteria shown to positively influence immune cell development, was present in greater relative abundance in WT mice for the first 32 weeks of life.[59] Taken together, these results indicate potential contributions from 3xTg-AD mice gut microbial communities in inflammatory processes and neurological health.

All three statistical approaches used in our study (ANCOM, Random Forest machine learning, and volatility analysis) demonstrated increased relative abundance in *Bacteroides* in 3xTg-AD mice. Notably, Random Forest identified the low abundance taxon, *Bacteroides acidifaciens,* as highly important in predicting mouse strain. Other species of *Bacteroides* have been implicated in health status and are likely key contributors to host-microbial interactions via the gut microbiome-brain axis. *Bacteroides fragilis* and *Bacteroides stercosis* function ecologically as keystone species, indicated by low relative abundance and disproportionately numerous interactions on microbial community dynamics.[60] *B. fragilis* can influence the gut microbiome-brain axis and reduce autism-like behaviors by modulating serum metabolites and GI inflammation.[61] *Bacteroides* were also increased in abundance in mice expressing a

variant of human APP (APPswe [Tg2576]) compared to control mice, and administration of *B. fragilis* promoted amyloid deposition in the APP/PS1 mice.[62] Another study, this time using 5xFAD mice, which model amyloidosis at an earlier time point than 3xTg-AD mice, demonstrated increased relative abundance of *Prevotella sp., Bacteroides acidifaciens,* and *Turicibacter sp.* in 5xFAD mice at 10 weeks of age. The 10 week time point in 5xFAD mice and the 24 week time point in 3xTg-AD mice (where we observed the first increase in *B. acidifaciens*) both represent development of amyloidosis in the respective models. This may indicate that changes in relative abundance of certain microbes is critical during the onset of amyloid-β exposure. These findings suggest the potential for amyloidosis to alter microbial communities in the gut of mice modeling AD amyloid-β plaques.

Bacteroides have also been observed as differentially abundant in human studies of AD, though the association with health or disease are conflicting. In one study of participants with AD and age-matched human controls, Vogt et al. demonstrated increased relative abundance of *Bacteroides* in patients with AD. Interestingly, this increase positively correlated with greater amyloid burden in the brain and CSF phospho-tau, indicating a greater disease burden.[16] In another study, Haran and colleagues also observed increased *Bacteroides* in patients with dementia compared to age-matched controls.[55] However, Zhuang et al. found that *Bacteroides* relative abundance decreased in patients with AD.[63] Taken together, these findings in humans support our findings in a mouse model, and suggests a role for gut-associated *Bacteroides* in progression of AD pathologies.

Mechanistically, species in the genus *Bacteroides* might influence neuroinflammatory processes in the brain. *Bacteroides fragilis* produces an endotoxin, lipopolysaccharide, that is unique to the species of Gram-negative bacteria (BF-LPS). BF-LPS may cross the gut epithelium and enter the bloodstream, inducing systemic inflammation and upregulation of pro-inflammatory cytokines via the NF-κB pathway.[64] BF-LPS is recognized by TLR-2, TLR-4, and CD41 microglial cells, potentially inciting microgliosis in the brain. We are currently investigating the role of *B. acidifaciens* in the ecology of the gut microbiota and hypothesize that it may also function as a keystone species and influence neurological health status through the gut microbiome-brain axis.

The complexity of the host-microbe interactions in 3xTg-AD mice was demonstrated in this study by the dynamic microbial communities and immune profiles. Our study characterized the gut microbiota temporally in 3xTg-AD mice modeling amyloid-β plaques and hyperphosphorylated tau to identify key changes in composition correlated with disease pathogenesis. The present study shows upregulation of biomarkers for microgliosis, astrogliosis, and intestinal inflammation. Analysis of the gut microbiome demonstrated an altered gut microbiota composition associated with 3xTg-AD early in life, including prior to pathology development, that is predictive of disease state. This is the first study of its kind to characterize the gut microbiota at 25 time points, ranging from pre-pathology to modeling of both amyloidosis and tauopathy. Additionally, it will provide a reference for future studies to determine frequency of fecal sampling in longitudinal gut microbiota analysis based on the well characterized evolving gut

microbiota composition in the present study. It is critical for future studies on the role of the gut microbiota-brain axis and AD to investigate multiple time points throughout disease progression due to changes in the gut microbiome and inflammatory profile as exemplified in the current study. Furthermore, focus on the functional microbiome through a multi-omics approach is essential in better understanding host - microbe interactions via the gut microbiota-brain axis in AD.

METHODS

Mouse Genotypes: 3xTg-AD (with overexpression of APP(Swe), PSEN1(M146V), and MAPT(P301L) transgenes) and Wild Type (B6129F2/J; WT) breeders were purchased from Jackson Laboratory (Bar Harbor, Maine). All mice included in this study were bred in-house at the Biological Sciences Vivarium at Northern Arizona University.

Mouse colonies: All mouse experiments were approved by the Institutional Animal Use and Care Committee of Northern Arizona University under protocol 18-016. Mice were purchased from Jackson Laboratory (3xTg-AD, WT), and allowed seven days to acclimate to the Animal Facility at Northern Arizona University. Mice were then combined into harems, housed in a 12 hour light/dark cycle, and provided food and water *ad libitum*. In-house bred mice were weaned at 21 days of age and female mice of the same strain were separated and housed in cages of three to five mice for the remainder of the animal study (n=88 total mice, n=57 3xTg-AD, n=31 WT). Weaned female mice were given one week to acclimate and adjust to their new food prior to the first sample collection.

Genotyping: Ear punches were collected at 4 weeks from 3xTg-AD mice for genotyping. DNA was extracted using the Qiagen Blood and Tissue kit (Qiagen, Hilden, Germany). PCR was run with the KAPA mouse genotyping kit and Jackson Laboratory approved primers for APPSwe and P301L transgenes. Amplicons were run on a 3% agarose gel to confirm the presence of bands representing APP(Swe) and MAPT(P301L) genes (ThermoFisher, Waltham, Massachusetts).

RT-qPCR: DNA and RNA were extracted in parallel from hippocampus and colon tissue samples using the Qiagen AllPrep kit. We performed gDNA clean ups on RNA using the Qiagen DNase Max kit . RNA was reverse transcribed using the Qiagen 2nd Strand Synthesis Kit (Qiagen, Hilden, Germany). A custom qPCR assay from Qiagen including various biomarkers for Th1/Th17 (*il2, il1beta, il-6, il-8, ifn-gamma, tnf-alpha, il17a*), astrocyte reactivity (*GFAP, STAT3, vimentin*), M1/M2 macrophage activation/microgliosis (*ccl2*, *il1β, il4, arg1, iNOS, cd206, il-10,* and *il-12*),[65,66] and LPS-induced neuroinflammation (NF-κB) were used.

Sample collection: Fecal samples were collected directly from each mouse fortnightly starting at 4 weeks until sacrifice for longitudinal gut microbiota analysis. Mice were euthanized with CO_2 at 8, 24, or 52 weeks. Gastrointestinal and brain samples were collected in a sterile Class II Biosafety Cabinet using sterile tools for each body site and mouse. Sample sizes are as follows; 3xTg-AD (n = 6 at 8 weeks, n = 15 at 24 weeks, n = 18 at 52 weeks) and WT (n = 10 at 8 weeks, n = 8 at 24 weeks, and n = 6 at 52

weeks). Colon and hippocampus were harvested, immediately placed in RNAlater and were stored at −80 °C until further processing.

Nucleic Acid Extraction and 16S rRNA gene sequencing: DNA and RNA were extracted in parallel from feces using the MagMAX Pathogen RNA/DNA Kit from ThermoFisher. Extractions were performed in a Class II Biosafety Cabinet using protocols adopted from eukaryotic cell culture to protect the samples from contamination (i.e., decontaminate all materials with 70% EtOH to bring into the BSC, double glove while in the BSC, and don single use PPE while working in the BSC). Modifications to the protocol include the use of Lysing Matrix E tubes (MP Biomedical, Irvine, California) for bacterial and fungal lysis. Both DNA and RNA were quantified using a NanoDrop 2000. Quantified DNA from fecal samples was used for 16S rRNA gene PCR. Using Earth Microbiome Project (EMP) primers (515F-806R), the V4 region of the 16S rRNA gene was amplified. Each PCR reaction contained 2.5 µl of PCR buffer (TaKaRa, 10x concentration, 1x final), 1 µl of the Golay barcode tagged forward primer (10 µM concentration, 0.4 µM final), 1 µl of bovine serum albumin (Thermofisher, 20 mg/mL concentration, 0.56 mg/µl final), 2 µl of dNTP mix (TaKaRa, 2.5 mM concentration, 200 µM final), 0.125 µl of HotStart ExTaq (TaKaRa, 5 U/µl, 0.625 U/µl final), 1 µL reverse primer (10 µM concentration, 0.4µM final), and 1 µL of template DNA. All PCR reactions were filled to a total 25 µL with UltraPure DNase, Rnase free water (Invitrogen), then placed on a ThermalCycler. ThermalCycler conditions were as follows, 98°C denaturing step for 2 minutes, 30 cycles of 98°C for 20 seconds, 50°C for 30 seconds, and 72°C for 45 seconds, a final step of 72°C for 10 minutes. PCR was

performed in a decontaminated PCR hood and consumables were decontaminated with 70% ethanol to bring into the hood, then exposed to UV light to prevent sample contamination. PCR was performed in triplicate and an additional negative control was included for each barcoded primer. 16S rRNA gene bands were visualized using a 3% agarose gel (ThermoFisher, Waltham, Massachusetts). Amplicons were quantified using fluorometry and pooled at equimolar ratios. Quality of the pool was assessed with the Bioanalyzer DNA 1000 chip (Agilent Technologies, Santa Clara, California) then combined with 1% PhiX for sequencing. A total of 4 pools were sequenced on the Illumina MiSeq using the 600-cycle MiSeq Reagent Kit V3 (Illumina, San Diego, California). Each pool contained mock communities and samples that overlapped over each sequencing run to identify potential sequencing bias. All sequencing was done on the Illumina MiSeq benchtop sequencing platform.

Bioinformatics Analysis: Microbiome bioinformatics were performed with QIIME 2 version 2021.2. A manifest of all commands used can be found in the supplemental information (Supplemental File 1). q2-DADA2 was used for sequence quality control and generation of amplicon sequence variants (ASVs) to provide the highest taxonomic specificity.[67] A phylogenetic tree was created using q2-fragment-insertion, which applies the SEPP algorithm, inserting short sequences into a reliable tree generated from a database of full-length sequences.[68] Taxonomy was assigned to reads using q2-feature-classifier and the Greengenes reference database, version 13_8.[68,69] Alpha diversity, including Faith's Phylogenetic Diversity,[70] Shannon Diversity Index,[71] and Observed ASVs were computed with q2-diversity[70]. Beta diversity (community dissimilarity)

metrics were computed with q2-diversity, including Bray-Curtis dissimilarity, Jaccard dissimilarity, weighted UniFrac,[70,72] and unweighted UniFrac[73] distances. Longitudinal analysis was performed with q2-longitudinal to assess temporal changes in bacterial communities.[74] Group comparisons of alpha diversity were performed with non-parametric Wilcoxon tests, and group comparisons of beta diversity were performed with non-parametric PERMANOVA[75]. ASVs and taxa that were differentially abundant across mouse strains were identified using ANCOM.[76] All P-values were corrected for multiple comparisons using the Benjamini-Hochberg False Discovery Rate correction. The Random Forest model sample classification was performed to predict mouse genotype using gut microbiome ASVs with q2-sample classifier.[77]

Statistical Analysis: Fold changes were calculated using $2^{-\Delta\Delta C_T}$.[78] Group comparisons of strain-age were performed with non-parametric Mann-Whitney. Violin plots were created using Prism-GraphPad version 9.1.1 (225).

Data availability. All raw sequence files and metadata can be accessed on NCBI's Sequence Read Archive under Project [to be provided upon acceptance].

Table S1: qPCR gene biomarkers included in the custom RT-qPCR assay

Marker types	**Genes**
Th1/Th17	*il2*, *il1beta, il-6, il-8, ifn-gamma, tnf-alpha, il17a*
astrocyte reactivity	*GFAP, STAT3, vimentin*
M1/M2 macrophage activation/microgliosis	*ccl2*, *il1β, il4, arg1, iNOS, cd206, il-10,* and *il-12*
LPS-induced neuroinflammation	NF-kB

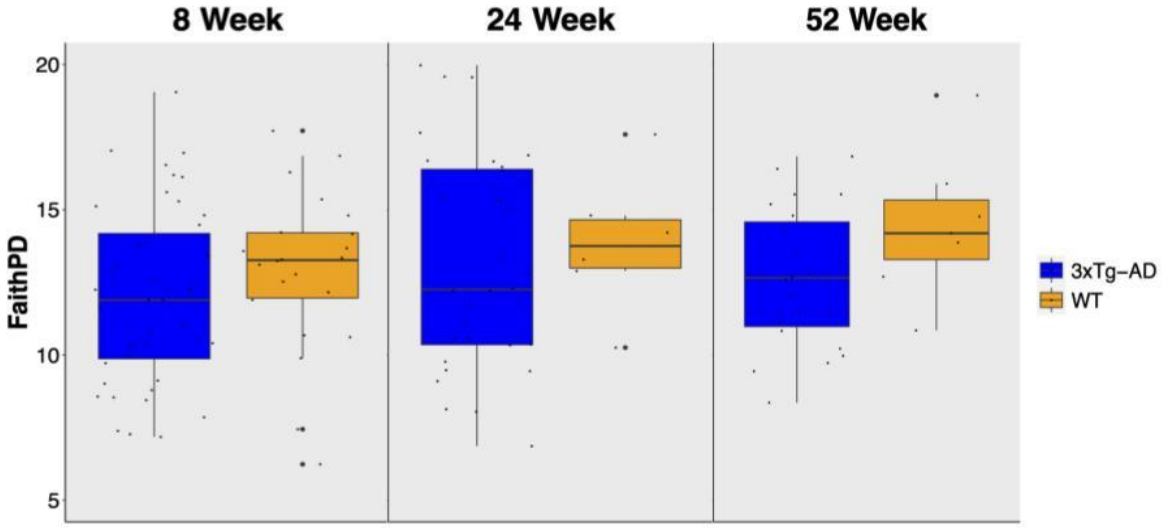

Figure S1: Faith's Phylogenetic Diversity in 8, 24, and 52 week 3xTg-AD and WT mice. 3xTg-AD mice demonstrate a non-significant trend towards lower Faith's Phylogenetic Diversity. A) 3xTg-AD and WT mice at 8 weeks (p-value = 0.098, Wilcoxon) B) 3xTg-AD and WT mice at 24 weeks (p-value = 0.63, Wilcoxon) C) 3xTg-AD and WT mice at 52 weeks (p-value = 0.17, Wilcoxon)

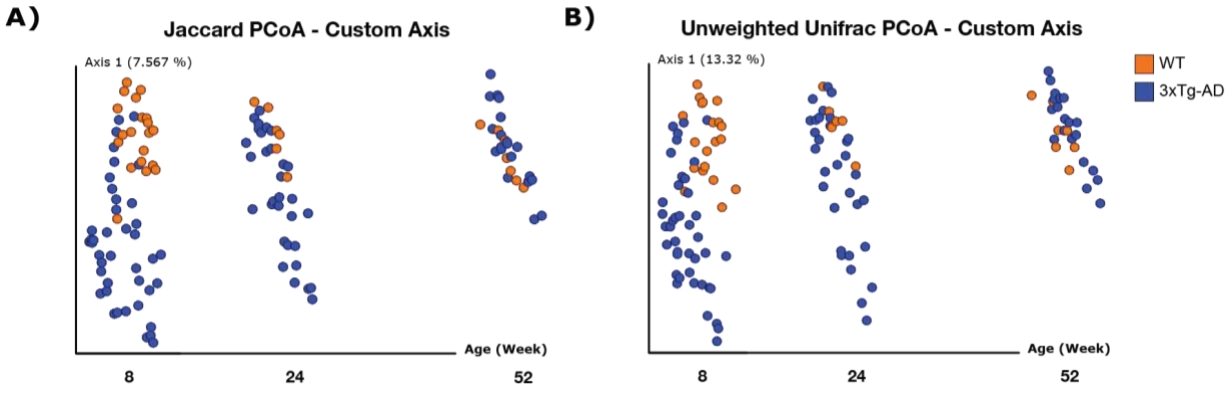

Figure S2: Jaccard dissimilarity metric and Unweighted Unifrac PCoA 1 plotted against time of 3xTg-AD and WT mice from 4 to 52 weeks demonstrate distinct gut microbiota compositions in early life in 3xTg-AD mice compared to WT mice. A) PCoA of Jaccard

dissimilarity metric, with key timepoints in pathology progression plotted as a PCoA 1 plotted against time (baseline: 8 weeks, amyloidosis: 24 weeks, tauopathy: 52 weeks). This demonstrates distinct gut microbiota compositions between 3xTg-AD and WT mice at 8 (PERMANOVA, p=0.001, f-statistic=5.56398) and 24 (PERMANOVA, p=0.025, f-statistic=1.38129) weeks of age, but not at 52 (PERMANOVA, p=0.054, f-statistic=1.33127) weeks of age B) PCoA of Unweighted UniFrac distance metric, with key timepoints in pathology progression plotted as a PCoA 1 plotted against time. This demonstrates distinct gut microbiota compositions between 3xTg-AD and WT mice at 8 (PERMANOVA, p=0.001, f-statistic=7.99616) and 24 (PERMANOVA, p=0.043, f-statistic=1.61199) weeks of age, but not at 52 (PERMANOVA, p=0.065, f-statistic=1.45748) weeks of age.

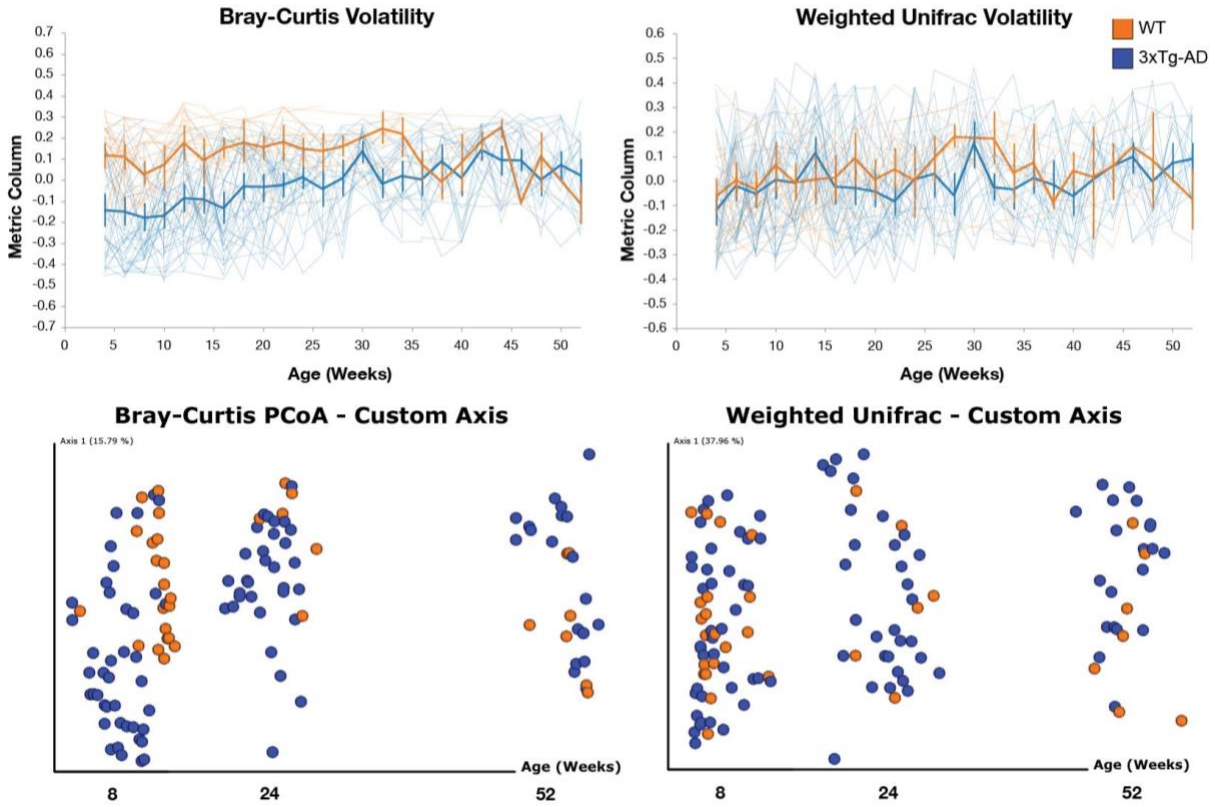

Figure S3: Beta-diversity metrics of 3xTg-AD and WT mice from 4 to 52 weeks of age and at 8, 24, and 52 weeks when comparing mouse strain. A) Bray-Curtis Axis 1 Volatility Plot from 4 to 52 weeks of age shows distinct gut microbiota compositions of 3xTg-AD and WT mice until 24 weeks of age. B) Weighted Unifrac Axis 1 Volatility Plot from 4 to 52 weeks of age. C) Bray-Curtis PCoA 1 plotted against time demonstrates distinct gut microbiota compositions between 3xTg-AD and WT mice at 8 (PERMANOVA, p=0.001, f-statistic=10.1743) and 24 (PERMANOVA, p=0.016, f-statistic=1.98555) weeks of age, but not at 52 (PERMANOVA, p=0.508, f-statistic=0.90456) weeks of age. D) Weighted Unifrac PCoA 1 plotted against time demonstrates distinct gut microbiota compositions between 3xTg-AD and WT mice at 8 (PERMANOVA, p=0.03, f-statistic=3.10426) , but not at 24 (PERMANOVA, p=0.566, f-

statistic=0.717805) and 52 (PERMANOVA, p=0.066) weeks of age.

Table S2: Differential abundance between 3xTg-AD and WT mice using Analysis of Composition of Microbiomes (ANCOM) at 8 weeks of age collapsed at genus level. W represents the number of features that the taxa is more abundant than.

Features Collapsed at Genus Level	W	Week
Bacteroides	57	8
Akkermansia	56	8
Turicibacter	56	8
Sutterella	53	8
Anaerostipes	53	8
F. Coriobacteriaceae	11	52
F. Mogibacteriaceae	9	52
Adlecreutzia	7	52
O. RF39	6	52
Prevotella	6	52
F. Erysipelotrichaceae	6	52
O. Streptophyta	6	52
Clostridium	5	52
Akkermansia	5	52

Bacillus	5	52

REFERENCES

1. Thursby, E. & Juge, N. Introduction to the human gut microbiota. *Biochemical Journal* vol. 474 1823–1836 (2017).
2. Kho, Z. Y. & Lal, S. K. The Human Gut Microbiome – A Potential Controller of Wellness and Disease. *Frontiers in Microbiology* vol. 9 (2018).
3. Mariat, D. *et al.* The Firmicutes/Bacteroidetes ratio of the human microbiota changes with age. *BMC Microbiol.* **9**, 123 (2009).
4. Lathrop, S. K. *et al.* Peripheral education of the immune system by colonic commensal microbiota. *Nature* **478**, 250–254 (2011).
5. Oliphant, K. & Allen-Vercoe, E. Macronutrient metabolism by the human gut microbiome: major fermentation by-products and their impact on host health. *Microbiome* **7**, 91 (2019).
6. Jandhyala, S. M. Role of the normal gut microbiota. *World Journal of Gastroenterology* vol. 21 8787 (2015).
7. McDonald, D. *et al.* American Gut: an Open Platform for Citizen Science Microbiome Research. *mSystems* **3**, (2018).
8. Turnbaugh, P. J. *et al.* An obesity-associated gut microbiome with increased capacity for energy harvest. *Nature* **444**, 1027–1031 (2006).
9. Alkanani, A. K. *et al.* Alterations in Intestinal Microbiota Correlate With Susceptibility to Type 1 Diabetes. *Diabetes* **64**, 3510–3520 (2015).

10. Teo, S. M. *et al.* The infant nasopharyngeal microbiome impacts severity of lower respiratory infection and risk of asthma development. *Cell Host Microbe* **17**, 704–715 (2015).

11. Rinninella, E. *et al.* What is the Healthy Gut Microbiota Composition? A Changing Ecosystem across Age, Environment, Diet, and Diseases. *Microorganisms* **7**, (2019).

12. Xu, C., Zhu, H. & Qiu, P. Aging progression of human gut microbiota. *BMC Microbiol.* **19**, 236 (2019).

13. Greenblum, S., Turnbaugh, P. J. & Borenstein, E. Metagenomic systems biology of the human gut microbiome reveals topological shifts associated with obesity and inflammatory bowel disease. *Proc. Natl. Acad. Sci. U. S. A.* **109**, 594–599 (2012).

14. Kang, D.-W. *et al.* Long-term benefit of Microbiota Transfer Therapy on autism symptoms and gut microbiota. *Sci. Rep.* **9**, 5821 (2019).

15. Hill-Burns, E. M. *et al.* Parkinson's disease and Parkinson's disease medications have distinct signatures of the gut microbiome. *Mov. Disord.* **32**, 739–749 (2017).

16. Vogt, N. M. *et al.* Gut microbiome alterations in Alzheimer's disease. *Sci. Rep.* **7**, (2017).

17. Martin, C. R., Osadchiy, V., Kalani, A. & Mayer, E. A. The Brain-Gut-Microbiome Axis. *Cell Mol Gastroenterol Hepatol* **6**, 133–148 (2018).

18. Carabotti, M., Scirocco, A., Maselli, M. A. & Severi, C. The gut-brain axis: interactions between enteric microbiota, central and enteric nervous systems. *Ann.*

Gastroenterol. Hepatol. **28**, 203–209 (2015).

19. Sochocka, M. *et al.* The Gut Microbiome Alterations and Inflammation-Driven Pathogenesis of Alzheimer's Disease—a Critical Review. *Molecular Neurobiology* vol. 56 1841–1851 (2019).

20. Sudo, N. Role of gut microbiota in brain function and stress-related pathology. *Biosci Microbiota Food Health* **38**, 75–80 (2019).

21. Collins, S. M. Interrogating the Gut-Brain Axis in the Context of Inflammatory Bowel Disease: A Translational Approach. *Inflamm. Bowel Dis.* **26**, 493–501 (2020).

22. Sinagra, E. *et al.* Microbiota-gut-brain axis and its affect inflammatory bowel disease: Pathophysiological concepts and insights for clinicians. *World J Clin Cases* **8**, 1013–1025 (2020).

23. Bullich, C., Keshavarzian, A., Garssen, J., Kraneveld, A. & Perez-Pardo, P. Gut Vibes in Parkinson's Disease: The Microbiota-Gut-Brain Axis. *Movement Disorders Clinical Practice* vol. 6 639–651 (2019).

24. Kowalski, K. & Mulak, A. Brain-Gut-Microbiota Axis in Alzheimer's Disease. *Journal of Neurogastroenterology and Motility* vol. 25 48–60 (2019).

25. Srikantha, P. & Mohajeri, M. H. The Possible Role of the Microbiota-Gut-Brain-Axis in Autism Spectrum Disorder. *Int. J. Mol. Sci.* **20**, (2019).

26. Camara-Lemarroy, C. R., Metz, L. M. & Yong, V. W. Focus on the gut-brain axis: Multiple sclerosis, the intestinal barrier and the microbiome. *World J. Gastroenterol.* **24**, 4217–4223 (2018).

27. Li, X.-L., Hu, N., Tan, M.-S., Yu, J.-T. & Tan, L. Behavioral and

psychological symptoms in Alzheimer's disease. *Biomed Res. Int.* **2014**, 927804 (2014).

28. 2020 Alzheimer's disease facts and figures. *Alzheimers. Dement.* (2020) doi:10.1002/alz.12068.

29. Elmaleh, D. R. *et al.* Developing Effective Alzheimer's Disease Therapies: Clinical Experience and Future Directions. *Journal of Alzheimer's Disease* vol. 71 715–732 (2019).

30. Ricciarelli, R. & Fedele, E. The Amyloid Cascade Hypothesis in Alzheimer's Disease: It's Time to Change Our Mind. *Current Neuropharmacology* vol. 15 (2017).

31. Kinney, J. W. *et al.* Inflammation as a central mechanism in Alzheimer's disease. *Alzheimers. Dement.* **4**, 575–590 (2018).

32. Hemonnot, A.-L., Hua, J., Ulmann, L. & Hirbec, H. Microglia in Alzheimer Disease: Well-Known Targets and New Opportunities. *Front. Aging Neurosci.* **11**, 233 (2019).

33. González-Reyes, R. E., Nava-Mesa, M. O., Vargas-Sánchez, K., Ariza-Salamanca, D. & Mora-Muñoz, L. Involvement of Astrocytes in Alzheimer's Disease from a Neuroinflammatory and Oxidative Stress Perspective. *Frontiers in Molecular Neuroscience* vol. 10 (2017).

34. C. Y. Daniel Lee, G. E. L. The role of microglia in amyloid clearance from the AD brain. *J. Neural Transm.* **117**, 949 (2010).

35. Cerovic, M., Forloni, G. & Balducci, C. Neuroinflammation and the Gut Microbiota: Possible Alternative Therapeutic Targets to Counteract Alzheimer's

Disease? *Front. Aging Neurosci.* **11**, (2019).

36. Scheuner, D. *et al.* Secreted amyloid β–protein similar to that in the senile plaques of Alzheimer's disease is increased in vivo by the presenilin 1 and 2 and APP mutations linked to familial Alzheimer's disease. *Nature Medicine* vol. 2 864–870 (1996).

37. Barghorn, S. *et al.* Structure, microtubule interactions, and paired helical filament aggregation by tau mutants of frontotemporal dementias. *Biochemistry* **39**, 11714–11721 (2000).

38. Triple-Transgenic Model of Alzheimer's Disease with Plaques and Tangles: Intracellular Aβ and Synaptic Dysfunction. *Neuron* **39**, 409–421 (2003).

39. Caruso, D. *et al.* Age-related changes in neuroactive steroid levels in 3xTg-AD mice. *Neurobiol. Aging* **34**, 1080–1089 (2013).

40. Oh, K.-J. *et al.* Staging of Alzheimer's Pathology in Triple Transgenic Mice: A Light and Electron Microscopic Analysis. *International Journal of Alzheimer's Disease* vol. 2010 1–24 (2010).

41. Sanguinetti, E. *et al.* Microbiome-metabolome signatures in mice genetically prone to develop dementia, fed a normal or fatty diet. *Sci. Rep.* **8**, 4907 (2018).

42. Bello-Medina, P. C. *et al.* Spatial Memory and Gut Microbiota Alterations Are Already Present in Early Adulthood in a Pre-clinical Transgenic Model of Alzheimer's Disease. *Frontiers in Neuroscience* vol. 15 (2021).

43. Chen, C. *et al.* Gut dysbiosis contributes to amyloid pathology, associated with C/EBPβ/AEP signaling activation in Alzheimer's disease mouse model.

Science Advances **6**, eaba0466 (2020).

44. Bonfili, L. *et al.* Microbiota modulation counteracts Alzheimer's disease progression influencing neuronal proteolysis and gut hormones plasma levels. *Sci. Rep.* **7**, 2426 (2017).

45. Transplantation of gut microbiota derived from Alzheimer's disease mouse model impairs memory function and neurogenesis in C57BL/6 mice. *Brain Behav. Immun.* **98**, 357–365 (2021).

46. Zaheer, S. *et al.* Enhanced expression of glia maturation factor correlates with glial activation in the brain of triple transgenic Alzheimer's disease mice. *Neurochem. Res.* **38**, 218 (2013).

47. Rosenbaum, C. *et al.* Activation of Myenteric Glia during Acute Inflammation In Vitro and In Vivo. *PLoS One* **11**, (2016).

48. Chatterjee, P. *et al.* Plasma glial fibrillary acidic protein is elevated in cognitively normal older adults at risk of Alzheimer's disease. *Transl. Psychiatry* **11**, 1–10 (2021).

49. Oddo, S. *et al.* Triple-transgenic model of Alzheimer's disease with plaques and tangles: intracellular Abeta and synaptic dysfunction. *Neuron* **39**, (2003).

50. Sarkar, A., Yoo, J. Y., Dutra, S. V. O., Morgan, K. H. & Groer, M. The Association between Early-Life Gut Microbiota and Long-Term Health and Diseases. *J. Clin. Med. Res.* **10**, (2021).

51. Huang, Y. *et al.* Possible association of Firmicutes in the gut microbiota of patients with major depressive disorder. *Neuropsychiatr. Dis. Treat.* **14**, 3329–3337

(2018).

52. Chen, Z. *et al.* Gut Microbial Profile Is Associated With the Severity of Social Impairment and IQ Performance in Children With Autism Spectrum Disorder. *Front. Psychiatry* **12**, 789864 (2021).

53. Kenna, J. E. *et al.* Changes in the Gut Microbiome and Predicted Functional Metabolic Effects in an Australian Parkinson's Disease Cohort. *Front. Neurosci.* **0**, (2021).

54. Ling, Z. *et al.* Structural and Functional Dysbiosis of Fecal Microbiota in Chinese Patients With Alzheimer's Disease. *Front Cell Dev Biol* **8**, 634069 (2020).

55. Haran, J. P. *et al.* Alzheimer's Disease Microbiome Is Associated with Dysregulation of the Anti-Inflammatory P-Glycoprotein Pathway. *MBio* **10**, (2019).

56. Seregin, S. S. *et al.* NLRP6 protects IL10−/− mice from colitis by limiting colonization of Akkermansia muciniphila. *Cell Rep.* **19**, 733 (2017).

57. Fung, T. C. *et al.* Intestinal serotonin and fluoxetine exposure modulate bacterial colonization in the gut. *Nature Microbiology* **4**, 2064–2073 (2019).

58. Iljazovic, A. *et al.* Perturbation of the gut microbiome by Prevotella spp. enhances host susceptibility to mucosal inflammation. *Mucosal Immunol.* **14**, 113–124 (2021).

59. Riboulet-Bisson, E. *et al.* Effect of Lactobacillus salivarius Bacteriocin Abp118 on the Mouse and Pig Intestinal Microbiota. *PLoS One* **7**, (2012).

60. Charles K. Fisher, P. M. Identifying Keystone Species in the Human Gut Microbiome from Metagenomic Timeseries Using Sparse Linear Regression. *PLoS One* **9**, (2014).

61. Hsiao, E. Y. *et al.* Microbiota modulate behavioral and physiological abnormalities associated with neurodevelopmental disorders. *Cell* **155**, 1451–1463 (2013).

62. Cox, L. M. *et al.* Calorie restriction slows age-related microbiota changes in an Alzheimer's disease model in female mice. *Scientific Reports* vol. 9 (2019).

63. Zhuang, Z.-Q. *et al.* Gut Microbiota is Altered in Patients with Alzheimer's Disease. *J. Alzheimers. Dis.* **63**, 1337–1346 (2018).

64. Lukiw, W. J. Bacteroides fragilis Lipopolysaccharide and Inflammatory Signaling in Alzheimer's Disease. *Front. Microbiol.* **7**, (2016).

65. Nawaz, A. *et al.* CD206 M2-like macrophages regulate systemic glucose metabolism by inhibiting proliferation of adipocyte progenitors. *Nat. Commun.* **8**, 286 (2017).

66. Davis, M. J. *et al.* Macrophage M1/M2 polarization dynamically adapts to changes in cytokine microenvironments in Cryptococcus neoformans infection. *MBio* **4**, e00264–13 (2013).

67. Callahan, B. J. *et al.* DADA2: High-resolution sample inference from Illumina amplicon data. *Nat. Methods* **13**, 581–583 (2016).

68. Janssen, S. *et al.* Phylogenetic Placement of Exact Amplicon Sequences Improves Associations with Clinical Information. *mSystems* **3**, (2018).

69. Bokulich, N. A. *et al.* Optimizing taxonomic classification of marker-gene amplicon sequences with QIIME 2's q2-feature-classifier plugin. *Microbiome* vol. 6 (2018).

70. Faith, D. P. Conservation evaluation and phylogenetic diversity. *Biological*

Conservation vol. 61 1–10 (1992).

71. Shannon, C. E. A Mathematical Theory of Communication. *Bell System Technical Journal* vol. 27 379–423 (1948).

72. Lozupone, C. A., Hamady, M., Kelley, S. T. & Knight, R. Quantitative and qualitative beta diversity measures lead to different insights into factors that structure microbial communities. *Appl. Environ. Microbiol.* **73**, 1576–1585 (2007).

73. Lozupone, C. & Knight, R. UniFrac: a new phylogenetic method for comparing microbial communities. *Appl. Environ. Microbiol.* **71**, 8228–8235 (2005).

74. Bokulich, N. A. *et al.* q2-longitudinal: Longitudinal and Paired-Sample Analyses of Microbiome Data. *mSystems* **3**, (2018).

75. Anderson, M. J. Permutational Multivariate Analysis of Variance (PERMANOVA). *Wiley StatsRef: Statistics Reference Online* 1–15 (2017) doi:10.1002/9781118445112.stat07841.

76. Mandal, S. *et al.* Analysis of composition of microbiomes: a novel method for studying microbial composition. *Microb. Ecol. Health Dis.* **26**, 27663 (2015).

77. Bokulich, N. A. *et al.* q2-sample-classifier: machine-learning tools for microbiome classification and regression. *bioRxiv* 306167 (2018) doi:10.1101/306167.

78. Dietmaier, W., Wittwer, C. & Sivasubramanian, N. *Rapid Cycle Real-Time PCR — Methods and Applications: Genetics and Oncology*. (Springer Science & Business Media, 2013).

CHAPTER 3: Engraftment of gut microbiota composition from aged 3xTg-AD mice modeling amyloidosis and tauopathy did not alter neuroinflammation in young 3xTg-AD mice.

ABSTRACT

The gut microbiota, the community of microbes that populate the gut, bidirectionally communicates with the brain via chemical messengers, termed the gut microbiota-brain axis. Shifts in the gut microbiota-brain axis are associated with development of Alzheimer's disease (AD), characterized by amyloid-β plaque deposition, neurofibrillary tangles, and neuroinflammation. *We hypothesize that remodeling the gut microbiota composition can shift key microbial communities, thereby altering the development of AD pathologies.* To assess the role of the functional microbiome on AD-associated neuroinflammation, we performed fecal microbiota transplants (FMT) from older (52-64 weeks) 3xTg-AD mice, modeling amyloidosis and tauopathy, to young 3xTg-AD (n=5) or WT mice (n=10). PBS was gavaged into 3xTg-AD (n=5) and WT mice (n=10) as a control. At 8 weeks, mice were treated with FMT or PBS for 5 consecutive days, followed by fortnightly maintenance doses until 24 weeks of age. The V4 region of the 16S rRNA gene was sequenced on the Illumina MiSeq. Data were analyzed using QIIME 2. Reverse transcription RT-qPCR was used to assess microgliosis, astrocytosis, and Th1/Th2 inflammation in the hippocampus and colon at 24 weeks of age. We observed partial engraftment of the gut microbiota from aged 3xTg-AD mice in FMT-treated mice. *Bacteroides acidifaciens* was increased in 3xTg-AD and WT mice receiving FMT from the 3xTg-AD mice. At 24 weeks, there was no difference in neuroinflammation between treatment groups. This study contributes to our

understanding of certain microbial features of the gut microbiota that may affect the onset and severity of AD pathologies.

IMPORTANCE

Fecal microbiota transplants have successfully treated *Clostridium difficile* hospital acquired infections, and have shown potential for treatment in neurological diseases related to altered gut microbiota compositions, including Parkinson's disease, Autism Spectrum Disorder, and Alzheimer's disease. Our study seeks to better understand the effects on the gut microbiota-brain axis in 3xTg-AD mice modeling Alzheimer's disease through transplantation from the gut microbiota composition of 3xTg-AD mice displaying full pathologies fortnightly into 8 week old 3xTg-AD and WT mice until 24 weeks of age. No changes in neuroinflammation between treatment groups were exhibited by 24 weeks of age, however successful partial engraftment of the gut microbiota composition by treatment group occurred, indicating early life gut microbiota may play a stronger role in the gut microbiota-brain axis.

Introduction

Microbial life, composed of bacteria, viruses, archaea, fungi, and their genomes, inhabit nearly every niche of the human body in what is collectively termed, the human microbiome. The gut microbiome houses the majority of the human microbiome, aiding in various aspects of human health, including nutrient absorption,[1] host homeostasis,[2] and resistance to foreign pathogen invasion.[3] Communication operates bidirectionally

between the central nervous system and the gastrointestinal tract via the gut microbiota-brain axis through neural, hormonal, immune and metabolic pathways.[3–6] Understanding these pathways offers insight into the development of targeted therapeutics aimed at recharacterizing the gut microbiome.[7]

Recent evidence suggests that the gut microbiota-brain axis may play an important role in the pathophysiology of Alzheimer's disease (AD).[4,8–10] AD is an irreversible, neurodegenerative disease that affects 1 in 10 people over the age of 65.[11] Patients with AD experience impaired physical and cognitive abilities, memory loss, and mood changes. Disease progression is slow, therefore patients may require caretakers for several years, which creates a financial and emotional burden to both the patient and their loved ones. Alzheimer's disease is characterized by three main pathologies; amyloid-β plaques, neurofibrillary tangles, and neuroinflammation.[4,12] Neuroinflammation in AD is characterized by a complex set of pathways, including dysfunctional microglia and astrocytes. Microglia are the resident macrophages of the central nervous system, while astrocytes function to support neuronal synaptic function and maintain the integrity of the blood brain barrier (BBB).[13,14] Microglia clear soluble amyloid-β via macropinocytosis, however, in the insoluble, fibrillary form, microglia are unable to clear amyloid-β deposits at the rate they are forming, leading to accumulation of amyloid-β plaques.[15] The chronic neuroinflammation in AD is further characterized by pro-inflammatory biochemical processes, including the release of proinflammatory cytokines, mainly IL-1β, TNF-α, and IL-6.[16] Emerging evidence points to neurotoxic metabolites of Gram-negative gut microbes, such as lipopolysaccharide (LPS), as key mediators of AD.[17]

The use of fecal microbiota transplantation (FMT) to alter health outcomes has been used to determine causality of microbial communities to disease severity or progression. A number of studies in mice modeling AD pathologies have shown reduced cognitive impairment, amyloidosis, tauopathy, and neuroinflammation proceeding gut microbiota intervention, including FMT from a healthy donor,[8] antibiotics,[18] and probiotics.[19] However, there have been few studies that explore directionality, using co-housing to allow for bi-directional transfer of microbial communities between mice modeling AD and WT mice. A study from Chen and colleagues demonstrate the impact of FMT in a study where young 3xTg-AD mice at 6 weeks old are co-housed with aged 3xTg-AD (12 months) mice or aged WT mice (12 months). The intervention led to a distinct gut microbiota composition in the young mice at 6 months of age cohoused with aged 3xTg-AD mice compared to those cohoused with WT mice. Further, the gut dysbiosis in the mice co-housed with aged 3xTg-AD mice led to decreased epithelial barrier integrity, upregulation of the C/EBPβ/AEP pathway in the brain, a reduction in synaptic function, and cognitive impairment.[20] In another study, where 5xFAD mice were co-housed with WT mice, a gut microbiota analysis at 7 months of age showed a distinct gut microbiota composition in co-housed WT mice compared to 5xFAD and WT mice without 5xFAD co-housing, suggesting partial transfer of the 5xFAD mouse microbiota phenotype. Interestingly, the cytokine array of the mouse brain homogenate from these mice shows WT mice co-housed with 5xFAD mice have more similar cytokine profiles to 5xFAD mice than the WT mice without 5xFAD co-housing. These studies, taken together, suggest the gut microbiota composition from mice modeling AD pathologies are not only transferable, but AD

murine models appear to have a stronger gut microbiota phenotype that is transferred to WT mice, linked to negative changes in immune, neural, and cognitive function.[21] To our knowledge, no clinical trials assessing FMT efficacy in people living with AD have been published, however, two case studies of individuals living with AD who received an FMT showed rapid improvement in cognitive function from pre-FMT to post-FMT treatment, measured by the Mini-Mental State Examination.[22,23] The body of literature demonstrating changes in the disease pathologies and cognition when the gut microbiota composition is transferred between mice modeling AD pathologies and WT mice, regardless of directionality, as well as the FMT treatments in two case studies of people living with AD, make a compelling case to explore the mechanisms involved.

Understanding how the gut microbiota-brain axis aggravates or alleviates disease progression could contribute to targeted therapies that restructure the microbiome toward a healthy state. Future therapies to manipulate the gut microbiota composition may provide a low-cost and minimally-invasive potential to reestablish healthy microbial communities in the gut of individuals with AD. Fecal microbiota transplantation (FMT) is an emerging technique in microbiota manipulation that involves transplantation of fecal matter containing gut microbes from a donor into a recipient.[8] FMTs have been used as an interventional strategy for recolonizing a disease-associated gut microbiota, *in vitro,* with minimal invasion to the host. Successful FMTs have been performed in treating hospital-acquired *Clostridium difficile* infections, where FMT from healthy donors effectively outcompetes the *C. difficile* and restores a healthy microbiome with minimal recurrence of *C. difficile* infection.[24] Beyond the potential for future therapies, FMTs allow researchers to study how the introduction of a donor

microbiota, associated with health or disease, may alter the progression and severity of disease. FMT clinical trials have been performed in patients with Parkinson's disease, and have indicated success in treating common symptoms of the disease including poor sleep, depression, anxiety, and resulted in motor skill improvement.[25] Previous studies indicate that transgenic mice modeling AD experience reduced tau hyperphosphorylation and cognitive decline as a result of FMT from a WT cohort.[8] This study seeks to elucidate whether FMTs from an aged triple transgenic mouse model (3xTg-AD) of AD can alter the gut microbiome of young 3xTg-AD and wild type (WT) mice, and investigate related changes in pathology development. We hypothesized that FMT from aged (12-19 month) 3xTg-AD mice would shift the gut microbiota of young 3xTg-AD and WT recipient mice to more closely resemble the phenotype associated with disease pathologies and aggravate neuroinflammation.

METHODS

Transgenic mouse models: Female 3xTg-AD (with overexpression of APP(Swe), PSEN1(M146V), and MAPT(P301L) transgenes; n=10) and female B6129F2/J (WT; n=20) mice were purchased from Jackson Laboratory (Bar Harbor, Maine). All mice were purchased from Jackson Laboratory, including aged, female 3xTg-AD donors, and allowed 5 days to acclimate. Mice were housed in a specific pathogen free environment at the vivarium at NAU.All animal experiments were approved by the Institutional Animal Use and Care Committee of NAU under protocol 18-016.

Sample collection: Fecal samples were collected directly from each mouse fortnightly starting at 8 weeks and continuing to 24 weeks, when mice were sacrificed for longitudinal gut microbiota and immune profile analysis. Mice were euthanized with CO_2 at 24 weeks of age. Gastrointestinal and brain samples were collected in a sterile Class II Biosafety Cabinet using sterile tools for each body site and mouse. Colon and hippocampus were harvested, immediately placed in RNAlater, and stored at −80 °C until further processing.

Fecal microbiota transplant: Fecal pellets were collected from 12-19 month old 3xTg-AD mice and stored at −80 °C in 1mL of sterile 1X phosphate buffer saline (PBS) per fecal pellet. Pellets were then thawed, combined with fresh fecal pellets in a 50/50 ratio, homogenized, and spun down at 4 degrees C for 15 minutes at 1200 rpm. 100uL of supernatant was transplanted via oral gavage into 3xTg-AD and WT mice beginning at 8 weeks of age for 5 consecutive days, followed by maintenance doses administered fortnightly from 10 weeks to 24 weeks of age. The control groups were administered sterile 1X PBS for the duration of the treatments. At 24 weeks, the mice were sacrificed to harvest feces and hippocampus. All samples were stored at −80 °C until further processing.

Nucleic Acid Extraction and 16S rRNA gene sequencing: DNA and RNA were extracted in parallel from feces using the MagMAX Pathogen RNA/DNA Kit from ThermoFisher. Extractions were performed in a Class II Biosafety Cabinet using protocols adopted from eukaryotic cell culture to protect the samples from contamination (i.e., decontaminate all materials with 70% EtOH to bring into the BSC, double glove while in the BSC, and don single use PPE while working in the BSC). Modifications to the protocol include the use of Lysing Matrix E tubes (MP Biomedical, Irvine, California) for bacterial and fungal lysis. Both DNA and RNA were quantified using a NanoDrop 2000. Quantified DNA from fecal samples was used for 16S rRNA gene PCR. Using Earth Microbiome Project (EMP) primers (515F-806R), the V4 region of the 16S rRNA gene was amplified. Each PCR reaction contained 2.5 µl of PCR buffer (TaKaRa, 10x concentration, 1x final), 1 µl of the Golay barcode tagged forward primer (10 µM concentration, 0.4 µM final), 1 µl of bovine serum albumin (Thermofisher, 20 mg/mL concentration, 0.56 mg/µl final), 2 µl of dNTP mix (TaKaRa, 2.5 mM concentration, 200 µM final), 0.125 µl of HotStart ExTaq (TaKaRa, 5 U/µl, 0.625 U/µl final), 1 µL reverse primer (10 µM concentration, 0.4µM final), and 1 µL of template DNA. All PCR reactions were filled to a total 25 µL with UltraPure DNase, Rnase free water (Invitrogen), then placed on a ThermalCycler. ThermalCycler conditions were as follows, 98°C denaturing step for 2 minutes, 30 cycles of 98°C for 20 seconds, 50°C for 30 seconds, and 72°C for 45 seconds, a final step of 72°C for 10 minutes. PCR was performed in a decontaminated PCR hood and consumables were decontaminated with 70% ethanol to bring into the hood, then exposed to UV light to prevent sample

contamination. PCR was performed in triplicate and an additional negative control was included for each barcoded primer. 16S rRNA gene bands were visualized using a 3% agarose gel (ThermoFisher, Waltham, Massachusetts). Amplicons were quantified using fluorometry and pooled at equimolar ratios. Quality of the pool was assessed with the Bioanalyzer DNA 1000 chip (Agilent Technologies, Santa Clara, California) then combined with 1% PhiX for sequencing. A total of 6 pools were sequenced on the Illumina MiSeq using the 600-cycle MiSeq Reagent Kit V3 (Illumina, San Diego, California). Each pool contained mock communities and samples that overlapped over each sequencing run to identify potential sequencing bias. All sequencing was done on the Illumina MiSeq.

Bioinformatics Analysis: Microbiome bioinformatics were performed with QIIME 2 version 2021.2. q2-DADA2 was used for sequence quality control and generation of amplicon sequence variants (ASVs) to provide the highest taxonomic specificity.[26] A phylogenetic tree was created using q2-fragment-insertion, which applies the SEPP algorithm, inserting short sequences into a reliable tree generated from a database of full-length sequences.[27] Taxonomy was assigned to reads using q2-feature-classifier and the Greengenes reference database, version 13_8.[27,28] Alpha diversity, including Faith's Phylogenetic Diversity,[29] Shannon Diversity Index,[30] and Observed ASVs were computed with q2-diversity[29]. Beta diversity (community dissimilarity) metrics were computed with q2-diversity, including Bray-Curtis dissimilarity, Jaccard dissimilarity, weighted UniFrac,[29,31] and unweighted UniFrac[32] distances. Longitudinal analysis was performed with q2-longitudinal to assess temporal changes in bacterial communities.[33]

Group comparisons of alpha diversity were performed with non-parametric Wilcoxon tests, and group comparisons of beta diversity were performed with non-parametric PERMANOVA[34]. ASVs and taxa that were differentially abundant across mouse genotypes and treatment groups were identified using ANCOM.[35] All P-values were corrected for multiple comparisons using the Benjamini-Hochberg False Discovery Rate correction.

qPCR Assay: DNA and RNA were extracted in parallel from hippocampus and colon samples using the Qiagen AllPrep kit. gDNA clean ups were performed on the RNA using the DNase Max kit (Qiagen, Hilden Germany). RNA was reverse transcribed using the 2nd strand synthesis kit (Qiagen, Hilden Germany). A custom qPCR assay from QIAGEN including various biomarkers for Th1/Th17 (*il2, il1beta, il-6, ifn-gamma, tnf-alpha*), astrocyte reactivity (*il-6*), and M1/M2 macrophage activation/microgliosis (*ccl2*, *il1β, il4, arg1, iNOS, il-10*)[36,37] were used.

Statistical Analysis: Fold changes were calculated using $2^{-\Delta\Delta C}$T.[38] Group comparisons of genotype-age were performed with non-parametric Mann-Whitney. Violin plots were created using Prism-GraphPad version 9.1.1 (225).

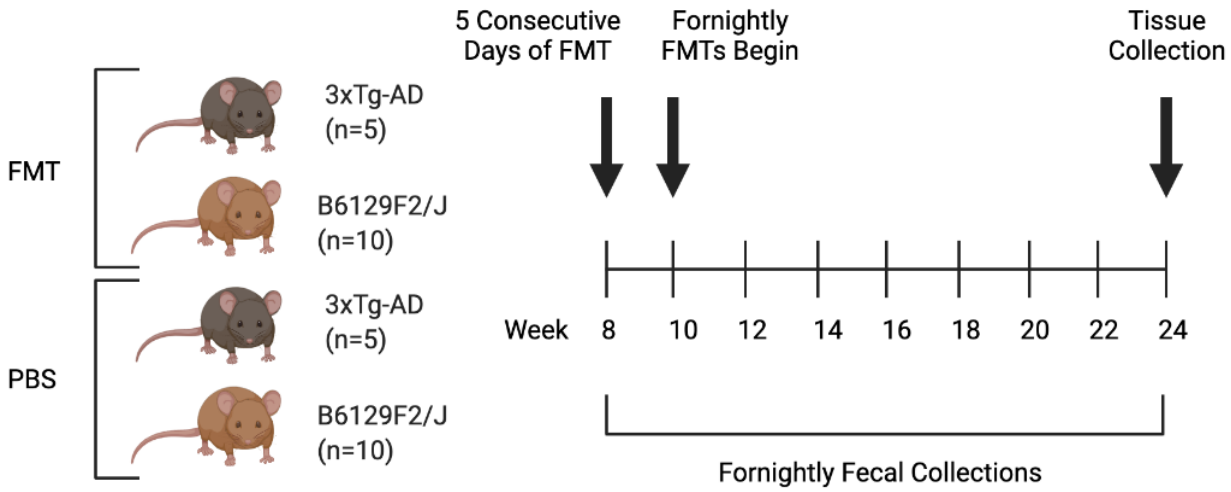

Figure 1: FMT Study Design. 3xTg-AD (n = 10) and B6129F2/J (n = 20) were separated into two treatment groups; fecal microbiota transplantation (FMT) and PBS (control). Beginning at 8 weeks of age, five consecutive days of treatment were administered (FMT or PBS), followed by fortnightly maintenance doses beginning at 10 weeks of age. Fecal samples were collected fortnightly from 8 to 24 weeks of age, when mice were sacrificed for tissue collection.

Fecal microbiota transplant (FMT) experimental design

To explore how FMT-induced shifts in the gut microbiota composition alters AD-associated neuroinflammation in mice, 3xTg-AD and WT mice were split further into four treatment groups, composed of 3xTg-AD-FMT treated mice, 3xTg-AD-PBS treated mice, WT-FMT treated mice, and WT-PBS treated mice. FMTs from female 3xTg-AD mice modeling AD pathologies (12-19 months old) were administered to 8 week old 3xTg-AD and WT mice for 5 consecutive days and fortnightly from 10 weeks to 24 weeks of age. Our recent results suggest that gut microbiome alterations precede pathology development from 8-24 weeks, so we rationalized that 24 weeks would be sufficient to observe changes in neuroinflammation and microbial composition in the

gut. Fecal samples were collected fortnightly for gut microbiome analysis from 8 weeks until 24 weeks of age (Figure 1).

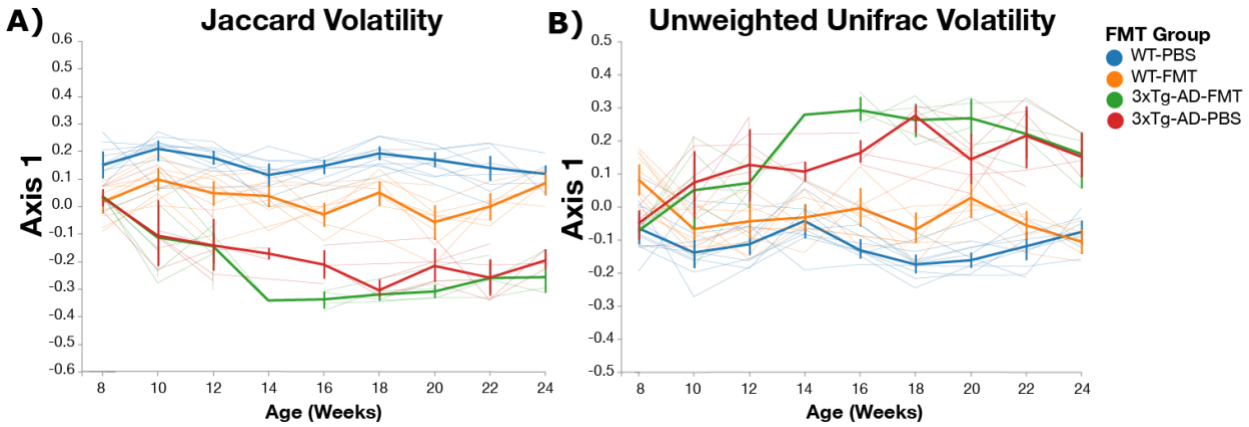

Figure 2: Volatility analysis of FMT Treatment Groups from 8 to 24 weeks demonstrates WT-FMT mice shift towards 3xTg-AD-FMT and 3xTg-AD PBS groups. A) Volatility plot of PCoA Axis 1 of the Jaccard dissimilarity index. This demonstrates differences in the shift of WT-FMT towards 3xTg-AD groups. Thick lines represent the average change in the gut microbiota on PC1 over time in the 4 treatment groups, and thin lines represent changes in the gut microbiota on PC1 over time in individual mice. B) Volatility plot of PCoA Axis 1 of Unweighted Unifrac distance metric. Thick lines represent the average change in the gut microbiota on PC1 over time in the 4 treatment groups, and thin lines represent changes in the gut microbiota on PC1 over time in individual mice.

Successful engraftment of the gut microbiota composition from 3xTg-AD mice into WT-FMT group

Success of FMTs are characterized by engraftment, or incorporation of the donor gut microbiota composition to the gut of the FMT recipient.[39] To assess the temporal compositional shifts from FMT, beta diversity metrics were run on the four treatment groups to analyze compositional differences between samples from 8 to 24 weeks of age. Jaccard dissimilarity, a non-phylogenetic, qualitative metric, demonstrated a shift of

WT-FMT treated mice towards a more similar gut microbiota composition to 3xTg-AD mice, suggesting the community of bacteria in WT-FMT treated mice and 3xTg-AD mice share more of the same amplicon sequence variants (ASVs) after the gut microbiota transplantation (Figure 2A). Comparisons of Jaccard distance metrics are significant at 8, 16, and 24 weeks of age (PERMANOVA q-value <0.01), except when comparing 3xTg-AD-FMT and 3xTg-AD-PBS at 24 weeks (PERMANOVA q-value = 0.111; Table S1A-C). Unweighted unifrac, a phylogenetic, qualitative metric, also demonstrated a shift of WT-FMT treated mice towards a more similar gut microbiota composition to 3xTg-AD mice, implying that phylogenetic similarity or dissimilarity of features is not a driving force in beta diversity metrics (Figure 2B). Unweighted Unifrac distance metrics are significant at 8, 16, and 24 weeks of age (PERMANOVA, q-value <0.01), except when comparing 3xTg-AD-FMT and 3xTg-AD-PBS at 24 weeks (PERMANOVA q-value = 0.095; Table S1D-F).

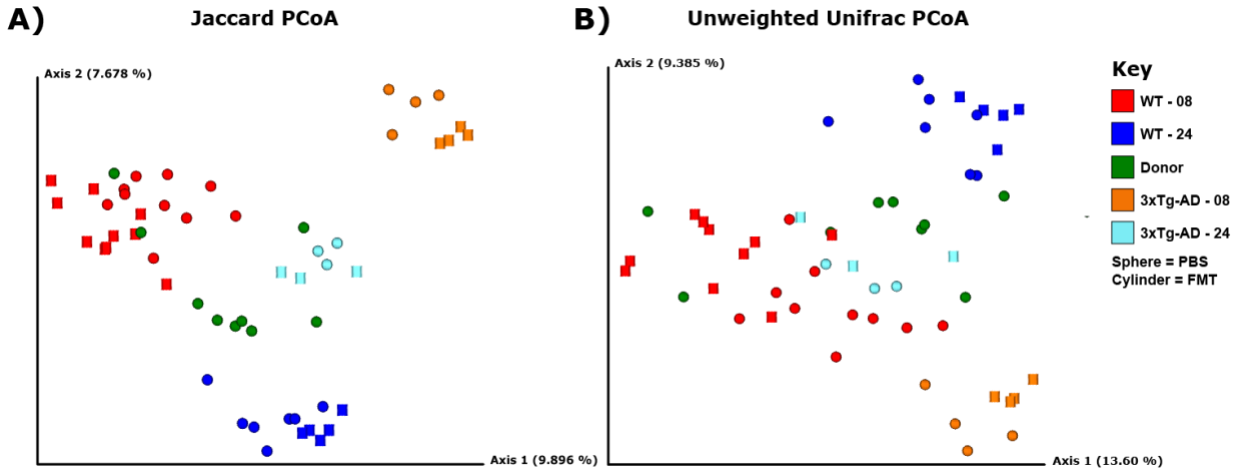

Figure 3: Jaccard and Unweighted Unifrac PCoA show composition shift towards Aged Donors in 3xTg-AD mice. A) PCoA of Jaccard dissimilarity index. Demonstrates 3xTg-AD mice shift towards an Aged Donor like community composition while WT mice at 24 weeks cluster away from Aged Donor's community composition. B) PCoA of

Unweighted Unifrac distance metric. Demonstrates 3xTg-AD mice shift towards an Aged Donor like community composition while WT mice at 24 weeks cluster away from Aged Donor's community composition.

3xTg-AD mice shift towards FMT donor community composition at 24 weeks of age when compared to WT mice

To examine how FMT treatment altered the gut microbiota composition of 3xTg-AD and WT mice by 24 weeks, we evaluated beta diversity at 8 week and 24 week samples from all four treatment groups, with FMT donor samples (Figure 3). All four groups reveal FMT associated gut microbiota composition changes were not strong enough to shift towards the FMT donor composition. Unsurprisingly, 3xTg-AD at 24 weeks were more similar to FMT donors than WT at 24 weeks. WT mice were more similar to FMT donor mice at 8 weeks than they were at 24 weeks, demonstrating a shift away from the disease-associated gut microbiota composition as they age.

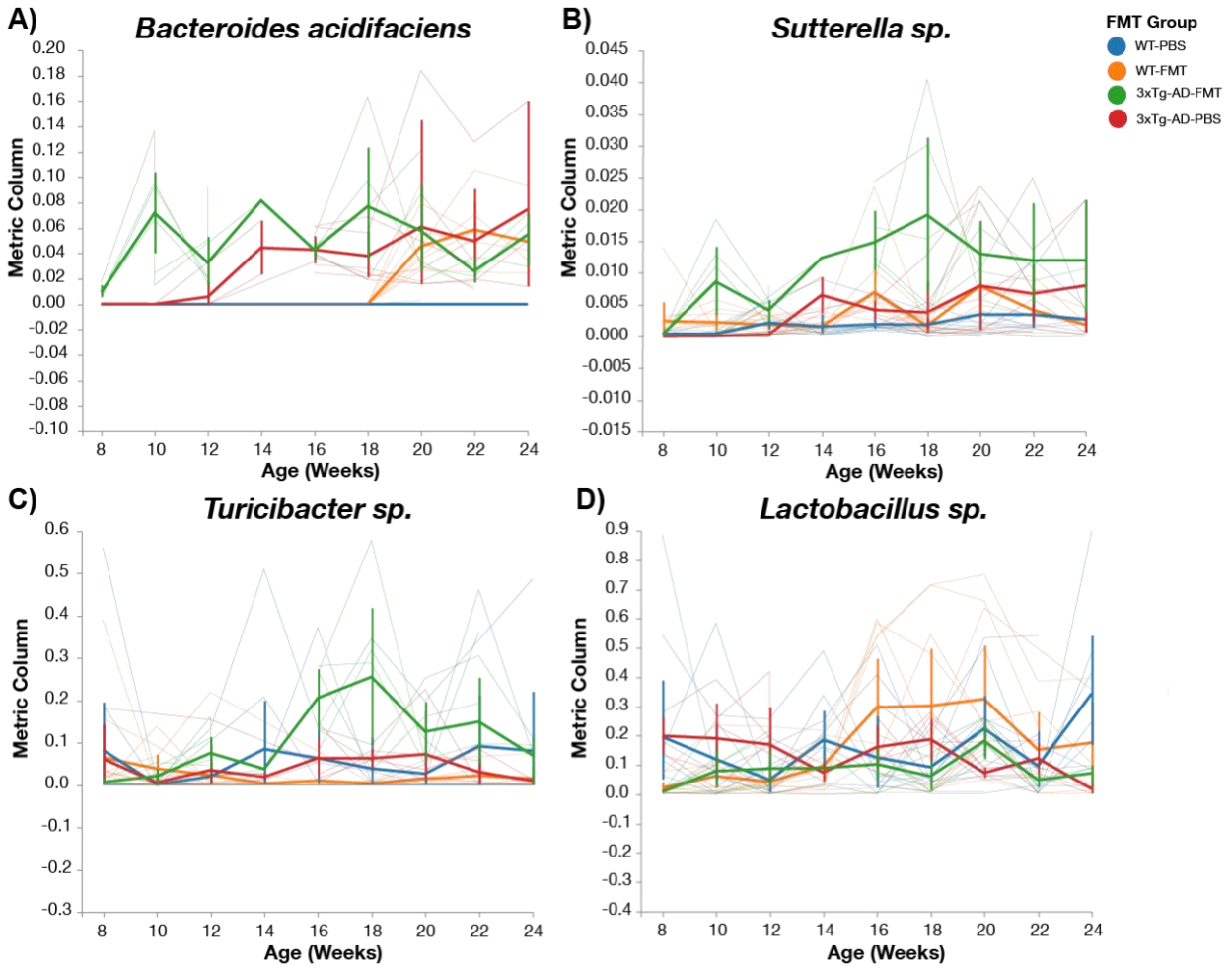

Figure 4. Feature volatility at species level.Thick lines represent the average change in the ASV over time in all 4 treatment groups, and thin lines represent changes in the ASV over time in individual mice. A) Feature volatility chart of *Bacteroides acidifaciens* demonstrates increasing abundance following initial FMT treatment in 3xTg-AD-FMT mice, and increases in 3xTg-AD-PBS around 14 weeks of age. WT-FMT mice experience increased *Bacteroides acidifaciens* about 12 weeks into FMT treatments.B) Feature volatility chart of *Sutterella sp*. demonstrates increasing abundance following initial FMT treatment in 3xTg-AD-FMT mice, while increasing abundance in 3xTg-AD-PBS and WT-FMT at 6 and 8 weeks, respectively, following initial FMT treatment. C) Feature volatility chart of *Turicibacter sp.* demonstrates increasing abundance in 3xTg-AD-FMT mice 8 weeks after the initial FMT treatment, while remaining relatively stable at low abundances in all other treatment groups. D) Feature volatility chart of *Lactobacillus sp.* demonstrates a relatively stable abundance for all treatment groups, however increasing in WT-FMT mice 6-10 weeks following initial FMT treatment.

Feature volatility reveals dynamic microbial communities endogenous to 3xTg-AD mice and transferable between phenotypes

To further characterize the engraftment success, q2-longitudinal was applied to identify dynamic features of the gut microbiota composition. *Bacteroides acidifaciens* increases in relative abundance in WT-FMT mice at 20 weeks of age, however, appears absent in WT-PBS mice. Interestingly, prior to 20 weeks of age in WT-FMT mice, *Bacteroides acidifaciens* was absent, suggesting multiple treatments were needed for effective transfer. In 3xTg-AD mice, *Bacteroides acidifaciens* was present as early as 8 weeks of age, yet the relative abundance in PBS treated mice was lower than FMT treated mice until 14-16 weeks of age. This delay in relative abundance of *Bacteroides acidifaciens* suggests that engraftment also occurred in FMT treated 3xTg-AD mice (Figure 4A). Similarly, *Sutterella sp*. increases in 3xTg-AD-FMT as early as 10 weeks of age, while remaining in low abundance in 3xTg-AD-PBS and WT-FMT mice at 14 and 16 weeks of age, respectively (Figure 4B). *Turicibacter sp.* increases in abundance in 3xTg-AD-FMT at 16 weeks of age, while remaining in relatively low abundance for 3xTg-AD-PBS, WT-FMT, and WT-PBS mice (Figure 4C). Curiously, a *Lactobacillus sp.* remains relatively stable at lower abundances in all 4 treatment groups, yet increases in WT-FMT mice from 16-20 weeks of age (Figure 4D).

Differential abundance of gut microbiota bacteria by treatment group

To identify differential abundance of bacteria in the gut microbiota composition of each treatment group, we used ANCOM (Analysis of Composition of Microbiomes) at the 8, 16, and 24 week timepoints (Table S2). *Bacteroides spp.* (W=52), *Lactobacillus spp.*

(W=52), and *Bacteroides acidifaciens* (W=52) were identified as differentially abundant among the treatment groups at 8 weeks of age. *Lactobacillus salivarius* (W=56), *Bacteroides spp.* (W=56), *Bacteroides acidifaciens* (W=54), *Lactobacillus* (W=54), *Prevotella spp.* (W=53), and *Akkermansia muciniphila* (W=51) were identified as differentially abundant among the treatment groups at 16 weeks of age. *Bacteroides acidifaciens* (W=66), *Lactobacillus* (W=64) and *Lactobacillus salivarius* (W=61) were identified as differentially abundant among the treatment groups at 24 weeks of age.

Next, we used ANCOM to compare the FMT treatment between mouse genotypes, at the 8, 16, and 24 week timepoints (3xTg-AD-FMT vs. WT-FMT, Table S3A). *Bacteroides acidifaciens* (W=50) was identified as differentially abundant among the treatment groups at 8 weeks of age between FMT treated 3xTg-AD and WT mice. *Lactobacillus sp.* (W=49) and *Bacteroides acidifaciens* (W=49) were identified as differentially abundant among the treatment groups at 16 weeks of age between FMT treated 3xTg-AD and WT mice. *Lactobacillus sp.* (W=50) was identified as differentially abundant among the treatment groups at 8 weeks of age between FMT treated 3xTg-AD and WT mice.

Finally, we sought to compare the PBS treatment mouse genotypes, at the 8, 16, and 24 week timepoints (3xTg-AD-PBS vs. WT-PBS, Table S3B). *Lactobacillus* (W=44) and *Bacteroides sp.* (W=43) were identified as differentially abundant among the treatment groups at 8 weeks of age between PBS treated 3xTg-AD and WT mice. *Bacteroides spp.* (W=43), *Bacteroides acidifaciens* (W=39), *Lactobacillus* (W=39), *Prevotella spp.*

(W=38), *Lactobacillus salivarius* (W=35), and *Akkermansia muciniphila* (W=34) were identified as differentially abundant among the treatment groups at 16 weeks of age between PBS treated 3xTg-AD and WT mice. *Bacteroides acidifaciens* (W=60), *Prevotella spp.* (W=52) and *Lactobacillus salivarius* (W=52) were identified as differentially abundant among the treatment groups at 24 weeks of age between PBS treated 3xTg-AD and WT mice.

Associations between bacterial microbiota and FMT treatment group over time using Linear Mixed Effects

We applied a Linear Mixed Effects (LME) model to determine the relationship of FMT treatment group (as a fixed effect) on gut microbiota diversity, leveraging the repeated measures for each mouse. When we performed pairwise comparisons at each timepoint, Faith's Phylogenetic Diversity (Faith's PD), an alpha diversity metric, was not significantly different in 3xTg-AD-FMT mice at 8 weeks compared to 3xTg-AD-PBS mice at 8 weeks (q-value = 0.178698, Kruskal-Wallis), 3xTg-AD mice at 16 weeks compared to WT mice at 16 weeks (q-value = 0.327986, Kruskal-Wallis), or 3xTg-AD-FMT mice at 24 weeks compared to 3xTg-AD-PBS mice at 24 weeks (q-value = 0.615229, Kruskal-Wallis (Figure S4)). There was a significant difference in Faith's PD between WT-FMT mice at 8 weeks compared to WT-PBS mice at 8 weeks (q-value = 0.030496, Kruskal-Wallis), while there was no significance at WT-FMT mice at 16 weeks compared to WT-PBS mice at 16 weeks (q-value = 0.757278, Kruskal-Wallis) or WT-FMT mice at 24 weeks compared to WT-PBS mice mice at 24 weeks (q-value = 0.684743, Kruskal-

Wallis (Figure S4)). When we leveraged LME to analyze the effect of FMT treatment + genotype on alpha diversity, Faith's PD was significantly lower in 3xTg-AD-FMT mice at baseline ($p < 0.001$). Faith's PD was consistently lower over time in WT-FMT ($p < 0.001$) and WT-PBS mice ($p < 0.001$) and higher over time in 3xTg-AD-FMT ($p = 0.002$), but not in 3xTg-AD-PBS ($p > 0.05$). To evaluate the effect of FMT treatment - genotype on microbial composition over time, we used LME on the first principle coordinate axis (PC1) from a PCoA generated from the Unweighted Unifrac dissimilarity metric. Gut microbial composition of 3xTg-AD-FMT mice was significantly distinct at baseline from WT treatment groups ($p < 0.011$). WT-FMT, 3xTg-AD-FMT and 3xTg-AD-PBS show significant differences over time ($p < 0.001$) when compared to WT-PBS, suggesting 3xTg-AD mice experience stronger shifts in gut microbial composition than WT mice without FMT treatment. FMT treatment + genotype did interact with time in modulating the gut microbiota composition, suggesting a possible impact of genotype on microbiome development ($p < 0.001$). Gut microbiota composition changed more drastically in FMT treatment mice regardless of mouse genotype from the baseline sample when compared to WT-PBS treated mice.

Inflammatory gene biomarkers in the hippocampus and colon

To assess severity of the inflammatory response in the hippocampus to the FMT treatments, we used a custom reverse transcriptase qPCR assay to evaluate 16 genes for AD-associated inflammatory biomarkers. Based on previous characterization of pathologies in the brain of 3xTg-AD mice, the hippocampus was selected for neuroinflammatory marker analysis.[40] Of the 16 genes assessed, five were T_H1/T_H17

markers, one was a astrogliosis markers, six were microgliosis markers, and four were controls/housekeeping genes (Table S4). Fold change was calculated for hippocampus at 24 weeks of age in all four treatment groups using the $2^{-\Delta\Delta C}$T method.[41] Arg1 is a biomarker for type 2 microgliosis, while Nos2 is a biomarker for type 1 microgliosis. Ccl2 is a biomarker for Aβ stimulated astrocytes and microglia[42,43]. We did not observe significant changes in inflammatory gene markers in the hippocampus across the four treatment groups ($p>0.05$, Mann-Whitney, Fig. 5A-C).

DISCUSSION

Studies have shown altered neuroinflammation[8], cognitive function,[44,45] and AD pathology burden[46] following gut microbiota alterations in mice, suggesting a role of the gut microbiota-brain axis in the development and severity of AD pathologies. In this study, we demonstrated successful engraftment using FMT treatments with no subsequent changes in AD- associated neuroinflammation. However, we did identify certain microbial features, including *Bacteroides acidifaciens, Sutterella sp., and Turicibacter sp.* that colonized 3xTg-AD-FMT treated mice, while less apparent in WT-FMT treated mice.

Increasing interest in understanding how to manipulate the gut microbiota to improve health has led to studies evaluating the health impacts of probiotics,[47] antibiotics,[48] prebiotics, and fecal microbiota transplants.[49] The beneficial impacts of these treatments relies heavily on their ability to alter the gut microbiota composition by providing nutrition to resident microbes or by directly altering the microbial composition.

Fecal microbiota transplants (FMT) require engraftment, or incorporation of foreign material, to alter the functional gut microbiome. The requirements for dictating a successful engraftment from FMT treatments are still unclear. In this study, we demonstrate that FMT alters the beta diversity, feature volatility, and abundance of taxa in a genotype-specific manner. While this study did not show changes in AD-associated neuroinflammation in FMT treated mice, we did demonstrate successful engraftment in FMT treated mice.

To engraft in the gut exogenous microbes must compete with the resident microbes through complex interactions to inhabit the gut microbiota, exhibited both at the community and individual level.[50] Jaccard and Unweighted Unifrac diversity metrics reveals community level engraftment suggested by a more similar gut microbiota compositions in WT-FMT treated mice to 3xTg-AD mice in both treatment groups than to their PBS treated WT mice. As a qualitative, non-phylogenetic metric for analyzing between sample diversity, Jaccard demonstrates engraftment of both low and high abundant taxa from 3xTg-AD donors to young WT mice. Further, the 3xTg-AD-FMT and 3xTg-AD-PBS mice show similar gut microbiota compositions, indicating that young 3xTg-AD mice share similar microbial communities with the older 3xTg-AD donor mice.

Identification of individual microbial engraftment illustrates the ability of the microbe to compete against endogenous communities for a spot in the gut microbiota. *Bacteroides acidifaciens* successfully engrafted in all FMT treated mice, but it took multiple doses of FMT to engraft in WT-FMT mice. Further, *B. acidifaciens* was indigenous in 3xTg-AD-

PBS mice and was completely absent in WT-PBS mice. Taken together, this indicates both transfer of maternal microbiome features during vaginal birth (in 3xTg-AD mice) and ability to engraft more effectively in 3xTg-AD-FMT than WT-FMT mice, demonstrating that the niche occupied by *B. acidifaciens* is likely genotype-specific Further, we observed increasing relative abundance of *B. acidifaciens* temporally, which can imply that *B. acidifaciens* is metabolically active in the gut microbiota and potentially involved the gut microbiota-brain axis and development of AD pathologies. Unfortunately, *B. acidifaciens* remains an understudied organism and has not been identified in humans.[51] First isolated from the mouse caecum in 2000, *B. acidifaciens* demonstrated phenotypic similarities to *Bacteroides fragilis* and is a member of the *B. fragilis group*.[52]

B. fragilis has previously been implicated in Alzheimer's disease in both mouse and human studies.[9,53,54] *B. fragilis* is a commensal gut microbe found in the mammalian gastrointestinal tract. However, *B. fragilis* also exerts strong neurological effects. In mice modeling Autism Spectrum Disorder, *B. fragilis* administration was beneficial; mice colonized with *B. fragilis* demonstrated improved social and behavioral behaviors, and reduced inflammation.[55] Moreover, the role of *B. fragilis* seems to be more neurotoxic in Alzheimer's Disease.[56] Most notably, *B. fragilis* produces lipopolysaccharide (BF-LPS),[57] an endotoxin that increases production of pro-inflammatory cytokines in the brain, and a toxin (fragilysin; BFT), which can disrupt the epithelial barrier.[58] BF-LPS and BFT have been shown to degrade intestinal barrier integrity, enter the bloodstream,

and cross the blood brain barrier in patients with AD and further exacerbate cytokine production in the brain.[59]

In addition to *Bacteroides acidifaciens*, *Sutterella sp*. and *Turicibacter sp.* increased in relative abundance in 3xTg-AD-FMT mice compared to the other treatment groups, suggesting successful engraftment of these features. *Sutterella* is considered a commensal gut microbe, with proinflammatory capacities, frequently associated with Inflammatory Bowel Diseases, Down Syndrome, and Autism Spectrum Disorder.[60] *Turicibacter sp.* has been identified in 3xTg-AD[61], 5xFAD[62,63], APP/PS1[62], and patients suffering from AD[9] as a microbial feature with altered relative abundance from healthy controls. While the role *Turicibacter sp.* plays in host health remain unclear, it does possess the capability to consume and regulate the uptake of serotonin in the intestines.[64] Serotonergic alterations (e.g., via use of selective serotonin reuptake inhibitors) have been linked to reduced AD pathology in a handful of clinical studies.[65] A recent study in 5xTg-FAD mice, modeling amyloidosis, found that *Turicibacter* was depleted in the gut microbiome of 5xTg-FAD mice.[63] In our study, we found that *Turicibacter* was increased in abundance in 3xTg-AD mice receiving FMT, possibly suggesting a role for this organism in AD via the gut microbiome-serotonin-AD axis.

While our study did not demonstrate changes in AD-associated neuroinflammation biomarkers between treatment groups at 24 weeks of age (Supplemental Figure 1A-C), the design of our FMT treatment did result in successful engraftment of the gut microbiota composition from older 3xTg-AD mice to young 3xTg-AD and WT mice. In

future FMT studies investigating neurological diseases and the gut microbiota composition, an extended treatment period for alterations in the disease pathologies should be considered. While we found no changes in inflammation or pathology severity, we believe that this could be a result of ending our study at 24 weeks of age, a time point where the 3xTg-AD mice model amyloidosis, but not tauopathy. Additionally, in a longitudinal study we performed simultaneously with the present study, we sampled 3xTg-AD and WT mice gut microbiota compositions over 52 weeks of age, and found that the gut microbiota composition of 3xTg-AD mice was significantly different in the first 24 weeks of age, and more similar to WT mice at 52 weeks of age[66]. With these findings, an FMT study transplanting between young 3xTg-AD and WT mice of the same age, or a cohousing of young 3xTg-AD and WT mice, with sampling to 52 weeks of age. This study design would allow for exploration of how the gut microbiota composition from young 3xTg-AD mice alters WT mice who are not genetically predisposed to AD and the neurological and inflammatory effects of the gut microbiota manipulation to better understand host-microbe interactions. Further, this would follow the canonical that early life gut microbiota perturbations may lead to adverse health outcomes later in life.[67]

CONCLUSIONS

The need for exploration of non-invasive treatments, including fecal microbiota transplantations, for Alzheimer's disease is crucial for the rapidly growing aging population. The present study showed successful engraftment of the gut microbiota composition in mice using a 5 day initial treatment followed by fortnightly maintenance

doses from older 3xTg-AD mice modeling Alzheimer's diseases pathologies to young 3xTg-AD and WT mice. Microbiome features that were differentiated between 3xTg-AD and WT mice included *Bacteroides acidifaciens, Lactobacillus salivarius*, *Turicibacter sp.*, and *Prevotella sp.* Interestingly, *Bacteroides acidifaciens*, a member of the *Bacteroides fragilis* group, was present in 3xTg-AD-FMT, 3xTg-AD-PBS, and WT-FMT treated mice, yet absent in WT mice. However, no changes in neuroinflammation were observed. Based on our findings, future studies that utilize FMT treatment from young transgenic AD mice, including co-housing studies, and extend the timeline for collection of samples to 52 weeks will provide a better understanding of long term treatment effects.

SUPPLEMENTAL MATERIALS

Table S1A: Pairwise PERMANOVA (Jaccard) of all 4 treatment groups at 8 weeks

Group 1	Group 2	Sample size	Permutations	pseudo-F	p-value	q-value
3xTg-AD-FMT	3xTg-AD-PBS	8	999	1.900780796	0.032	0.032
3xTg-AD-FMT	WT-FMT	14	999	4.332847434	0.003	0.0036
3xTg-AD-FMT	WT-PBS	14	999	4.061195442	0.003	0.0036
3xTg-AD-PBS	WT-FMT	14	999	3.614524349	0.002	0.0036
3xTg-AD-PBS	WT-PBS	14	999	3.47345118	0.001	0.003

WT-FMT	WT-PBS	20	999	2.416265499	0.001	0.003

Table S1B: Pairwise PERMANOVA (Jaccard) of all 4 treatment groups at 16 weeks

Group 1	Group 2	Sample size	Permutations	pseudo-F	p-value	q-value
3xTg-AD-FMT	3xTg-AD-PBS	8	999	2.385024346	0.027	0.027
3xTg-AD-FMT	WT-FMT	10	999	2.652654708	0.006	0.0105
3xTg-AD-FMT	WT-PBS	9	999	3.453636489	0.011	0.0132
3xTg-AD-PBS	WT-FMT	10	999	2.188799447	0.006	0.0105
3xTg-AD-PBS	WT-PBS	9	999	2.816490424	0.007	0.0105
WT-FMT	WT-PBS	11	999	1.741135455	0.002	0.0105

Table S1C: Pairwise PERMANOVA (Jaccard) of all 4 treatment groups at 24 weeks

Group 1	Group 2	Sample size	Permutations	pseudo-F	p-value	q-value
3xTg-AD-FMT	3xTg-AD-PBS	6	999	2.274584593	0.111	0.111
3xTg-AD-FMT	WT-FMT	8	999	3.599115159	0.017	0.0228
3xTg-AD-FMT	WT-PBS	10	999	3.394753937	0.011	0.022
3xTg-AD-PBS	WT-FMT	8	999	3.582518392	0.019	0.0228
3xTg-AD-PBS	WT-PBS	10	999	3.348039411	0.007	0.021

WT-FMT	WT-PBS	12	999	1.726733826	0.001	0.006

Table S1D: Pairwise PERMANOVA (Unweighted Unifrac) of all 4 treatment groups at 8 weeks

Group 1	Group 2	Sample size	Permutations	pseudo-F	p-value	q-value
3xTg-AD-FMT	3xTg-AD-PBS	8	999	2.323920943	0.034	0.034
3xTg-AD-FMT	WT-FMT	14	999	6.247418376	0.004	0.0048
3xTg-AD-FMT	WT-PBS	14	999	4.217075386	0.004	0.0048
3xTg-AD-PBS	WT-FMT	14	999	5.476731172	0.004	0.0048
3xTg-AD-PBS	WT-PBS	14	999	3.550703856	0.001	0.003
WT-FMT	WT-PBS	20	999	3.128878175	0.001	0.003

Table S1E: Pairwise PERMANOVA (Unweighted Unifrac) of all 4 treatment groups at 16 weeks

Group 1	Group 2	Sample size	Permutations	pseudo-F	p-value	q-value
3xTg-AD-FMT	3xTg-AD-PBS	8	999	2.630177612	0.032	0.032
3xTg-AD-FMT	WT-FMT	10	999	3.42509336	0.007	0.015
3xTg-AD-FMT	WT-PBS	9	999	5.048285806	0.016	0.0192
3xTg-AD-PBS	WT-FMT	10	999	2.5301344	0.008	0.015

3xTg-AD-PBS	WT-PBS	9	999	3.7544345	0.01	0.015
WT-FMT	WT-PBS	11	999	1.70560583	0.007	0.015

Table S1F: Pairwise PERMANOVA (Unweighted Unifrac) of all 4 treatment groups at 24 weeks

Group 1	Group 2	Sample size	Permutations	pseudo-F	p-value	q-value
3xTg-AD-FMT	3xTg-AD-PBS	6	999	2.08242525	0.095	0.095
3xTg-AD-FMT	WT-FMT	8	999	3.798316658	0.027	0.0324
3xTg-AD-FMT	WT-PBS	10	999	3.268371352	0.006	0.03
3xTg-AD-PBS	WT-FMT	8	999	4.690298039	0.021	0.0315
3xTg-AD-PBS	WT-PBS	10	999	4.075052721	0.011	0.03
WT-FMT	WT-PBS	12	999	1.628618124	0.015	0.03

Table S2: Differential abundance between all 4 treatment groups using Analysis of Composition of Microbiomes (ANCOM) collapsed at species level at week 8, 16, and 24. W represents the number of features that the taxa is more abundant than.

Features Collapsed at Genus Level	W	Week
Bacteroides spp.	52	8
Lactobacillus spp.	52	8
Bacteroides acidifaciens	52	8

Lactobacillus salivarius	56	16
Bacteroides spp.	56	16
Bacteroides acidifaciens	54	16
Lactobacillus	54	16
Prevotella spp.	53	16
Akkermansia muciniphila	51	16
Bacteroides acidifaciens	66	24
Lactobacillus	64	24
Lactobacillus salivarius	61	24

Table S3A: Differential abundance between 3xTg-AD and WT mice treated with FMT using Analysis of Composition of Microbiomes (ANCOM) collapsed at species level at week 8, 16, and 24. W represents the number of features that the taxa is more abundant than.

Features Collapsed at Genus Level	**W**	**Week**	**Treatment**
Bacteroides acidifaciens	50	8	FMT
Lactobacillus sp.	49	16	FMT
Bacteroides acidifaciens	49	16	FMT
Lactobacillus sp.	53	24	FMT

Table S3B: Differential abundance between 3xTg-AD and WT mice treated with PBS using Analysis of Composition of Microbiomes (ANCOM) collapsed at species level at week 8, 16, and 24. W represents the number of features that the taxa is more

abundant than.

Features Collapsed at Genus Level	W	Week	Treatment
Lactobacillus sp.	44	8	PBS
Bacteroides sp.	43	8	PBS
Bacteroides sp.	43	16	PBS
Bacteroides acidifaciens	39	16	PBS
Lactobacillus sp.	39	16	PBS
Prevotella spp.	38	16	PBS
Lactobacillus salivarius	35	16	PBS
Akkermansia muciniphila	34	16	PBS
Bacteroides acidifaciens	60	24	PBS
Prevotella spp.	52	24	PBS
Lactobacillus sp.	52	24	PBS

Table S4: qPCR gene biomarkers included in the custom RT-qPCR assay

Marker types	Genes
Th1/Th17	*il2, il1beta, il-6, ifn-gamma, tnf-alpha*
astrocyte reactivity	*il-6*

M1/M2 macrophage activation/microgliosis	*ccl2*, *il1β, il4, arg1, iNOS, il-10*
control/housekeeping	*GAPDH, GDC, PPC, RTC (QIAGEN)*

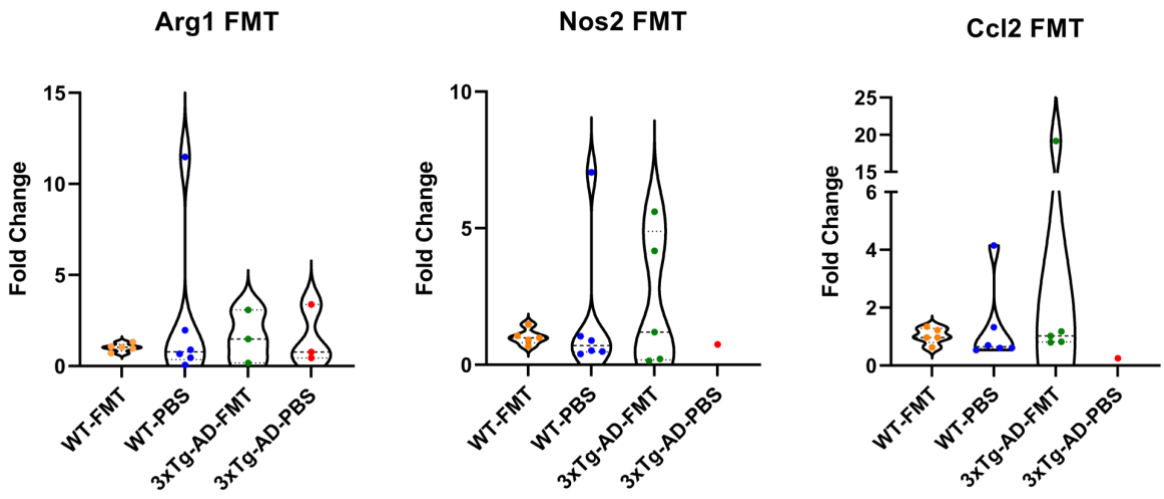

Supplemental Figure 1. Relative gene expression of Arg1, Nos2 and Ccl2 in the hippocampus at 24 weeks of age. Hippocampus from 3xTg-AD-FMT, 3xTg-AD-PBS, WT-FMT, and WT-PBS mice were collected at 24 weeks of age. No statistical significance found. A) Gene expression of Nos2. B) Gene expression of Arg1. C) Gene expression of Ccl2. Samples that did not amplify have been excluded from the violin plots and statistical analysis.

REFERENCES

1. Jumpertz, R. *et al.* Energy-balance studies reveal associations between gut microbes, caloric load, and nutrient absorption in humans. *Am. J. Clin. Nutr.* **94**, 58–65 (2011).

2. Lyte, M. The microbial organ in the gut as a driver of homeostasis and disease. *Med. Hypotheses* **74**, 634–638 (2010).

3. O'Hara, A. M. & Shanahan, F. The gut flora as a forgotten organ. *EMBO Rep.* **7**, 688–693 (2006).

4. Bonfili, L. *et al.* Microbiota modulation counteracts Alzheimer's disease progression influencing neuronal proteolysis and gut hormones plasma levels. *Sci. Rep.* **7**, 2426 (2017).

5. Rhee, S. H., Pothoulakis, C. & Mayer, E. A. Principles and clinical implications of the brain-gut-enteric microbiota axis. *Nat. Rev. Gastroenterol. Hepatol.* **6**, 306–314 (2009).

6. Westfall, S. *et al.* Microbiome, probiotics and neurodegenerative diseases: deciphering the gut brain axis. *Cell. Mol. Life Sci.* **74**, 3769–3787 (2017).

7. Borsom, E. M., Lee, K. & Cope, E. K. Do the Bugs in Your Gut Eat Your Memories? Relationship between Gut Microbiota and Alzheimer's Disease. *Brain sciences* **10**, (2020).

8. Sun, J. *et al.* Fecal microbiota transplantation alleviated Alzheimer's disease-like pathogenesis in APP/PS1 transgenic mice. *Transl. Psychiatry* **9**, 189 (2019).

9. Vogt, N. M. *et al.* Gut microbiome alterations in Alzheimer's disease. *Sci. Rep.* **7**, 13537 (2017).

10. Shen, L., Liu, L. & Ji, H.-F. Alzheimer's Disease Histological and Behavioral Manifestations in Transgenic Mice Correlate with Specific Gut Microbiome State. *J. Alzheimers. Dis.* **56**, 385–390 (2017).

11. Alzheimer's Association. 2019 Alzheimer's disease facts and figures. *Alzheimers. Dement.* **15**, 321–387 (2019).

12. Pistollato, F. *et al.* Role of gut microbiota and nutrients in amyloid

formation and pathogenesis of Alzheimer disease. *Nutr. Rev.* **74**, 624–634 (2016).

13. Hemonnot, A.-L., Hua, J., Ulmann, L. & Hirbec, H. Microglia in Alzheimer Disease: Well-Known Targets and New Opportunities. *Front. Aging Neurosci.* **11**, 233 (2019).

14. González-Reyes, R. E., Nava-Mesa, M. O., Vargas-Sánchez, K., Ariza-Salamanca, D. & Mora-Muñoz, L. Involvement of Astrocytes in Alzheimer's Disease from a Neuroinflammatory and Oxidative Stress Perspective. *Frontiers in Molecular Neuroscience* vol. 10 Preprint at https://doi.org/10.3389/fnmol.2017.00427 (2017).

15. C. Y. Daniel Lee, G. E. L. The role of microglia in amyloid clearance from the AD brain. *J. Neural Transm.* **117**, 949 (2010).

16. Cerovic, M., Forloni, G. & Balducci, C. Neuroinflammation and the Gut Microbiota: Possible Alternative Therapeutic Targets to Counteract Alzheimer's Disease? *Front. Aging Neurosci.* **11**, (2019).

17. Fassbender, K. *et al.* The LPS receptor (CD14) links innate immunity with Alzheimer's disease. *FASEB J.* **18**, 203–205 (2004).

18. Guilherme, M. dos S., dos Santos Guilherme, M., Nguyen, V. T. T., Reinhardt, C. & Endres, K. Impact of Gut Microbiome Manipulation in 5xFAD Mice on Alzheimer's Disease-Like Pathology. *Microorganisms* vol. 9 815 Preprint at https://doi.org/10.3390/microorganisms9040815 (2021).

19. Webberley, T. S. *et al.* The Impact of Probiotic Supplementation on Cognitive, Pathological and Metabolic Markers in a Transgenic Mouse Model of Alzheimer's Disease. *Frontiers in Neuroscience* vol. 16 Preprint at https://doi.org/10.3389/fnins.2022.843105 (2022).

20. Chen, C. *et al.* Gut dysbiosis contributes to amyloid pathology, associated with C/EBPβ/AEP signaling activation in Alzheimer's disease mouse model. *Science Advances* vol. 6 Preprint at https://doi.org/10.1126/sciadv.aba0466 (2020).

21. Wang, X. *et al.* Sodium oligomannate therapeutically remodels gut microbiota and suppresses gut bacterial amino acids-shaped neuroinflammation to inhibit Alzheimer's disease progression. *Cell Res.* **29**, 787–803 (2019).

22. Hazan, S. Rapid improvement in Alzheimer's disease symptoms following fecal microbiota transplantation: a case report. *Journal of International Medical Research* vol. 48 030006052092593 Preprint at https://doi.org/10.1177/0300060520925930 (2020).

23. Park, S.-H. *et al.* Cognitive function improvement after fecal microbiota transplantation in Alzheimer's dementia patient: a case report. *Current Medical Research and Opinion* vol. 37 1739–1744 Preprint at https://doi.org/10.1080/03007995.2021.1957807 (2021).

24. Kelly, C. R. *et al.* Fecal microbiota transplant for treatment of Clostridium difficile infection in immunocompromised patients. *Am. J. Gastroenterol.* **109**, 1065–1071 (2014).

25. Xue, L.-J. *et al.* Fecal microbiota transplantation therapy for Parkinson's disease: A preliminary study. *Medicine* **99**, e22035 (2020).

26. Callahan, B. J. *et al.* DADA2: High-resolution sample inference from Illumina amplicon data. *Nat. Methods* **13**, 581–583 (2016).

27. Janssen, S. *et al.* Phylogenetic Placement of Exact Amplicon Sequences Improves Associations with Clinical Information. *mSystems* **3**, (2018).

28. Bokulich, N. A. *et al.* Optimizing taxonomic classification of marker-gene amplicon sequences with QIIME 2's q2-feature-classifier plugin. *Microbiome* vol. 6 Preprint at https://doi.org/10.1186/s40168-018-0470-z (2018).

29. Faith, D. P. Conservation evaluation and phylogenetic diversity. *Biological Conservation* vol. 61 1–10 Preprint at https://doi.org/10.1016/0006-3207(92)91201-3 (1992).

30. Shannon, C. E. A Mathematical Theory of Communication. *Bell System Technical Journal* vol. 27 379–423 Preprint at https://doi.org/10.1002/j.1538-7305.1948.tb01338.x (1948).

31. Lozupone, C. A., Hamady, M., Kelley, S. T. & Knight, R. Quantitative and qualitative beta diversity measures lead to different insights into factors that structure microbial communities. *Appl. Environ. Microbiol.* **73**, 1576–1585 (2007).

32. Lozupone, C. & Knight, R. UniFrac: a new phylogenetic method for comparing microbial communities. *Appl. Environ. Microbiol.* **71**, 8228–8235 (2005).

33. Bokulich, N. A. *et al.* q2-longitudinal: Longitudinal and Paired-Sample Analyses of Microbiome Data. *mSystems* **3**, (2018).

34. Anderson, M. J. Permutational Multivariate Analysis of Variance (PERMANOVA). *Wiley StatsRef: Statistics Reference Online* 1–15 Preprint at https://doi.org/10.1002/9781118445112.stat07841 (2017).

35. Mandal, S. *et al.* Analysis of composition of microbiomes: a novel method for studying microbial composition. *Microb. Ecol. Health Dis.* **26**, 27663 (2015).

36. Nawaz, A. *et al.* CD206 M2-like macrophages regulate systemic glucose metabolism by inhibiting proliferation of adipocyte progenitors. *Nat. Commun.* **8**,

286 (2017).

37. Davis, M. J. *et al.* Macrophage M1/M2 polarization dynamically adapts to changes in cytokine microenvironments in Cryptococcus neoformans infection. *MBio* **4**, e00264–13 (2013).

38. Dietmaier, W., Wittwer, C. & Sivasubramanian, N. *Rapid Cycle Real-Time PCR — Methods and Applications: Genetics and Oncology*. (Springer Science & Business Media, 2013).

39. Du Toit, A. Principles of microbiota engraftment. *Nat. Rev. Microbiol.* **16**, 186–186 (2018).

40. Oh, K.-J. *et al.* Staging of Alzheimer's Pathology in Triple Transgenic Mice: A Light and Electron Microscopic Analysis. *International Journal of Alzheimer's Disease* vol. 2010 1–24 Preprint at https://doi.org/10.4061/2010/780102 (2010).

41. Rao, X., Huang, X., Zhou, Z. & Lin, X. An improvement of the 2ˆ(-delta delta CT) method for quantitative real-time polymerase chain reaction data analysis. *Biostat. Bioinform. Biomath.* **3**, 71–85 (2013).

42. Kiyota, T. *et al.* CCL2 affects β-amyloidosis and progressive neurocognitive dysfunction in a mouse model of Alzheimer's disease. *Neurobiol. Aging* **34**, (2013).

43. Cherry, J. D., Olschowka, J. A. & O'Banion, M. K. Neuroinflammation and M2 microglia: the good, the bad, and the inflamed. *J. Neuroinflammation* **11**, 98 (2014).

44. D'Amato, A. *et al.* Faecal microbiota transplant from aged donor mice

affects spatial learning and memory via modulating hippocampal synaptic plasticity-and neurotransmission-related proteins in young recipients. *Microbiome* **8**, 140 (2020).

45. Fujii, Y. *et al.* Fecal metabolite of a gnotobiotic mouse transplanted with gut microbiota from a patient with Alzheimer's disease. *Bioscience, Biotechnology, and Biochemistry* vol. 83 2144–2152 Preprint at https://doi.org/10.1080/09168451.2019.1644149 (2019).

46. Dodiya, H. B. *et al.* Synergistic depletion of gut microbial consortia, but not individual antibiotics, reduces amyloidosis in APPPS1-21 Alzheimer's transgenic mice. *Sci. Rep.* **10**, 1–10 (2020).

47. Kawakubo-Yasukochi, T. *et al.* Hepatic glycogenolysis is determined by maternal high-calorie diet via methylation of Pygl and it is modified by oteocalcin administration in mice. *Mol Metab* **54**, 101360 (2021).

48. Zarrinpar, A. *et al.* Antibiotic-induced microbiome depletion alters metabolic homeostasis by affecting gut signaling and colonic metabolism. *Nat. Commun.* **9**, 2872 (2018).

49. Kang, D.-W. *et al.* Microbiota Transfer Therapy alters gut ecosystem and improves gastrointestinal and autism symptoms: an open-label study. *Microbiome* **5**, (2017).

50. Wilson, B. C. *et al.* Strain engraftment competition and functional augmentation in a multi-donor fecal microbiota transplantation trial for obesity. *Microbiome* **9**, 1–16 (2021).

51. Nakajima, A. *et al.* A Soluble Fiber Diet Increases Bacteroides fragilis

Group Abundance and Immunoglobulin A Production in the Gut. *Appl. Environ. Microbiol.* **86**, (2020).

52. Miyamoto, Y. & Itoh, K. Bacteroides acidifaciens sp. nov., isolated from the caecum of mice. *Int. J. Syst. Evol. Microbiol.* **50 Pt 1**, 145–148 (2000).

53. Haran, J. P. *et al.* Alzheimer's Disease Microbiome Is Associated with Dysregulation of the Anti-Inflammatory P-Glycoprotein Pathway. *mBio* vol. 10 Preprint at https://doi.org/10.1128/mbio.00632-19 (2019).

54. Zhao, Y., Jaber, V. & Lukiw, W. J. Secretory Products of the Human GI Tract Microbiome and Their Potential Impact on Alzheimer's Disease (AD): Detection of Lipopolysaccharide (LPS) in AD Hippocampus. *Front. Cell. Infect. Microbiol.* **7**, 318 (2017).

55. Hsiao, E. Y. *et al.* Microbiota modulate behavioral and physiological abnormalities associated with neurodevelopmental disorders. *Cell* **155**, 1451–1463 (2013).

56. Wexler, H. M. Bacteroides: the Good, the Bad, and the Nitty-Gritty. *Clin. Microbiol. Rev.* **20**, 593 (2007).

57. Hill, J. M. & Lukiw, W. J. Microbial-generated amyloids and Alzheimer's disease (AD). *Front. Aging Neurosci.* **7**, 9 (2015).

58. Choi, V. M. *et al.* Activation of Bacteroides fragilis toxin by a novel bacterial protease contributes to anaerobic sepsis in mice. *Nat. Med.* **22**, 563–567 (2016).

59. Lukiw, W. J. Bacteroides fragilis Lipopolysaccharide and Inflammatory Signaling in Alzheimer's Disease. *Front. Microbiol.* **7**, (2016).

60. Hiippala, K., Kainulainen, V., Kalliomäki, M., Arkkila, P. & Satokari, R. Mucosal Prevalence and Interactions with the Epithelium Indicate Commensalism of Sutterella spp. *Front. Microbiol.* **0**, (2016).

61. Sanguinetti, E. *et al.* Microbiome-metabolome signatures in mice genetically prone to develop dementia, fed a normal or fatty diet. *Scientific Reports* vol. 8 Preprint at https://doi.org/10.1038/s41598-018-23261-1 (2018).

62. Chen, Y. *et al.* Gut Microbiome Alterations Precede Cerebral Amyloidosis and Microglial Pathology in a Mouse Model of Alzheimer's Disease. *BioMed Research International* vol. 2020 1–15 Preprint at https://doi.org/10.1155/2020/8456596 (2020).

63. Dunham, S. J. B. *et al.* Longitudinal analysis of the gut microbiome in the 5xfAD mouse model of Alzheimer's disease. Preprint at https://doi.org/10.1101/2022.03.02.482725.

64. Khoury, R., Mdawar, B. & Ghossoub, E. Selective serotonin reuptake inhibitors and Alzheimer's disease. *Neural Regeneration Research* vol. 15 41 Preprint at https://doi.org/10.4103/1673-5374.264445 (2020).

65. Aaldijk, E. & Vermeiren, Y. The role of serotonin within the microbiota-gut-brain axis in the development of Alzheimer's disease: A narrative review. *Ageing Res. Rev.* **75**, 101556 (2022).

66. Borsom, E. M. *et al.* Predicting neurodegenerative disease using pre-pathology gut microbiota composition: a longitudinal study in mice modeling Alzheimer's disease pathologies. Preprint at https://doi.org/10.21203/rs.3.rs-1538737/v1.

67. Sarkar, A., Yoo, J. Y., Dutra, S. V. O., Morgan, K. H. & Groer, M. The Association between Early-Life Gut Microbiota and Long-Term Health and Diseases. *J. Clin. Med. Res.* **10**, (2021).

CHAPTER 4: Shallow shotgun metagenomic sequencing of observational and interventional studies in 3xTg-AD mice Alzheimer's disease pathologies reveals unique species- and strain- level gut microbes

ABSTRACT

There is mounting evidence to support the involvement of the gut microbial communities and their impact on host health in Alzheimer's disease (AD) via the gut microbiota-brain axis, yet only one study to date has employed the highly accurate taxonomic profiling of shallow shotgun metagenomic sequencing (SSMS) in 5xFAD mice, which model amyloid-β plaques. For the first time in 3xTg-AD mice, which model amyloid-β plaques

and neurofibrillary tangles, we investigate the gut microbiota composition using SSMS to provide accurate species and strain level taxonomic classification. In an observational study, fecal samples were sequenced at three time points; 2 months (pre-pathology, n=6 3xTg-AD, n=10 WT), 6 months (modeling amyloidosis, n=15 3xTg-AD, n=8 WT), and 12 months (modeling amyloidosis and neurofibrillary tangles, n=18 3xTg-AD, n=6 WT). Secondarily, we performed a fecal microbiota transplant (FMT) from aged 3xTg-AD mice (12-19 months) into young WT and 3xTg-AD mice. In this study, samples were sequenced pre-FMT treatment at 2 months of age (n=5 3xTg-AD, n=10 WT), and after 16 weeks of FMT treatment at 6 months of age (n=5 3xTg-AD, n=10 WT). Alpha diversity, beta diversity, differential abundance, and a clustered heatmap analysis were performed with QIIME2. In the longitudinal study, observed features are reduced in 3xTg-AD mice at 6 months compared to WT mice (Kruskal-Wallis all group, p-value = 0.046), and Bray-Curtis demonstrates distinct differences between 3xTg-AD and WT mice at 2, 6, and 12 months of age. *Ligilactobacillus* species are differentially abundant when comparing WT and 3xTg-AD mice at 2 and 6 months, while the heatmap reveals difference in relative proportion of species in *Bacteroides* and *Turicibacter* between mouse genotype and time points. In the FMT study, observed features are increased in PBS-treated WT mice compared to the other groups at 6 months (Kruskal-Wallis all group, p=0.025), and Bray-Curtis demonstrates distinct differences between treatment groups at 2 and 6 months of age. *Ligilactobacillus* species are differentially abundant between FMT treatment groups at 2 and 6 months, while the heatmap reveals difference in relative proportion of *Limosiloactobacillus reuteri, Duncaniella dubosii,* and species in *Bacteroides* and *Turicibacter* between FMT treatment group before and after

treatment. These analyses reveal new findings on the distinct gut microbiota composition associated with AD pathologies, with and without FMT intervention, using SSMS.

INTRODUCTION

The discovery of the 16S rRNA gene for microbial classification by Carl Woese in 1977 has allowed scientists to uncover the 98-99% of microbes that are unculturable in the lab setting.[1] The communities of microbes and their genetic material that inhabit a defined niche, termed the microbiome, has revolutionized our understanding of complex microbial ecosystems and their interactions.[2] Further, the field of microbiome sciences has revealed the invisible world of microorganisms that have evolved to benefit ecosystems, including the intricate microbial life within and on the human body.[3] Early microbiome studies used gene amplification methods, including 16S rRNA gene, ITS1/ITS2, and 18S rRNA gene to classify bacterial, fungal, and eukaryotic microbial communities.[4] However, amplicon sequencing limits the resolution of microbial classification due to short sequence reads of one, or a few, hypervariable genes.[5] The future of microbiome studies relies on the use of RNAseq, metabolomics, proteomics, and shotgun sequencing, collectively known as multi-omics, to elucidate the functional capacities of the microbiome, and their impact on host health.[6]

Neurodegenerative diseases are associated with shifts in the gut microbial communities of both murine models[7–10] and patients with Parkinson's disease,[11] Huntington's disease,[12] multiple sclerosis,[13] and Alzheimer's disease (AD).[14] AD is the most common

cause of dementia, affecting 1 in 9 people over the age of 65.[15] Recent studies have investigated how a shift in the microbiome composition,[16–18] or the absence of the gut microbiota,[19] affects disease manifestation in transgenic mice modeling AD pathologies. Probiotic and fecal microbiota transplantation methods have shown to alleviate or exacerbate cognitive impairment[20] and amyloidosis[20] in transgenic AD murine models.[20–22] Yet, few studies have used shotgun metagenomic sequencing to provide deeper resolution of microbial communities across all three domains of life in the gastrointestinal tract in AD.[23–26]

In this study, we sought to further characterize the gut microbiome in 3xTg-AD mice using shallow shotgun metagenomic sequencing (SSMS) to reveal strain- and species-level microbes, and their metabolic potential, in one observational and one interventional study design. We hypothesized that SSMG would greatly improve the taxonomic resolution over our prior studies using 16S rRNA gene sequencing. Further, our prior studies have demonstrated that *Bacteroides* may play a critical role in the pathologies associated with AD, however, we were unable to accurately speciate *Bacteroides* using 16S rRNA gene sequencing. A second aim of our study was to differentiate the *Bacteroides* species within the 3xTg-AD gut microbiome.

METHODS

Transgenic mouse models: 3xTg-AD (with overexpression of APP(Swe), PSEN1(M146V), and MAPT(P301L) transgenes) and Wild Type (B6129F2/J; WT) breeders and FMT study mice were purchased from Jackson Laboratory (Bar Harbor,

Maine). All mouse experiments were approved by the Institutional Animal Use and Care Committee of Northern Arizona University under protocol 18-016.

Longitudinal study mouse colonies: Mice were purchased from Jackson Laboratory (3xTg-AD, WT), and allowed seven days to acclimate to the Animal Facility at Northern Arizona University. Mice were then combined into harems, housed in a 12 hour light/dark cycle, and provided food and water *ad libitum*. In-house bred mice were weaned at 21 days of age and female mice of the same strain were separated and housed in cages of three to five mice for the remainder of the animal study (n=88 total mice, n=57 3xTg-AD, n=31 WT). Weaned female mice were given one week to acclimate and adjust to their new food prior to the first sample collection. Fecal samples were collected directly from each mouse fortnightly starting at 4 weeks until sacrifice for longitudinal gut microbiota analysis and were stored at −80 °C until further processing.

Mice were euthanized with CO_2 at 8, 24, or 52 weeks. Sample sizes are as follows; 3xTg-AD (n = 6 at 2 months, n = 15 at 6 months, n = 18 at 12 months) and WT (n = 10 at 2 months, n = 8 at 6 months, and n = 6 at 12 months).

FMT Study: All mice were purchased from Jackson Laboratory, including aged 3xTg-AD donors, and allowed 5 days to acclimate. Cages housed 5 mice and were provided food and water *ad libitum.* Fecal samples were collected directly from each mouse fortnightly starting at 8 weeks until sacrifice for longitudinal gut microbiota analysis and were stored at −80 °C until further processing. Mice were euthanized with CO_2 at 24

weeks of age. Sample sizes are as follows; 3xTg-AD-FMT (n = 5), 3xTg-AD-PBS (n = 5), WT-PBS (n = 10), and WT-PBS (n = 10). For immunohistochemistry (not included in this manuscript), 2-3 mice were sacrificed per group using transcardial perfusion and do not have 24 week fecal sample timepoints.

Genotyping: Ear punches were collected at 4 weeks from 3xTg-AD mice for genotyping. DNA was extracted using the Qiagen Blood and Tissue kit (Qiagen, Hilden, Germany). PCR was run with the KAPA mouse genotyping kit and Jackson Laboratory approved primers for APPSwe and P301L transgenes. Amplicons were run on a 3% agarose gel to confirm the presence of bands representing APP(Swe) and MAPT(P301L) genes (ThermoFisher, Waltham, Massachusetts).

Nucleic Acid Extraction and shallow shotgun metagenomic sequencing: DNA and RNA were extracted in parallel from feces using the MagMAX Pathogen RNA/DNA Kit from ThermoFisher. Extractions were performed in a Class II Biosafety Cabinet using protocols adopted from eukaryotic cell culture to protect the samples from contamination (i.e., decontaminate all materials with 70% EtOH to bring into the BSC, double glove while in the BSC, and don single use PPE while working in the BSC). Modifications to the protocol include the use of Lysing Matrix E tubes (MP Biomedical, Irvine, California) for bacterial and fungal lysis. Both DNA and RNA were quantified using a NanoDrop 2000. Library was prepped with the Nextera XT DNA Library Prep Kit and indexed with TG Nextera® XT Index Kit v2 Set A (Illumina, San Diego, California). DNA libraries were quantified using fluorometry and pooled at equimolar ratios. Quality

of the pool was assessed with the Bioanalyzer DNA 1000 chip (Agilent Technologies, Santa Clara, California) then combined with 1% PhiX for sequencing. A total of 4 pools were sequenced using the NextSeq 500/550 High Output Kit v2.5 (150 Cycles) (Illumina, San Diego, California). All sequencing was done on the Illumina NextSeq.

Bioinformatics Analysis: Shotgun sequence reads were processed utilizing a tailor-made bioinformatic workflow designed to automate and improve the computational reproducibility of operational taxonomic unit (OTU) based metagenomic analyses. Sequence read quality was assessed using a combination of fastqc and multiqc.[27] Host DNA was identified as reads contaminants and were removed using KneadData (https://github.com/biobakery/kneaddata).[28] Species-level taxonomic classifications and relative abundance estimations of microbial reads were performed using Kraken2 and Bracken.[29,30] Kraken2 is a taxonomic profiling program that classifies archaea, bacteria, viruses, fungi, and other eukaryotic microbes, while Bracken is a taxonomic profiling program limited to the classification of archaea and bacteria. Sequence references were downloaded and compiled together from the NCBI nucleotide database (https://www.ncbi.nlm.nih.gov/nuccore/). Subsequent report files were compiled into a single BIOM formatted file using kraken-biom (https://github.com/smdabdoub/kraken-biom). Microbiome bioinformatics were performed with QIIME 2 version 2022.2. Taxonomy was assigned to reads using q2-feature-classifier and the NCBI reference database.[31,32] Observed features were computed with q2-diversity[33]. Beta diversity (community dissimilarity) metrics were computed with q2-diversity, including Bray-Curtis dissimilarity and Jaccard dissimilarity distances. Group comparisons of alpha diversity were performed with non-parametric Wilcoxon tests, and group comparisons of beta

diversity were performed with non-parametric PERMANOVA[34]. Taxa that were differentially abundant across mouse genotypes or mouse genotype-treatment groups were identified using ANCOM.[35] All P-values were corrected for multiple comparisons using the Benjamini-Hochberg False Discovery Rate correction. The heatmaps were produced with q2-sample-classifier filtering for a minimum abundance of 0.001 and minimum prevalence of 0.25.[36]

RESULTS

Analysis of gut microbiota composition using SSMS in observational and interventional studies

To assess species- and strain- level bacteria, archaea, fungi, viruses, and other eukaryotic microbes in an observational study, we collected fecal samples from 2, 6, and 12 months of age from 3xTg-AD and B6129F2/J (WT) mice. These three timepoints represent the gut microbiota composition associated with pre-pathology, amyloidosis, and amyloidosis with tauopathy (Figure S1). For the interventional study, a fecal microbiota transplantation was performed from female donor mice (12-19 months of age) to 2 month old 3xTg-AD and WT mice for five consecutive days, followed by fortnightly FMT treatments until 6 months of age. Fecal samples were collected at 2 months and 6 months and from donor mice to assess which microbial features were engrafted from the donor microbiota by 6 months of age.

Sequencing depth using 16S rRNA gene sequencing compared to SSMS

To demonstrate the improved sequencing depth for SSMS compared to 16S rRNA gene sequencing, we computed the average sequencing depth for the observational and interventional studies by sequencing technique. The average sequencing depth for the observational study using 16S rRNA gene sequencing had a sample frequency of 26,098 on average, while SSMS yielded 2.74 million reads on average per sample after trimming. Similarly, the average depth for the observational study using 16S rRNA gene sequencing had a sample frequency of 21,694, while SSMS yielded 2.09 million reads on average per sample after trimming.

Non-phylogenetic alpha diversity metrics reveal 3xTg-AD mice have lower microbial diversity associated with disease pathology modeling

To investigate the differences within and between gut microbiota composition, alpha and beta diversity analysis were performed on the longitudinal and observation studies in 3xTg-AD mice. Alpha diversity, or within sample diversity, was analyzed using Observed Features and Shannon Diversity Index at 2, 6, and 12 months of age using Kraken2 and Bracken. Kraken2 is a taxonomic profiling program that classifies archaea, bacteria, viruses, fungi, and other eukaryotic microbes, while Bracken is a taxonomic profiling program limited to the classification of archaea and bacteria.

In the longitudinal mouse study with Bracken, we observed reduced alpha diversity (observed features) at 2 and 6 months of in WT mice compared to 3xTg-AD mice, though this only reached statistical significance at 6 months of age (Fig 1B; Kruskal-

Wallis, p-value = 0.045). No statistically significant difference in alpha diversity was observed at 12 months of age between WT and 3xTg-AD mice (Fig. 1C). It is possible that the lower sampling frequency at 2 months (Kruskal-Wallis, p-value = 0.17791) and 12 months (Kruskal-Wallis, p-value = 0.200217) decreased the statistical power of the comparisons, as we computed a power size of 8 samples/genotype/timepoint in a previous power calculation using R (pwr.anova.test(k=6, n=8, f=.55,sig.level=.05)). In the longitudinal study with Kraken 2, we observed non significant trend towards decreased observed features in WT mice at 2 months (Kruskal-Wallis, p-value = 0.391267) and 6 months (Kruskal-Wallis, p-value = 0.067889) of age compared to 3xTg-AD mice, and a non significant trend towards increased observed features in WT compared to 3xTg-AD mice at 12 months of age (Kruskal-Wallis, p-value = 0.200217).

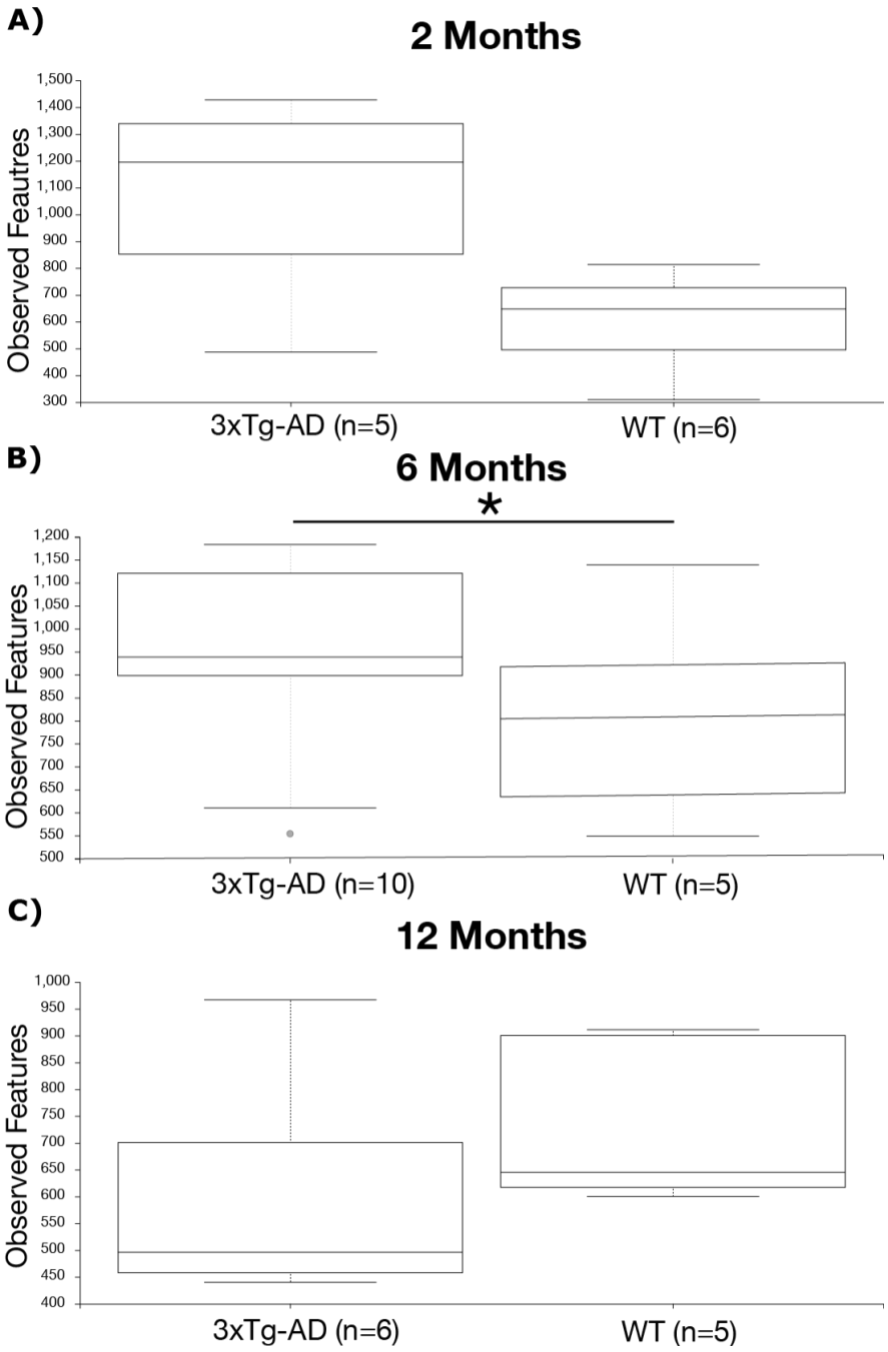

Figure 1. Observed Features at 2, 6, and 12 months of age in 3xTg-AD and WT mice using Bracken. A) Observed features trend towards a non-significant decrease in WT mice compared to 3xTg-AD at 2 months of age (Kruskal-Wallis, p-value = 0.17791). B) Observed features are significantly decreased in WT mice compared to 3xTg-AD at 6 months of age (Kruskal-Wallis, p-value = 0.04461). C) Observed features trend towards a non-significant increase in WT mice compared to 3xTg-AD at 12 months of age (Kruskal-Wallis, p-value = 0.200217).

Weighted beta diversity metrics suggest highly abundant taxa are driving differences in 3xTg-AD mice compared to WT mice

Beta diversity (between-sample) metrics were used to identify compositional differences in the bacterial gut microbiota between 3xTg-AD and WT mice at 2, 6, and 12 months of age. We applied Bray Curtis dissimilarity index and Jaccard similarity index, which are weighted and unweighted metrics, respectively, with taxonomy from Bracken and Kraken2. PCoA of Jaccard using Kraken2 (Figure 2A) and Bracken (Figure 2C) show separation between 3xTg-AD and WT mice at 2 months of age [(Kraken2 PERMANOVA, p=0.028, f-statistic=1.292549; Bracken PERMANOVA, p=0.018, f-statistic=1.348104)], but not at 6 months [(Kraken2 PERMANOVA, p=0.234, f-statistic=1.028158; Bracken PERMANOVA, p=0.299, f-statistic=1.019968)] or 12 months of age [(Kraken2 PERMANOVA, p=0.142, 1.061627; Bracken PERMANOVA, p=0.051, f-statistic=1.114975)]. PCoA of Bray Curtis using Kraken2 (Figure 2B) and Bracken (Figure 2D) shows separation between 3xTg-AD and WT mice at 2 months [(Kraken2 PERMANOVA, p=0.001, f-statistic=6.610184; Bracken PERMANOVA, p=0.005, f-statistic=6.652388)], 6 months [(Kraken2 PERMANOVA, p=0.001, f-statistic=3.668729; Bracken PERMANOVA, p=0.001, f-statistic=3.703339)], and 12 months (Kraken2 PERMANOVA, p=0.015, f-statistic=3.518673; Bracken PERMANOVA, p=0.021, f-statistic=3.428344)] of age. These findings suggest high abundance microbial communities are driving the differences between 3xTg-AD and WT mice, which contrasts our previous findings where unweighted metrics showed more separation between mouse genotype.

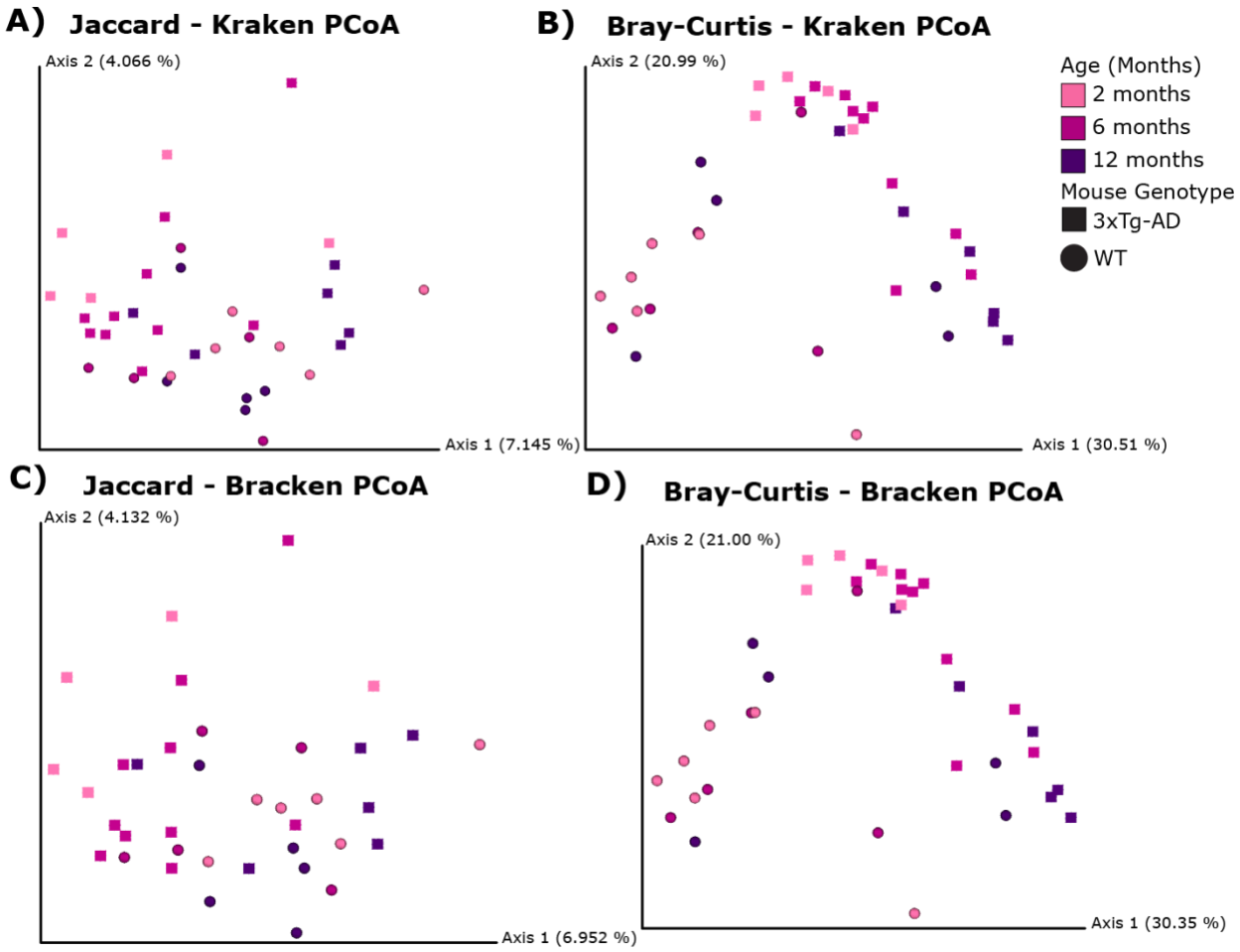

Figure 2. Weighted metric beta diversity PCoA demonstrates a strong separation between 3xTg-AD and WT mice at 2, 6, and 12 months of age. A) PCoA of Jaccard similarity index using Kraken2. This plot shows clear separation by mouse genotype at 2 months (PERMANOVA, p=0.028, f-statistic=1.292549), but no clear separation based on age or mouse genotype at 6 months (PERMANOVA, p=0.234, f-statistic=1.028158) or 12 months of age (PERMANOVA, p=0.142, 1.061627). B) PCoA of Bray-Curtis dissimilarity index using Kraken2. This plot demonstrates clear separation by mouse genotype at 2 months (PERMANOVA, p=0.001, f-statistic=6.610184), 6 months (PERMANOVA, p=0.001, f-statistic=3.668729), and 12 months of age (PERMANOVA, p=0.015, f-statistic=3.518673).C) PCoA of Jaccard dissimilarity index using Bracken. This plot shows clear separation by mouse genotype at 2 months (PERMANOVA, p=0.018, f-statistic=1.348104), but no clear separation based on age or mouse genotype at 6 months (PERMANOVA, p=0.299, f-statistic=1.019968) or 12 months of age (PERMANOVA, p=0.051, f-statistic=1.114975). D) PCoA of Bray-Curtis dissimilarity index using Bracken.This plot demonstrates clear separation by mouse genotype at 2 months at 2 months (PERMANOVA, p=0.005, f-statistic=6.652388), 6 months (PERMANOVA, p=0.001, f-statistic=3.703339), or 12 months of age (PERMANOVA, p=0.021, f-statistic=3.428344).

Identifying microbial features that differentiate mouse genotype using a heatmap

To further explore the relative proportions of important microbial features between mouse genotypes, a heatmap was produced with the parameters including microbial features with prevalence of at least 0.001 in at least 25% of the longitudinal samples at 2, 6, and 12 months of age (Figure 3). The clustered heatmap shows increased abundance of *Ligilactobacillus animali*s, *Ligilactobacillus murinis*, and *Ligilactobacillus sp.* in WT mice compared to 3xTg-AD mice at all the time points. *Turicibacter sp., Turicibacter sanguinis*, and *Turicibacter sp.* H121 were enriched at 2 months of age, but depleted by 6 and 12 month age time points. By 12 months of age, 3xTg-AD mice are enriched with *Bacteroides CBA7301, Bacteroides xylanisolvens, Bacteroides caccae*, *Bacteroides ovatus, Bacteroides thetaiotaomicron,* and *Bacteroides fragilis*. Finally, *Faecalibacterium rodentium* is enriched in 3xTg-AD mice at 6 and 12 months of age.

Figure 3. Heat map of microbial features in the longitudinal study. Relative proportion of microbial features parameters with a prevalence of at least 0.001 in at least 25% of the longitudinal samples at 2, 6, and 12 months of age.

Differential abundance analysis reveals three Ligilactoabillus species drive differences between the gut microbiota composition between 3xTg-AD and WT mice

To identify differentially abundant microbial communities at each time point, Analysis of Compositions of Microbiomes (ANCOM) was run at 2, 6, and 12 months on longitudinal mice and 2 and 6 months in FMT mice. At 2 and 12 months of age, *Ligilactobacillus animali*s, *Ligilactobacillus murinis*, and *Ligilactobacillus sp.* were differentially abundant between 3xTg-AD and WT mice, but not at 6 months of age. A sub-analysis was performed where *Ligilactobacillus animali*s, *Ligilactobacillus murinis*, and *Ligilactobacillus sp.* were filtered to investigate other taxa that are differentially abundant, but not significant when compared to *Ligilactobacillus sp.* that are highly enriched in the gut microbiota composition.

Table 1: Differential abundance between 3xTg-AD and WT mice using Analysis of Composition of Microbiomes (ANCOM) collapsed at species level at 2, 6, and 12 months. W represents the number of features that the taxa is more abundant than.

Features Collapsed at Species Level	W	Month
Ligilactobacillus animalis	7771	2
Ligilactobacillus murinus	7771	2
Ligilactobacillus sp.	7771	2
Ligilactobacillus murinus	7940	12
Ligilactobacillus sp.	7940	12
Ligilactobacillus animalis	3967	12

Observed features decreased in all treatment groups compared to PBS treated WT mice following 16 weeks of FMT treatment.

Observed features, an alpha diversity metric that measures the number of unique taxa found in sample groups, was explored to identify differences across FMT treatment groups. At 2 months of age, when FMT treatments begin, there are no differences across all four treatment groups (FMT - 3xTg-AD, FMT - WT, PBS - 3xTg-AD, and PBS - WT) in all group (Kruskal-Wallis all group, p-value = 0.32311) or pairwise comparisons (Supplemental Table 1) using Bracken data (Figure 4A). At 6 months of age, following 12 weeks of FMT treatments, there was a significant difference between FMT treatment groups (p-value = 0.04387) using Bracken data (Figure 4B). Observed features were significantly increased in PBS treated WT mice when compared to FMT treated 3xTg-AD (Kruskal-Wallis all group, p-value = 0.025347), PBS - treated 3xTg-AD mice (Kruskal-Wallis pairwise, p-value = 0.049535), but not PBS treated WT mice (Kruskal-Wallis pairwise, p-value = 0.025347). Using the Kraken2 data, we observed no difference in observed features between all four treatment groups at 2 months (Kruskal-Wallis pairwise, p-value = 0.257286) and 6 months (Kruskal-Wallis pairwise, p-value = 0.055772) of age.

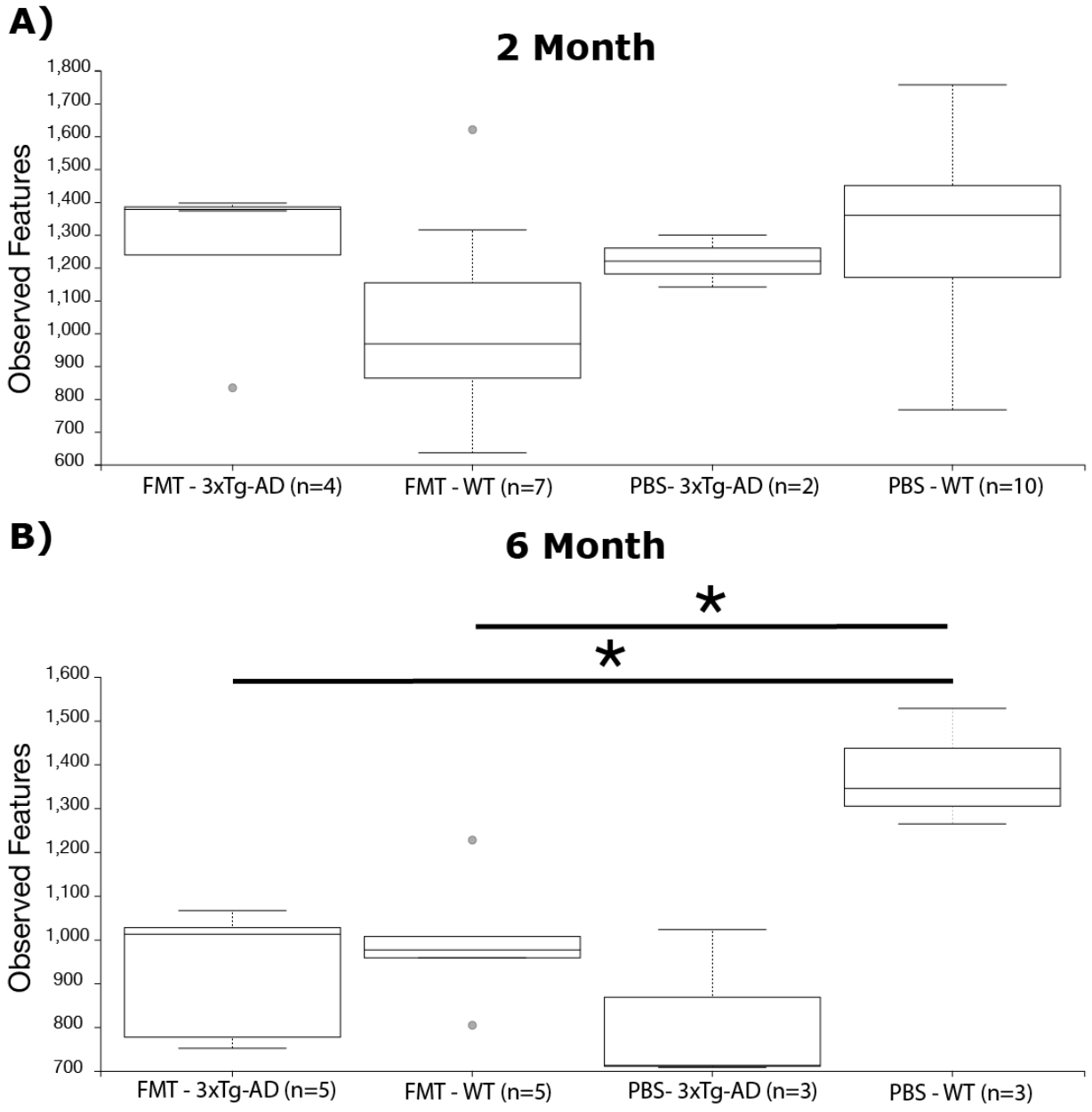

Figure 4. Observed Features at 2 and 6 months of age in FMT and PBS treated 3xTg-AD and WT mice using Bracken. A) Observed features do not differ between all four treatment groups (FMT - 3xTg-AD, FMT - 3xTg-AD, PBS - 3xTg-AD, and PBS - WT) at 2 months of age, when FMT treatment begins (Kruskal-Wallis all group, p-value = 0.32311). B) Observed features are significantly different between all four treatment groups at 6 months of age, following the 12 weeks of FMT treatment (Kruskal-Wallis all group, p-value = 0.04387).

Weighted beta diversity metrics suggest highly abundant taxa are driving differences between mouse genotype at 2 months and by treatment group at 6 months

Beta diversity metrics were used to identify compositional differences in the bacterial gut microbiota between all four treatment groups at 2 months of age and 6 months of age, representing pre-FMT treatment and post-FMT treatment. To explore these differences in microbiota composition, we produced PCoA plots of Jaccard similarity index and Bray Curtis dissimilarity index, which are unweighted and weighted metrics, respectively, with taxonomy from Bracken and Kraken2. PCoA of Jaccard using Kraken2 (Figure 5A) and Bracken (Figure 5C) show separation all treatment groups at 2 months of age [(Kraken2 PERMANOVA, $p<0.05$; Bracken PERMANOVA, $p<0.05$], regardless of treatment group, except FMT - 3xTg-AD compared to PBS - 3xTg-AD and PBS - 3xTg-AD compared to PBS - WT (Supp. Tables 2A and 2B). At 6 months, PCoA of Jaccard using Kraken2 (Figure 5A) and Bracken (Figure 5C) show separation between all treatment groups [(Kraken2 PERMANOVA, $p<0.05$; Bracken PERMANOVA, $p<0.05$], except FMT - 3xTg-AD compared to PBS - 3xTg-AD and PBS - 3xTg-AD compared to PBS - WT (Supp. Tables 2C and 2D). PCoA of Bray Curtis using Kraken2 (Figure 5A) and (Figure 5B) and Bracken (Figure 5D) show separation all treatment groups at 2 months of age [(Kraken2 PERMANOVA, $p<0.05$; Bracken PERMANOVA, $p<0.05$], regardless of treatment group, except FMT - 3xTg-AD compared to PBS - 3xTg-AD, FMT - WT compared to PBS - WT, and PBS - 3xTg-AD compared to PBS - WT (Supp. Tables 2D and 2E). At 6 months, PCoA of Jaccard using Kraken2 (Figure 4B) and Bracken (Figure 4D) show separation between all treatment groups [(Kraken2

PERMANOVA, p<0.05; Bracken PERMANOVA, p<0.05], except FMT - 3xTg-AD compared to PBS - 3xTg-AD, FMT - WT compared to PBS - WT, and PBS - 3xTg-AD compared to PBS - WT (Supp. Tables 2F and 2G). These findings suggest high abundance microbial communities are driving the differences between mouse genotype at 2 months of age, regardless of treatment group, and drive differences by treatment group at 6 months of age.

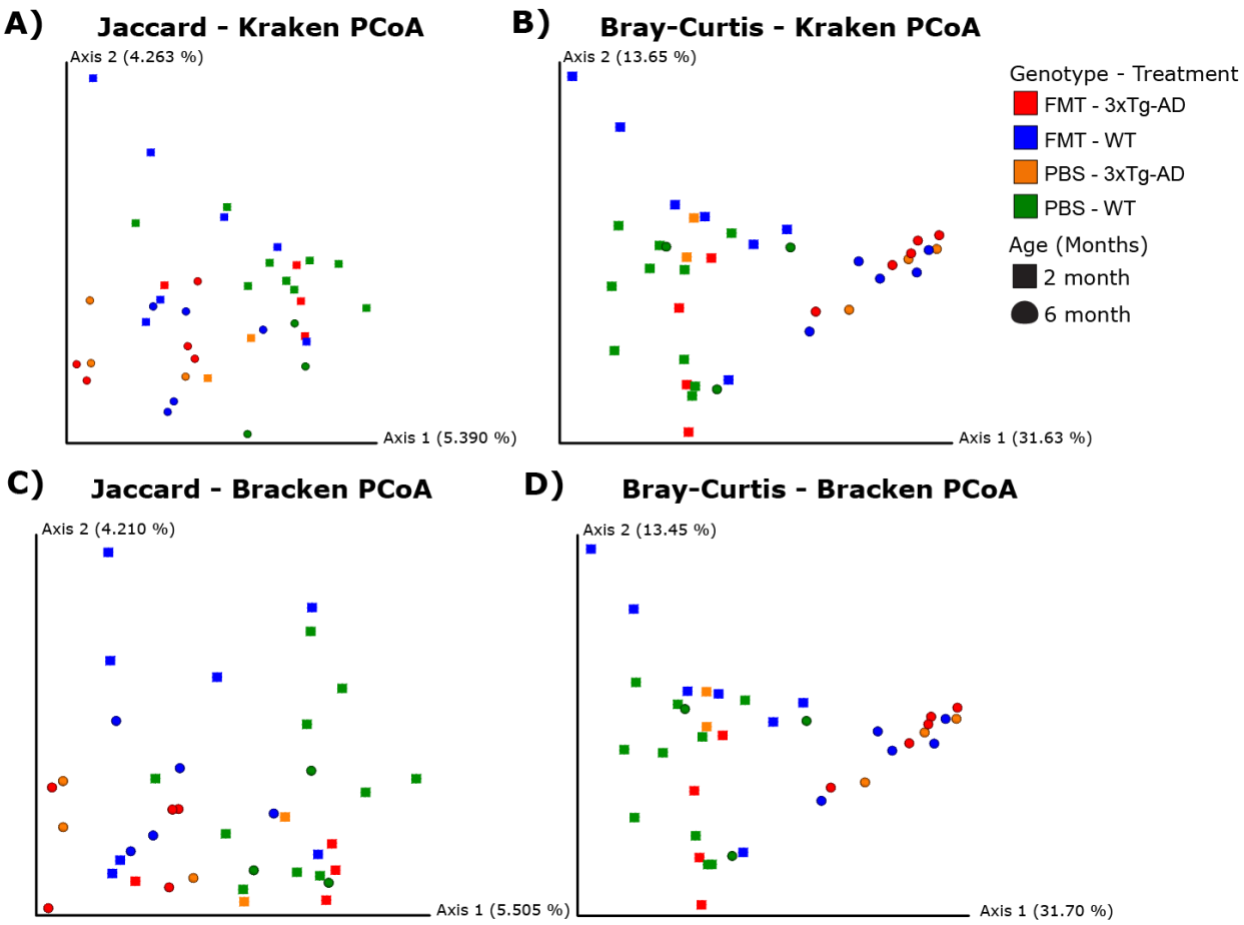

Figure 4. Non-phylogenetic beta diversity PCoA in the FMT Study. A) PCoA of Jaccard similarity index using Kraken2. This plot shows separation by mouse genotype at 2 months (PERMANOVA, p=0.001, f-statistic=1.20248) and by treatment groups at 6 months (PERMANOVA, p=0.001, f-statistic=1.23128). B) PCoA of Bray-Curtis dissimilarity index using Kraken2. This plot shows separation by mouse genotype at 2 months(PERMANOVA, p=0.004, f-statistic=2.44187) and by treatment groups at 6

months (PERMANOVA, p=0.001, f-statistic=2.48154). C) PCoA of Jaccard dissimilarity index using Bracken. This plot shows separation by mouse genotype at 2 months (PERMANOVA, p=0.001, f-statistic=1.23201) and by treatment groups at 6 months (PERMANOVA, p=0.001, f-statistic=1.21016). D) PCoA of Bray-Curtis dissimilarity index using Bracken. This plot shows separation by mouse genotype at 2 months (PERMANOVA, p=0.003, f-statistic=2.45507) and by treatment groups at 6 months (PERMANOVA, p=0.002, f-statistic=2.45218).

Identifying microbial features that differentiate FMT treatment groups using a heatmap

To further investigate the relative proportions of important microbial features in each FMT treatment group, a heatmap was produced with the parameters including microbial features with prevalence of at least 0.001 in at least 25% of the longitudinal samples at 2 and 6 months of age (Figure 6). The clustered heatmap shows decreased abundance of *Limosiloactobacillus reuteri* in WT mice at 2 and 6 months compared to 3xTg-AD mice, regardless of treatment group. *Turicibacter sp., Turicibacter sanguinis*, and *Turicibacter sp.* H121 were elevated at 2 months in WT and 3xTg-AD mice, but depleted in WT mice compared to 3xTg-AD mice at 6 months. *Duncaniella dubosii* is enriched in FMT treated 3xTg-AD and WT mice at 6 months compared to 2 months. FMT treated 3xTg-AD, FMT treated WT mice, and PBS treated 3xTg-AD mice were enriched with *Bacteroides CBA7301, Bacteroides xylanisolvens, Bacteroides caccae*, *Bacteroides ovatus* compared to PBS treated WT mice at 6 months. *Bacteroides thetaiotaomicron* was enriched in WT mice at 2 months compared to 3xTg-AD mice, regardless of treatment group.

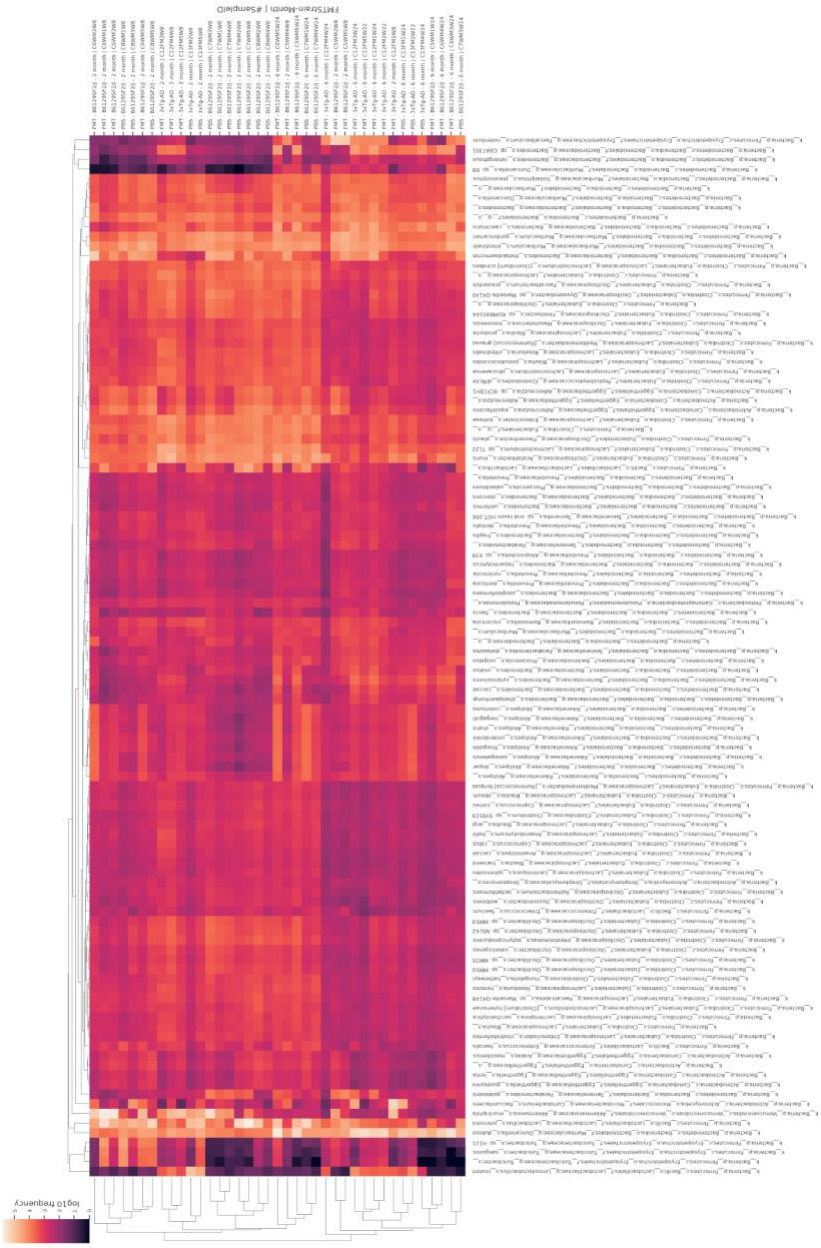

Figure 6. Heat map of microbial features in the FMT study. Relative proportion of microbial features parameters with a prevalence of at least 0.001 in at least 25% of the longitudinal samples at 2 and 6 months of age.

Differential abundance analysis reveals three Ligilactoabillus species drive differences between the gut microbiota composition between FMT treatment groups

Limosiloactobacillus reuteri was differentially abundant when comparing FMT treated 3xTg-AD and FMT treated WT mice, as well as PBS treated 3xTg-AD and PBS treated WT mice at 2 and 6 months of age. These findings suggest *Limosiloactobacillus reuteri* was unaffected by the FMT treatments. *Ligilactobacillus murinus* was differentially abundant in FMT treated 3xTg-AD and PBS treated 3xTg-AD mice at 6 months of age, as well as PBS treated 3xTg-AD and PBS treated WT mice at 6 months of age. Finally, *Ligilactobacillus animalis* was differentially abundant between PBS treated 3xTg-AD and PBS treated WT, but not between FMT treated 3xTg-AD and FMT treated WT mice at 6 months of age. We hypothesize that introduction of microbes via FMT treatment may outcompete *Ligilactobacillus animalis* in FMT treated WT mice by 6 months of age, which is 16 weeks into consecutive fortnightly treatments.

Table 2: Differential abundance between all 4 treatment groups using Analysis of Composition of Microbiomes (ANCOM) collapsed at species level at 2 and 6 months. W represents the number of features that the taxa is more abundant than.

Features Collapsed at Species Level	W	Higher Abundance	Comparison	Month
Limosiloactobacillus reuteri	7516	FMT - 3xTg-AD	FMT - WT	2
Limosiloactobacillus reuteri	8155	PBS - 3xTg-AD	PBS - WT	2
Ligilactobacillus murinus	7457	PBS - 3xTg-AD	FMT - 3xTg-AD	6
Limosiloactobacillus reuteri	7898	FMT - 3xTg-AD	FMT - WT	6

Ligilactobacillus murinus	8145	PBS - 3xTg-AD	PBS - WT	6
Limosiloactobacillus reuteri	8145	PBS - 3xTg-AD	PBS - WT	6
Ligilactobacillus animalis	8143	PBS - 3xTg-AD	PBS - WT	6

DISCUSSION

We have demonstrated SSMS yields higher taxonomic resolution when compared to 16S rRNA gene sequencing, and overall supports our previous findings. Using SSMS, we identified differences in alpha and beta diversity metrics between mouse genotypes and treatment groups, as well as microbial features at the species- and strain- level that are differentially abundant in observational and interventional studies in 3xTg-AD mice modeling AD pathologies. Further, the data presented supports our findings using 16S rRNA gene sequencing, while providing deeper insight into the species and strain level of the microbes identified in our previous work.

Gut microbiota alpha diversity is commonly used to assess host health.[37] Reduced alpha diversity is often associated with a disease state in both mice and humans, which is being explored as a biomarker of neurological diseases, including AD.[38] Our observational study reveals fewer observed features in 3xTg-AD mice at 6 months, when amyloidosis is first modeled. This may be attributed to the antimicrobial properties of amyloid-β peptides, which have been shown to impact the gut microbiota in 5xFAD mice.[39] However, other studies in 3xTg-AD mice found no differences in alpha diversity when comparing 3 and 5 month 3xTg-AD female mice[40] and no differences in alpha

diversity at 8, 12, 18, and 24 week old 3xTg-AD male mice compared to age-matched WT mice.[41] These differences may be attributed to our use of SSMS, compared to the 16S rRNA gene sequencing used in the other studies, as we found no differences in alpha diversity on samples when sequenced the 16S rRNA gene amplicon.[42]

Interestingly, in our 16S rRNA gene sequencing data, we observed that low abundance taxa were driving differences, illustrated by significant separation between 3xTg-AD and WT mice in unweighted beta diversity metrics (Jaccard Similarity Index and Unweighted Unifrac), but not in weighed beta diversity metrics (Bray-Curtis Dissimilarity Index and Weighted Unifrac). However, using SSMS, we observed high abundance taxa were driving differences, illustrated by significant separation between 3xTg-AD and WT mice in weighted beta diversity metrics (Bray-Curtis Dissimilarity Index), but not in unweighted beta diversity metrics (Jaccard Similarity Index). While the 16S rRNA gene sequencing data analysis of beta diversity did include more samples per time point, the differences between sequencing time may be due to more accurate taxonomic profiling and more reads per sample using SSMS. Further, we hypothesize that certain highly abundant taxonomic features are driving the significant differences in weighted metric between 3xTg-AD and WT mice. Based on differential abundance testing (ANCOM), relative abundance testing, and the heatmap, *Ligilactobacillus murinus*, *Ligilactobacillus animalis and Ligilactobacillus sp.* are depleted in 3xTg-AD mice compared to WT mice.

To date, only one other study has used SSMS on a transgenic mouse model of AD. A study by Dunham and colleagues investigated the gut microbiota using fecal and cecal

samples from 5xFAD mice at 4, 8, 12, and 18 months of age.[26] 5xFAD model amyloidosis at 2 months of age and do not model neurofibrillary tangles, whereas the mouse model used here (3xTg-AD) model amyloidosis at 6 months of age and neurofibrillary tangles at 12 months of age. In 5xFAD mice, they observed similar species in the mouse gut microbiome using SSMG, including *Ligilactobacillus murinus*, *Ligilactobacillus animalis, Limosiloactobacillus reuteri*, *Turicibacter sp.* H121. The majority of observed differences were at 18 months of age, when WT mice had increased levels of *L. reuteri* and *Turicibacter* sp H121 compared to 5xFAD mice. . In 3xTg-AD mice, we observed increased relative proportions of *Turicibacter sp.* H121 at 2 months, but abundance decreased as mice aged to 6 and 12 months to levels similar to WT mice. In our WT mice, we show increased abundance of *Ligilactobacillus murinus* and *Ligilactobacillus animalis* at 2 and 12 months of age, but not at 6 months. Interestingly, we observed changes in the microbiome in early, pre-pathology timepoints, which is in contrast to the study performed in 5xFAD mice (they did not sample pre-pathology development). Since these are two distinct models of AD, we don't expect to see exact convergence of findings, though we were encouraged to see similar taxonomic groups in these two mouse models using SSMG, despite differences in location and genotype.

In our FMT study, there was no difference in alpha diversity between FMT treatment groups (FMT - 3xTg-AD, FMT - WT, PBS - 3xTg-AD, and PBS - WT) at prior to FMT treatment at 2 months, as we anticipated due to no prior intervention. However, following the FMT treatment, FMT - 3xTg-AD, FMT - WT, PBS - 3xTg-AD demonstrated

fewer observed features compared to WT - PBS mice, suggesting that FMT treatment and / or AD pathology modeling led to decreased alpha diversity. To our knowledge, no other study transferring an AD-associated gut microbiota composition via co-housing or FMT treatment has led to a significant change in alpha diversity.[43,44]

Beta diversity analysis on our FMT study revealed that following treatment, there is not a significant difference in gut microbiota composition using Bray-Curtis or Jaccard metrics between FMT and PBS treated 3xTg-AD mice, suggesting that FMTs did not significantly alter 3xTg-AD mice composition. No significant difference in composition was shown between FMT treated WT mice and PBS treated 3xTg-AD mice using Bray-Curtis or Jaccard metrics, implying that the FMT treatment did shift the WT phenotype toward a 3xTg-AD phenotype. Finally, no difference was shown between PBS - WT and PBS - 3xTg-AD mice at 6 months of age using Bray-Curtis, but was significantly different using Jaccard, suggesting that less abundant taxa are driving differences between the groups.

Based on differential abundance testing (ANCOM), *Limosiloactobacillus reuteri, Ligilactobacillus murinus,* and *Ligilactobacillus animalis* between FMT treatment groups. Interestingly, *Limosiloactobacillus reuteri* demonstrates increased abundance in 3xTg-AD mice compared to WT mice before (2 months) and after (6 months) FMT treatment. Additionally, *Ligilactobacillus murinus* and *Ligilactobacillus animalis* demonstrate increased abundance in 3xTg-AD - PBS mice compared to other treatment groups. This finding is similar to a study using SSMS to assess the gut microbiota of 5xFAD mice, which demonstrated increased *Ligilactobacillus murinus* at 18 months in 5xFAD mice

compared to WT mice.[26] A heatmap was used to observe changes in lower abundance taxa, which were not significant in ANCOM, even when run after filtering out *Ligilactobacillus murinus, Ligilactobacillus sp.* and *Ligilactobacillus animalis. Turicibacter sp., Turicibacter sanguinis*, and *Turicibacter sp.* H121 were enriched in 3xTg-AD and WT mice at 2 months, yet only remained enriched in 3xTg-AD mice following treatment, regardless of treatment group. AD-associated gut microbiota phenotypes have shown increased *Turicibacter species* in studies investigating AD mouse models,[26,45,46] yet decreased in studies investigating human patients living with AD.[14,47] *Duncaniella dubosii,* a feature not identified in our 16S rRNA gene sequencing, was enriched in FMT treated 3xTg-AD and WT mice at 6 months, compared to the FMT treatment groups at 2 months. Dunham and colleagues show decreased abundance of *Duncaniella* sp. PC9 and *Duncaniella* sp. B8 at 18 months in 5xFAD mice using SSMS, yet has not been identified in any studies using 16S rRNA gene sequencing on mice modeling AD. We hypothesize this is attributable to the high taxonomic resolution of SSMS, which exemplifies the need for more SSMS studies to improve our understanding of the gut microbial communities associated with AD pathologies. Finally, *Bacteroides CBA7301, Bacteroides xylanisolvens, Bacteroides caccae*, *Bacteroides ovatus* were enriched in FMT treated 3xTg-AD, FMT treated WT mice, and PBS treated 3xTg-AD compared to PBS treated WT mice at 6 months. These findings suggest FMT treatment or predisposition to AD pathologies both led to an increase in several *Bacteroides* species. The genus *Bacteroides* are composed of Gram-negative bacteria that produce lipopolysaccharide, an endotoxin that aggravates AD-associate neuroinflammation and amyloid-β deposition.[48] Taken together, these differences in the gut microbiota

composition between treatment groups following FMT treatment using SSMS reveal new insights into microbial features that were not identified using 16S rRNA gene sequencing.

The improved taxonomic resolution of SSMS was shown in these observational and interventional studies investigating the gut microbiota composition in 3xTg-AD mice modeling amyloidosis and tauopathy. Our interventional study demonstrated distinct gut microbiota composition between 3xTg-AD and WT mice at 2, 6, and 12 months using beta diversity metrics, with differences in abundance of species in the *Ligilactobacillus, Turicibacter,* and *Bacteroides* genera. Our FMT study showed increased alpha diversity in PBS treated WT compared to all other treatment groups, with differences in abundance of species in the *Limosiloactobacillus, Ligilactobacillus, Duncaniella, Turicibacter,* and *Bacteroides* genera.

CONCLUSIONS

To develop microbiota-targeted therapeutic strategies for Alzheimer's disease, we need accurate and precise understanding of the gut microbiota composition associated with disease pathologies. The use of shallow shotgun metagenomic sequencing to improve taxonomic classification is imperative as we investigate disease mechanisms and potential interventions to treat AD. This study demonstrates SSMS improves relative abundance predictions, shows higher taxonomic resolution, and uncovers taxa not found in traditional 16S rRNA gene sequencing. Based on these findings, future studies

on the gut microbiota-brain axis and Alzheimer's disease should implement SSMS to improve study outcomes.

SUPPLEMENTAL MATERIALS

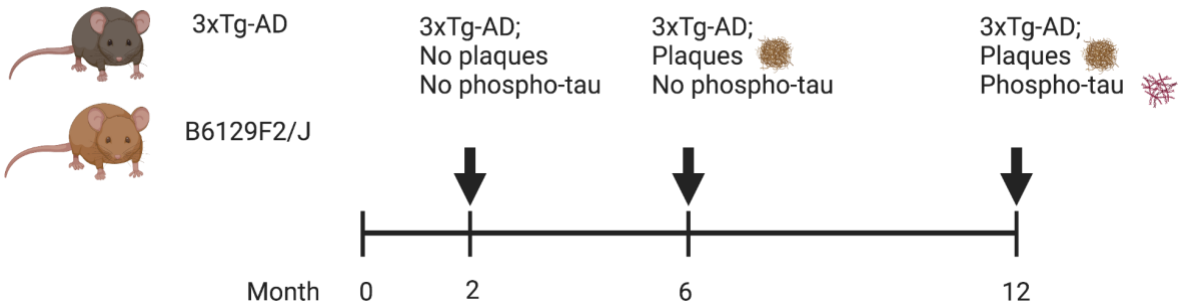

Supplemental Figure 1. Longitudinal Study Design. Fecal sample collections from 3xTg-AD and WT mice at 8 weeks (pre-pathologies), 24 weeks (amyloidosis), and 52 weeks (amyloidosis and tauopathy). Image created using Biorender.com.

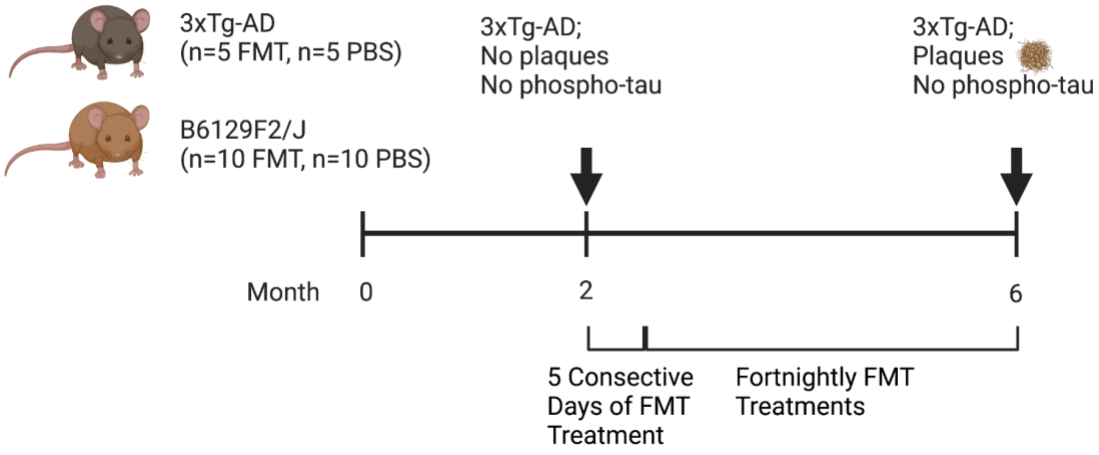

Supplemental Figure 2. FMT Study Design. 3xTg-AD (n = 10) and WT (n = 20) were separated into two treatment groups; fecal microbiota transplantation (FMT) and PBS (control). Beginning at 8 weeks of age, five consecutive days of treatment were administered (FMT or PBS), followed by fortnightly maintenance doses beginning at 10 weeks of age. Fecal samples were collected at 8 and 24 weeks of age. Image created using Biorender.com.

Table S1A: Pairwise Comparisons by FMT treatment groups at 2 months using Bracken

Group 1	Group 2	H	p-value	q-value
FMT - 3xTg-AD (n=5)	FMT - WT (n=7)	1.285714	0.256839	0.513679
FMT - 3xTg-AD (n=5)	PBS - 3xTg-AD (n=2)	0.857143	0.354539	0.569663
FMT - 3xTg-AD (n=5)	PBS - WT (n=10)	0.32	0.571608	0.571608
FMT - WT (n=7)	PBS - 3xTg-AD (n=2)	0.771429	0.379775	0.569663
FMT - WT (n=7)	PBS - WT (n=10)	2.752381	0.09711	0.569663
PBS - 3xTg-AD (n=2)	PBS - WT (n=10)	0.415385	0.519249	0.571608

Table S1B: Pairwise Comparisons by FMT treatment groups at 6 months using Bracken

Group 1	Group 2	H	p-value	q-value
FMT - 3xTg-AD (n=5)	FMT - WT (n=5)	0.010909	0.916815	0.916815
FMT - 3xTg-AD (n=5)	PBS - 3xTg-AD (n=3)	1.8	0.179712	0.269569
FMT - 3xTg-AD (n=5)	PBS - WT (n=3)	5	0.025347	0.076042
FMT - WT (n=5)	PBS - 3xTg-AD (n=3)	1.088889	0.296718	0.356061
FMT - WT (n=5)	PBS - WT (n=3)	5	0.025347	0.076042
BS - 3xTg-AD (n=3)	PBS - WT (n=3)	3.857143	0.049535	0.099069

Table S1C: Pairwise Comparisons by FMT treatment groups at 2 months using Kraken2

Group 1	Group 2	H	p-value	q-value
FMT - 3xTg-AD (n=4)	FMT - WT (n=7)	1.285714	0.256839	0.513679
FMT - 3xTg-AD (n=4)	PBS - 3xTg-AD (n=2)	0.857143	0.354539	0.531809
FMT - 3xTg-AD (n=4)	PBS - WT (n=10)	0.02	0.887537	0.887537
FMT - WT (n=7)	PBS - 3xTg-AD (n=2)	1.371429	0.241567	0.513679
FMT - WT (n=7)	PBS - WT (n=10)	3.438095	0.063709	0.382255

PBS - 3xTg-AD (n=2)	PBS - WT (n=10)	0.415385	0.519249	0.623099

Table S1D: Pairwise Comparisons by FMT treatment groups at 2 months using Kraken2

Group 1	Group 2	H	p-value	q-value
FMT - 3xTg-AD (n=5)	FMT - WT (n=5)	0.010909	0.916815	0.916815
FMT - 3xTg-AD (n=5)	PBS - 3xTg-AD (n=3)	0.555556	0.456057	0.547268
FMT - 3xTg-AD (n=5)	PBS - WT (n=3)	5	0.025347	0.076042
FMT - WT (n=5)	PBS - 3xTg-AD (n=3)	1.088889	0.296718	0.445076
FMT - WT (n=5)	PBS - WT (n=3)	5	0.025347	0.076042
PBS - 3xTg-AD (n=3)	PBS - WT (n=3)	3.857143	0.049535	0.099069

Table S2A: Pairwise PERMANOVA (Jaccard - Bracken) of all 4 treatment groups at 2 months

Group 1	Group 2	Sample size	Permutations	pseudo-F	p-value	q-value
FMT - 3xTg-AD	FMT - WT	11	999	1.312269	0.006	0.018
FMT - 3xTg-AD	PBS - 3xTg-AD	6	999	1.101791	0.071	0.071
FMT - 3xTg-AD	PBS - WT	14	999	1.276537	0.006	0.018
FMT - WT	PBS - 3xTg-AD	9	999	1.226093	0.056	0.0672
FMT - WT	PBS - WT	17	999	1.224207	0.016	0.032
PBS - 3xTg-AD	PBS - WT	12	999	1.184519	0.022	0.033

Table S2B: Pairwise PERMANOVA (Jaccard - Kraken2) of all 4 treatment groups at 2 months

Group 1	Group 2	Sample size	Permutations	pseudo-F	p-value	q-value
FMT - 3xTg-AD	FMT - WT	11	999	1.342244	0.005	0.015
FMT - 3xTg-AD	PBS - 3xTg-AD	6	999	1.045425	0.287	0.287

FMT - 3xTg-AD	PBS - WT	14	999	1.26397	0.004	0.015
FMT - WT	PBS - 3xTg-AD	14	999	1.26397	0.004	0.015
FMT - WT	PBS - WT	9	999	1.197856	0.103	0.1236
PBS - 3xTg-AD	PBS - WT	17	999	1.13994	0.051	0.0765

Table S2C: Pairwise PERMANOVA (Jaccard - Bracken) of all 4 treatment groups at 6 months

Group 1	Group 2	Sample size	Permutations	pseudo-F	p-value	q-value
FMT - 3xTg-AD	FMT - WT	11	999	1.372916	0.004	0.012
FMT - 3xTg-AD	PBS - 3xTg-AD	6	999	1.025513	0.336	0.336
FMT - 3xTg-AD	PBS - WT	14	999	1.205438	0.004	0.012
FMT - WT	PBS - 3xTg-AD	9	999	1.202408	0.081	0.0972
FMT - WT	PBS - WT	17	999	1.205539	0.028	0.056
PBS - 3xTg-AD	PBS - WT	12	999	1.168685	0.05	0.075

Table S2D: Pairwise PERMANOVA (Jaccard - Kraken2) of all 4 treatment groups at 6 months

Group 1	Group 2	Sample size	Permutations	pseudo-F	p-value	q-value
FMT - 3xTg-AD	FMT - WT	11	999	1.363529	0.009	0.027
FMT - 3xTg-AD	PBS - 3xTg-AD	6	999	1.040883	0.182	0.182
FMT - 3xTg-AD	PBS - WT	14	999	1.254939	0.001	0.006
FMT - WT	PBS - 3xTg-AD	9	999	1.241094	0.059	0.0708
FMT - WT	PBS - WT	17	999	1.217913	0.024	0.0375
PBS - 3xTg-AD	PBS - WT	12	999	1.185397	0.025	0.0375

Table S2E: Pairwise PERMANOVA (Bray-Curtis - Bracken) of all 4 treatment groups at 2 months

Group 1	Group 2	Sample size	Permutations	pseudo-F	p-value	q-value
FMT - 3xTg-AD	FMT - WT	11	999	2.662255	0.015	0.045
FMT - 3xTg-AD	PBS - 3xTg-AD	6	999	3.229289	0.053	0.0795
FMT - 3xTg-AD	PBS - WT	14	999	3.144929	0.008	0.045
FMT - WT	PBS - 3xTg-AD	9	999	1.464203	0.214	0.214
FMT - WT	PBS - WT	17	999	2.640202	0.026	0.052
PBS - 3xTg-AD	PBS - WT	12	999	1.828204	0.08	0.096

Table S2F: Pairwise PERMANOVA (Bray-Curtis - Kraken2) of all 4 treatment groups at 2 months

Group 1	Group 2	Sample size	Permutations	pseudo-F	p-value	q-value
FMT - 3xTg-AD	FMT - WT	11	999	2.660177	0.026	0.052
FMT - 3xTg-AD	PBS - 3xTg-AD	6	999	3.291544	0.072	0.0864
FMT - 3xTg-AD	PBS - WT	14	999	3.133815	0.009	0.042
FMT - WT	PBS - 3xTg-AD	9	999	1.479432	0.201	0.201
FMT - WT	PBS - WT	17	999	2.579893	0.014	0.042
PBS - 3xTg-AD	PBS - WT	12	999	1.831228	0.071	0.0864

Table S2G: Pairwise PERMANOVA (Bray-Curtis - Bracken) of all 4 treatment groups at 6 months

Group 1	Group 2	Sample size	Permutations	pseudo-F	p-value	q-value
FMT - 3xTg-AD	FMT - WT	11	999	2.719967	0.017	0.042
FMT - 3xTg-AD	PBS - 3xTg-AD	6	999	3.368204	0.061	0.0828
FMT - 3xTg-AD	PBS - WT	14	999	3.113561	0.003	0.018

FMT - WT	PBS - 3xTg-AD	9	999	1.497337	0.204	0.204
FMT - WT	PBS - WT	17	999	2.563084	0.021	0.042
PBS - 3xTg-AD	PBS - WT	12	999	1.829487	0.069	0.0828

Table S2H: Pairwise PERMANOVA (Bray-Curtis - Kraken2) of all 4 treatment groups at 6 months

Group 1	Group 2	Sample size	Permutations	pseudo-F	p-value	q-value
FMT - 3xTg-AD	FMT - WT	11	999	2.752449	0.024	0.048
FMT - 3xTg-AD	PBS - 3xTg-AD	6	999	3.36523	0.062	0.093
FMT - 3xTg-AD	PBS - WT	14	999	3.222682	0.011	0.048
FMT - WT	PBS - 3xTg-AD	9	999	1.493346	0.213	0.213
FMT - WT	PBS - WT	17	999	2.601309	0.016	0.048
PBS - 3xTg-AD	PBS - WT	12	999	1.802226	0.093	0.1116

REFERENCES

1. Woo, P. C. Y., Lau, S. K. P., Teng, J. L. L., Tse, H. & Yuen, K.-Y. Then and now: use of 16S rDNA gene sequencing for bacterial identification and discovery of novel bacteria in clinical microbiology laboratories. *Clin. Microbiol. Infect.* **14**, 908–934 (2008).
2. Ursell, L. K., Metcalf, J. L., Parfrey, L. W. & Knight, R. Defining the human microbiome. *Nutrition Reviews* vol. 70 S38–S44 Preprint at https://doi.org/10.1111/j.1753-4887.2012.00493.x (2012).
3. Relman, D. A. The human microbiome: ecosystem resilience and health. *Nutr.*

Rev. **70**, S2 (2012).

4. Liu, Y.-X. *et al.* A practical guide to amplicon and metagenomic analysis of microbiome data. *Protein Cell* **12**, 315–330 (2021).

5. Brumfield, K. D., Huq, A., Colwell, R. R., Olds, J. L. & Leddy, M. B. Microbial resolution of whole genome shotgun and 16S amplicon metagenomic sequencing using publicly available NEON data. *PLoS One* **15**, e0228899 (2020).

6. Jiang, D. *et al.* Microbiome Multi-Omics Network Analysis: Statistical Considerations, Limitations, and Opportunities. *Frontiers in Genetics* vol. 10 Preprint at https://doi.org/10.3389/fgene.2019.00995 (2019).

7. Gandy, K. A. O., Zhang, J., Nagarkatti, P. & Nagarkatti, M. The role of gut microbiota in shaping the relapse-remitting and chronic-progressive forms of multiple sclerosis in mouse models. *Sci. Rep.* **9**, 1–17 (2019).

8. Gorecki, A. M. *et al.* Altered Gut Microbiome in Parkinson's Disease and the Influence of Lipopolysaccharide in a Human α-Synuclein Over-Expressing Mouse Model. *Front. Neurosci.* **0**, (2019).

9. Gubert, C. *et al.* Gene-Environment-Gut Interactions in Huntington's Disease Mice Are Associated with Environmental Modulation of the Gut Microbiome. *SSRN Electronic Journal* Preprint at https://doi.org/10.2139/ssrn.3904352.

10. Borsom, E. M., Lee, K. & Cope, E. K. Do the Bugs in Your Gut Eat Your Memories? Relationship between Gut Microbiota and Alzheimer's Disease. *Brain Sciences* vol. 10 814 Preprint at https://doi.org/10.3390/brainsci10110814 (2020).

11. Khedr, E. M. *et al.* Gut microbiota in Parkinson's disease patients: hospital-based study. *The Egyptian Journal of Neurology, Psychiatry and*

Neurosurgery vol. 57 Preprint at https://doi.org/10.1186/s41983-021-00407-z (2021).

12. Wasser, C. I. *et al.* Gut dysbiosis in Huntington's disease: associations among gut microbiota, cognitive performance and clinical outcomes. *Brain Communications* vol. 2 Preprint at https://doi.org/10.1093/braincomms/fcaa110 (2020).

13. Cantoni, C. *et al.* Alterations of host-gut microbiome interactions in multiple sclerosis. *EBioMedicine* **76**, 103798 (2022).

14. Vogt, N. M. *et al.* Gut microbiome alterations in Alzheimer's disease. *Scientific Reports* vol. 7 Preprint at https://doi.org/10.1038/s41598-017-13601-y (2017).

15. 2022 Alzheimer's disease facts and figures. *Alzheimers. Dement.* **18**, 700–789 (2022).

16. Kim, N. *et al.* Transplantation of gut microbiota derived from Alzheimer's disease mouse model impairs memory function and neurogenesis in C57BL/6 mice. *Brain Behav. Immun.* **98**, 357–365 (2021).

17. Mezö, C. *et al.* Different effects of constitutive and induced microbiota modulation on microglia in a mouse model of Alzheimer's disease. *Acta Neuropathologica Communications* **8**, 1–19 (2020).

18. van Olst, L. *et al.* Contribution of Gut Microbiota to Immunological Changes in Alzheimer's Disease. *Frontiers in Immunology* vol. 12 Preprint at https://doi.org/10.3389/fimmu.2021.683068 (2021).

19. Harach, T. *et al.* Reduction of Abeta amyloid pathology in APPPS1

transgenic mice in the absence of gut microbiota. *Sci. Rep.* **7**, 41802 (2017).

20. Sun, J. *et al.* Fecal microbiota transplantation alleviated Alzheimer's disease-like pathogenesis in APP/PS1 transgenic mice. *Transl. Psychiatry* **9**, (2019).

21. Tan, C. *et al.* Neuroprotective Effects of Probiotic-Supplemented Diet on Cognitive Behavior of 3xTg-AD Mice. *J. Healthc. Eng.* **2022**, 4602428 (2022).

22. Guilherme, M. dos S., dos Santos Guilherme, M., Nguyen, V. T. T., Reinhardt, C. & Endres, K. Impact of Gut Microbiome Manipulation in 5xFAD Mice on Alzheimer's Disease-Like Pathology. *Microorganisms* vol. 9 815 Preprint at https://doi.org/10.3390/microorganisms9040815 (2021).

23. Jeong, S. *et al.* Whole genome shotgun metagenomic sequencing to identify differential abundant microbiome features between dementia and mild cognitive impairment (MCI) in AD subjects. *Alzheimer's & Dementia* vol. 17 Preprint at https://doi.org/10.1002/alz.051914 (2021).

24. Peng, W. *et al.* Association of gut microbiota composition and function with a senescence-accelerated mouse model of Alzheimer's Disease using 16S rRNA gene and metagenomic sequencing analysis. *Aging* vol. 10 4054–4065 Preprint at https://doi.org/10.18632/aging.101693 (2018).

25. Laske, C. *et al.* Signature of Alzheimer's Disease in Intestinal Microbiome: Results From the AlzBiom Study. *Frontiers in Neuroscience* vol. 16 Preprint at https://doi.org/10.3389/fnins.2022.792996 (2022).

26. Dunham, S. J. B. *et al.* Longitudinal analysis of the gut microbiome in the 5xfAD mouse model of Alzheimer's disease. *bioRxiv* 2022.03.02.482725 (2022)

doi:10.1101/2022.03.02.482725.

27. Ewels, P., Magnusson, M., Lundin, S. & Käller, M. MultiQC: summarize analysis results for multiple tools and samples in a single report. *Bioinformatics* vol. 32 3047–3048 Preprint at https://doi.org/10.1093/bioinformatics/btw354 (2016).

28. McIver, L. J. *et al.* bioBakery: a meta'omic analysis environment. *Bioinformatics* vol. 34 1235–1237 Preprint at https://doi.org/10.1093/bioinformatics/btx754 (2018).

29. Lu, J., Breitwieser, F. P., Thielen, P. & Salzberg, S. L. Bracken: estimating species abundance in metagenomics data. *PeerJ Computer Science* vol. 3 e104 Preprint at https://doi.org/10.7717/peerj-cs.104 (2017).

30. Lu, J. & Salzberg, S. L. Ultrafast and accurate 16S rRNA microbial community analysis using Kraken 2. *Microbiome* **8**, 124 (2020).

31. Janssen, S. *et al.* Phylogenetic Placement of Exact Amplicon Sequences Improves Associations with Clinical Information. *mSystems* **3**, (2018).

32. Bokulich, N. A. *et al.* Optimizing taxonomic classification of marker-gene amplicon sequences with QIIME 2's q2-feature-classifier plugin. *Microbiome* vol. 6 Preprint at https://doi.org/10.1186/s40168-018-0470-z (2018).

33. Faith, D. P. Conservation evaluation and phylogenetic diversity. *Biological Conservation* vol. 61 1–10 Preprint at https://doi.org/10.1016/0006-3207(92)91201-3 (1992).

34. Anderson, M. J. Permutational Multivariate Analysis of Variance (PERMANOVA). *Wiley StatsRef: Statistics Reference Online* 1–15 Preprint at https://doi.org/10.1002/9781118445112.stat07841 (2017).

35. Mandal, S. *et al.* Analysis of composition of microbiomes: a novel method for studying microbial composition. *Microb. Ecol. Health Dis.* **26**, 27663 (2015).

36. Bokulich, N. A. *et al.* q2-sample-classifier: machine-learning tools for microbiome classification and regression. *bioRxiv* 306167 (2018) doi:10.1101/306167.

37. Manor, O. *et al.* Health and disease markers correlate with gut microbiome composition across thousands of people. *Nat. Commun.* **11**, 1–12 (2020).

38. Li, Z. *et al.* Differences in Alpha Diversity of Gut Microbiota in Neurological Diseases. *Front. Neurosci.* **16**, 879318 (2022).

39. Dos Santos Guilherme, M. *et al.* Impact of Acute and Chronic Amyloid-β Peptide Exposure on Gut Microbial Commensals in the Mouse. *Front. Microbiol.* **11**, 1008 (2020).

40. Bello-Medina, P. C. *et al.* Spatial Memory and Gut Microbiota Alterations Are Already Present in Early Adulthood in a Pre-clinical Transgenic Model of Alzheimer's Disease. *Front. Neurosci.* **15**, 595583 (2021).

41. Bonfili, L. *et al.* Microbiota modulation counteracts Alzheimer's disease progression influencing neuronal proteolysis and gut hormones plasma levels. *Scientific Reports* vol. 7 Preprint at https://doi.org/10.1038/s41598-017-02587-2 (2017).

42. Borsom, E. M. *et al.* Predicting neurodegenerative disease using pre-pathology gut microbiota composition: a longitudinal study in mice modeling Alzheimer's disease pathologies. Preprint at https://doi.org/10.21203/rs.3.rs-1538737/v1.

43. Soriano, S. *et al.* Fecal microbiota transplantation derived from Alzheimer's disease mice worsens brain trauma outcomes in wild-type controls. Preprint at https://doi.org/10.1101/2021.11.23.469725.

44. Chen, C. *et al.* Gut dysbiosis contributes to amyloid pathology, associated with C/EBPβ/AEP signaling activation in Alzheimer's disease mouse model. *Science Advances* vol. 6 Preprint at https://doi.org/10.1126/sciadv.aba0466 (2020).

45. Dodiya, H. B. *et al.* Gut microbiota–driven brain Aβ amyloidosis in mice requires microglia. *Journal of Experimental Medicine* vol. 219 Preprint at https://doi.org/10.1084/jem.20200895 (2022).

46. Chen, Y. *et al.* Gut Microbiome Alterations Precede Cerebral Amyloidosis and Microglial Pathology in a Mouse Model of Alzheimer's Disease. *BioMed Research International* vol. 2020 1–15 Preprint at https://doi.org/10.1155/2020/8456596 (2020).

47. Wu, S., Liu, X., Jiang, R., Yan, X. & Ling, Z. Roles and Mechanisms of Gut Microbiota in Patients With Alzheimer's Disease. *Frontiers in Aging Neuroscience* vol. 13 Preprint at https://doi.org/10.3389/fnagi.2021.650047 (2021).

48. Kim, H. S. *et al.* Gram-negative bacteria and their lipopolysaccharides in Alzheimer's disease: pathologic roles and therapeutic implications. *Transl. Neurodegener.* **10**, 49 (2021).

CHAPTER 5: Gut microbiota adaptations to the environment of in-house bred versus vendor bred B6129F2/J mice on the gut microbiota composition in the first six months of life

ABSTRACT

The use of murine models in research on microbe-host interaction is an essential tool for pre-clinical microbiome studies. The gut microbiome, or the collective microbes and their genomes that inhabit the gastrointestinal tract, plays an important role in various aspects of health, including metabolite production, digestion of macronutrients, and immune modulation. Over the last two decades, the gut microbiome has been implicated in the pathophysiology of many diseases, notably inflammatory bowel disease, autism spectrum disorder, and type-2 diabetes. With the need for new research on the gut microbiota and human disease, the use of laboratory models in gut microbiome research is essential translational research. However, recent studies have shown significant changes in the gut microbiome of mice from different vendors, introducing confounding factors that may alter research outcomes. Due to the profound effects of early life gut microbiota perturbations on host health, minimizing these across microbiome studies will result in reproducible, robust outcomes. We show for the first time, to our knowledge, a temporal difference in gut microbiota composition of mice purchased directly from the vendor and mice purchased from the vendor to breed in house. With these findings, it is essential to design experiments investigating the gut microbiome of mice, and other laboratory animal models, to be bred in the same environment to reduce environmental alterations in the gut microbiota composition.

INTRODUCTION

Microbial life, mainly bacteria, archaea, fungi, and viruses, that inhabit a defined niche, collectively compose a microbiota.[1] The human microbiota, or the microbes that live in and on the human body, contribute to various bodily processes, such as immune support, digestion, and prevention of pathogen colonization.[2] Numerous studies have shown correlation of dysbiosis of the gut microbiota composition and disease in different body systems, including the gastrointestinal, nervous, immune, and vascular system.[3] With a new understanding of how body systems connect to gut microbiota alterations, and the advances in Next Generation Sequencing techniques, the field of microbiome research is expanding quickly, and relying heavily on animals, including mice, to model disease.[4] Mice provide low-cost, reproducible models for a variety of diseases via genetic engineering,[5] exposure to pathogens,[6] or chemically induced inflammation,[7] all of which are connected to the gut microbiota. However, confounding effects, such as strain, sex, group housing, diet, age, inter-individual variability, and maternal effects play a role in shaping the gut microbiota composition in laboratory mice.[8] Understanding longitudinal effects of the maternal and environmental influences on the gut microbiota will allow researchers to standardize practices in breeding and collection of high-quality data. This research demonstrates that maternal effect can last up to, and potentially beyond, 12 months of age, meaning that mice purchased from a vendor make poor comparative cohorts to those bred in house. For optimal and reproducible results, minimizing factors such as the maternal effect is essential for increasing data quality in microbiota studies.

Previous research has shown significant compositional differences in the gut microbiota between vendors. A study on 21 animal facilities across Germany showed significant differences in microbial features, alpha-, and beta- diversity of the gut microbiota in C57BL/6J mice[9]. A different study showed A/J, BALB/cJ, and C57BL/6J 3 week old mice purchased from two different vendors, Jackson Laboratories and Harlan Sprague Dawley, cluster distinctly on the first axis of PCA plots at 3.5, 7.5, 10.5, and 24 weeks of age.[10] Wolff and colleagues demonstrated altered gut microbiota compositions in C57BL/6J mice from three different vendors, and yet, yielding no significant differences in host immune response to lipopolysaccharide injection.[11] Taken together, these studies demonstrate that the facility roden models are purchased from can have profound effects on the gut microbiota composition.

In the current study, we were interested in assessing if the breeding location of Jackson Laboratory B6129F2/J mice, a common wild-type model, impacted gut microbiota composition. We observed unique gut microbiota compositions using alpha- and beta-diversity metrics between Jackson Laboratory B6129F2/J mice bred at Jackson Laboratories and B6129F2/J mice bred at Northern Arizona University using mice purchased from Jackson Laboratories. To our knowledge, this is the first study to show temporal differences in the gut microbiota composition between mice bred at the vendor and mice bred in-house from the same genotype as mice purchased from a vendor.

METHODS

Mouse colonies: All mouse experiments were approved by the Institutional Animal Use and Care Committee of Northern Arizona University under protocol 18-016.

Jackson-bred: Female B6129F2/J mice were purchased from Jackson Laboratories at 3 weeks of age and given one week to acclimate and adjust to rodent chow prior to the first fecal sample collection.

Northern Arizona University bred: Male and female B6129F2/J mice purchased from Jackson Laboratory were allowed 5 days to acclimate, then combined into harems, housed in a 12 hour light/dark cycle, and provided food and water *ad libitum*. Pups were housed with their mother until weaning at 21 days of age. Weaned female mice were given one week to acclimate and adjust to their new food prior to the first fecal sample collection.

Sample collection: Fecal samples were collected directly from each mouse fortnightly from 4 to 52 weeks of age. Fecal samples were stored at −80 °C until further processing.

16S rRNA gene sequencing: Fecal samples are collected directly from the mice, and stored in sterile 1X PBS at −80 °C until processing. The DNA from fecal samples were extracted using the MagMAX Pathogen RNA/DNA Kit from ThermoFisher. Modifications to the protocol include the use of Lysing Matrix E tubes (MP Biomedical) for tissue lysis.

DNA was quantified using a NanoDrop 2000. Quantified DNA from fecal samples was used for 16S rRNA gene PCR. Using EMP primers (515F-806R), the V4 region of the 16S rRNA gene was amplified. Each PCR reaction contained 2.5 µl of PCR buffer (TaKaRa, 10x concentration, 1x final), 1 µl of the Golay barcode tagged forward primer (10 µM concentration, 0.4 µM final), 1 µl of bovine serum albumin (Thermofisher, 20 mg/mL concentration, 0.56 mg/µl final), 2 µl of dNTP mix (TaKaRa, 2.5 mM concentration, 200 µM final), 0.125 µl of HotStart ExTaq (TaKaRa, 5 U/µl, 0.625 U/µl final), 1 µL reverse primer (10 µM concentration, 0.4µM final), and 1 µL of template DNA. All PCR reactions were filled to a total 25 µL with UltraPure DNase,Rnase free water (Invitrogen), then placed on a ThermalCycler. ThermalCycler conditions were as follows, 98°C denaturing step for 2 minutes, 30 cycles of 98°C for 20 seconds, 50°C for 30 seconds, and 72°C for 45 seconds, a final step of 72°C for 10 minutes. PCR was performed in triplicate for each sample and an additional negative control was included for each barcoded primer. A post-PCR quality control step was performed using a 2% agarose gel (ThermoFisher), followed by quantification of amplicons using the fluorometry. Quality of the pool was assessed with the Bioanalyzer DNA 1000 chip (Agilent Technologies) then combined with 1% PhiX. A total of 7 pools were sequenced on the Illumina MiSeq using the 600-cycle MiSeq Reagent Kit V3 (Illumina). Each pool contained mock community samples that overlapped over each sequencing run to avoid sequencing bias. All sequencing was done on the Illumina MiSeq at TGen North.

Bioinformatics Analysis: Microbiome bioinformatics on 16S rRNA gene sequences were performed with QIIME 2. q2-DADA2 was used for sequence quality control and

resolution of amplicon sequence variants (ASVs) to provide the highest taxonomic specificity[12]. A phylogenetic tree was created using q2-fragment-insertion, which applies the SEPP algorithm, inserting short sequences into a reliable database of full-length sequences[13]. Taxonomy was assigned to reads using q2-feature-classifier[13,14]. Alpha diversity (community richness) metrics was computed with q2-diversity, including Faith's Phylogenetic Diversity, Observed OTUs, and Shannon diversity. Beta diversity (community dissimilarity) metrics was computed with q2-diversity, including Bray-Curtis dissimilarity, Jaccard, weighted UniFrac, and unweighted UniFrac distances. Longitudinal analysis was computed with q2-longitudinal to assess temporal changes in microbial compositions[15]. These diversity metrics, along with taxonomic profiles of samples, were used to compare microbiome compositions between breeder location of mice. Group comparisons of alpha diversity were performed with non-parametric Kruskal-Wallis tests, and group comparisons of beta diversity were performed with non-parametric PERMANOVA. ASVs and taxa that were differentially abundant across disease groups were identified using ANCOM. All P-values were corrected for multiple comparisons using the Benjamini-Hochberg False Discovery Rate correction.

RESULTS

Longitudinal analysis of breeder location effects on gut microbiota composition

To examine the effects of breeding location on the temporal gut microbiota composition of B6129F2/J mice, we compared female B6129F2/J mice bred at Jackson Laboratory and shipped to Northern Arizona University (NAU) and female B6129F2/J mice bred at Jackson Laboratory (JAX). Fecal samples were collected directly from each mouse

fortnightly from 4 to 52 weeks of age, and the 16S rRNA gene was amplified to explore changes in the gut microbiota composition between breeder locations. Sequencing data was analyzed using QIIME 2.

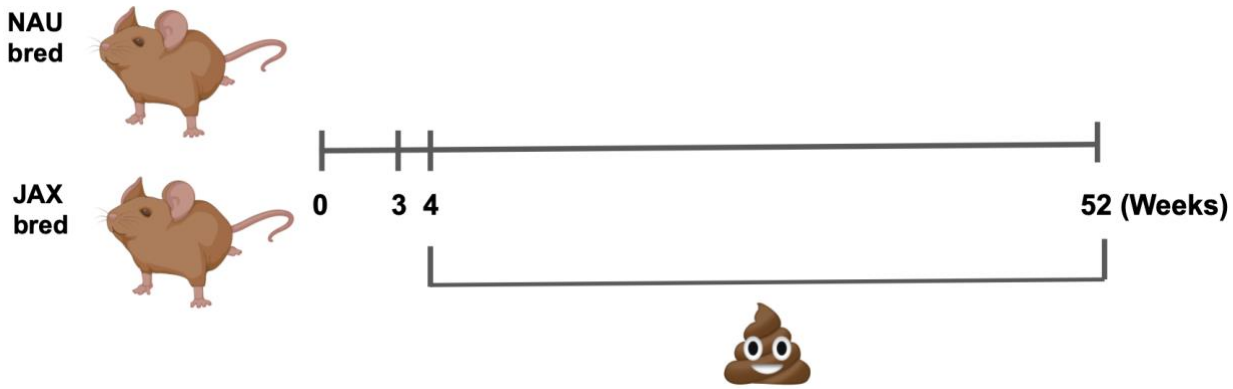

Figure 1. Sample collection overview. Fecal sample collections from female Northern Arizona University (NAU) and Jackson Laboratory (JAX) bred B6129F2/J mice began at 4 weeks of age and continued fortnightly until sacrifice at 8 weeks. Image created using Biorender.com.

JAX and NAU bred mice have distinct gut microbiota composition in the first 6 months of life

Beta diversity metrics were used to identify temporal compositional differences in the bacterial gut microbiota of female NAU and JAX bred B6129F2/J mice. We applied Jaccard and Unweighted Unifrac, which are unweighted (qualitative) beta diversity metrics, and Bray-Curtis and Weighted Unifrac, which are weighted (quantitative) beta diversity metrics to our samples. Volatility analysis demonstrates a distinct gut microbiota composition for the first 26 weeks of age using Jaccard diversity (Fig. 2A) and 32 weeks using Unweighted Unifrac (Fig. 2B) between NAU and JAX bred B6129F2/J mice. As mice age, the composition of the gut microbiota becomes more similar between the breeder locations (Figure 1). To analyze the differences in

composition at 8 weeks, 24 weeks, and 52 weeks, a PCoA of Jaccard and Unweighted Unifrac distances were generated with PCoA 1 plotted against time, highlighting the key three timepoints. The gut microbiota composition was statistically distinct, using Jaccard and Unweighted Unifrac metrics, between NAU and JAX bred B6129F2/J mice in early life, shown at 8 weeks of age. However, the gut microbiota composition became more similar at later time points, demonstrated at 24 and 52 weeks of age (Fig. 3, (PERMANOVA, p=0.054, f-statistic=1.33127), (PERMANOVA, p=0.065, f-statistic=1.45748) weeks of age . Weighted beta diversity metrics show a similar, though less robust, pattern at the baseline and 24 week timepoints. Volatility analysis and PCoA of the Bray-Curtis dissimilarity metric demonstrates distinct gut microbiota compositions between NAU and JAX bred B6129F2/J mice at 8 (PERMANOVA, p=0.001, f-statistic=10.1743) weeks of age, but not at 24 (PERMANOVA, p=0.016, f-statistic=1.98555) and 52 (PERMANOVA, p=0.508, f-statistic=0.90456) weeks of age (Fig. S3A, Fig. S3C). A PCoA of the Weighted Unifrac distance metric also demonstrates distinct gut microbiota compositions between NAU and JAX bred B6129F2/J mice at 8 (PERMANOVA, p=0.03, f-statistic=3.10426), but not at 24 (PERMANOVA, p=0.566, f-statistic=0.717805) and 52 (PERMANOVA, p=0.066) weeks of age (Fig. S3B, Fig. S3D). Taken together, these results indicate qualitative (not weighted by abundance of taxa) metrics suggesting the strongest drivers of different microbial communities are the less abundant taxa in the murine gut microbiota.

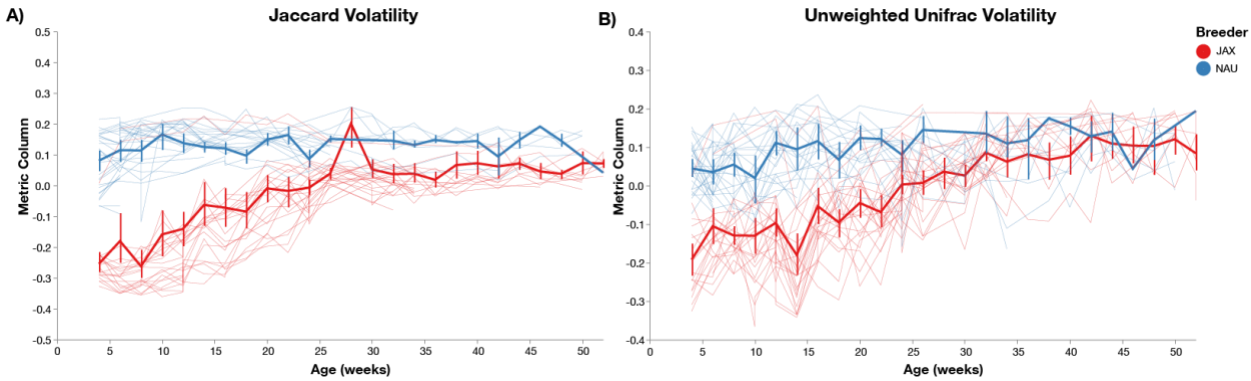

Figure 2. Volatility analysis of JAX and NAU bred mice from 4 to 52 weeks demonstrate distinct gut microbiota compositions in early life between breeder locations. A) Volatility plot of PCoA Axis 1 of the Jaccard dissimilarity index. This demonstrates differences in the gut microbiota until 26 weeks of age by breeder location. Thick lines represent the average change in the gut microbiota on PC1 over time in JAX and NAU bred mice, and thin lines represent changes in the gut microbiota on PC1 over time in individual mice. B) Volatility plot of PCoA Axis 1 of Unweighted Unifrac distance metric demonstrates differences in the gut microbiota until 32 weeks of age by breeder location. Thick lines represent the average change in the gut microbiota on PC1 over time in JAX and NAU bred mice, and thin lines represent changes in the gut microbiota on PC1 over time in individual mice.

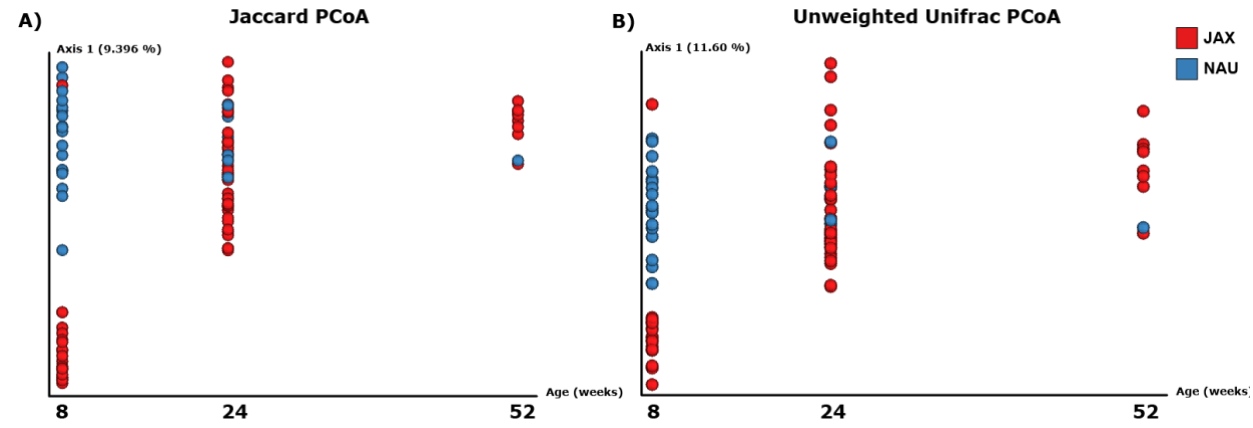

Figure 3. Beta-diversity metrics of 3xTg-AD and WT mice at 8, 24, and 52 weeks of age. A) Jaccard PCoA 1 plotted against time demonstrates distinct gut microbiota compositions between JAX and NAU bred mice mice at 8 (PERMANOVA, p=0.001, f-statistic=7.088606) and 24 (PERMANOVA, p=0.001, f-statistic=1.904089) weeks of age, but not at 52 (PERMANOVA, p=0.315, f-statistic=1.148262)) weeks of age. B) Unweighted Unifrac PCoA 1 plotted against time demonstrates distinct gut microbiota compositions between JAX and NAU bred mice mice at 8 (PERMANOVA, p=0.001, f-statistic=7.37656),and 24 (PERMANOVA, p=0.003, f-statistic=2.146992) weeks of age, but not at 52 (PERMANOVA, p=0.52, f-statistic=1.135859) weeks of age.

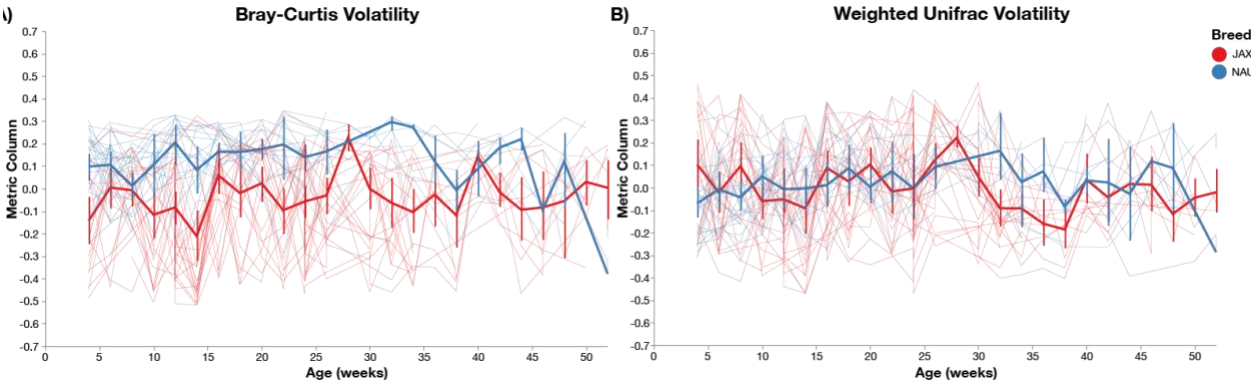

Figure 4. Volatility analysis of JAX and NAU bred mice from 4 to 52 weeks demonstrate distinct gut microbiota compositions in early life between breeder locations. A) Volatility plot of PCoA Axis 1 of the Bray-Curtis dissimilarity index. This demonstrates no distinct differences in gut microbiota composition over time by breeder location. Thick lines represent the average change in the gut microbiota on PC1 over time in JAX and NAU bred mice, and thin lines represent changes in the gut microbiota on PC1 over time in individual mice. B) Volatility plot of PCoA Axis 1 of Weighted Unifrac distance metric demonstrates no distinct differences in gut microbiota composition over time between breeder location. Thick lines represent the average change in the gut microbiota on PC1 over time in JAX and NAU bred mice, and thin lines represent changes in the gut microbiota on PC1 over time in individual mice.

Table 1: Differential abundance between JAX and NAU bred mice using Analysis of Composition of Microbiomes (ANCOM) at 8, 24, and 52 weeks of age collapsed at species level. W represents the number of features that the taxa is more abundant than.

Features Collapsed at Species Level	W	Week
Lactobacillus salivarius	1199	8
Family *S24-7*	1188	8
Lactobacillus sp.	1184	8
Family *S24-7*	1184	8
Family *S24-7*	1183	8

Family *S24-7*	1179	8
Family Rikenellaceae	1178	8
Family *S24-7*	1177	8
Adlercreutzia sp.	1177	8
Family *S24-7*	1174	8
Ruminococcus gnavus	1139	8
Family *S24-7*	1521	24
Bacteroides acidifaciens	1490	24
Family *S24-7*	1403	24
Order Clostridiales	183	52
Clostridiales	168	52
Clostridium cocleatum	168	52

Identifying bacterial features that are differentially abundant between breeder locations

To identify the amplicon sequence variants (ASVs) that are driving the differences in gut microbiota composition between 3xTg-AD and WT mice, feature volatility plots were produced using the QIIME 2 plug-in, q2-longitudinal. We identified one bacterial feature when collapsed at the genus level. The longitudinal feature analysis demonstrates a

temporal trend of increasing relative abundance of the genera *Prevotella* in JAX bred B6129F2/J mice compared to NAU bred B6129F2/J mice (Figure 4).

Differential abundance analysis of ASVs using analysis of composition of microbiomes (ANCOM) revealed a differential abundance of 1229 ASVs between NAU and JAX bred mice at 8 weeks of age, however we will focus on the top 11 ASV's (Supplementary Table S1). At 8 weeks of age, *Lactobacillus salivarius* (W=1199), Family *S24-7* (W=1188), *Lactobacillus sp.* (W=1184,) Family *S24-7* (W=1184), Family *S24-7* (W=1183), Family *S24-7* (W=1179), Family Rikenellaceae (W=1178), Family *S24-7* (W=1177), and *Adlercreutzia sp.* (W=1177) were enriched in NAU bred mice, while Family *S24-7* (W=1174) and *Ruminococcus gnavus* (W=1139) were enriched in JAX bred mice (Table 1). At 24 weeks of age, Family *S24-7* (W=1521), *Bacteroides acidifaciens* (W=1490), and Family *S24-7* (W=1403) were enriched in NAU bred mice (Table 1). At 52 weeks of age, *Order Clostridiales* (W=183), *Clostridiales* (W=168), and *Clostridium cocleatum* (W=168) were enriched in NAU bred mice (Table 1).

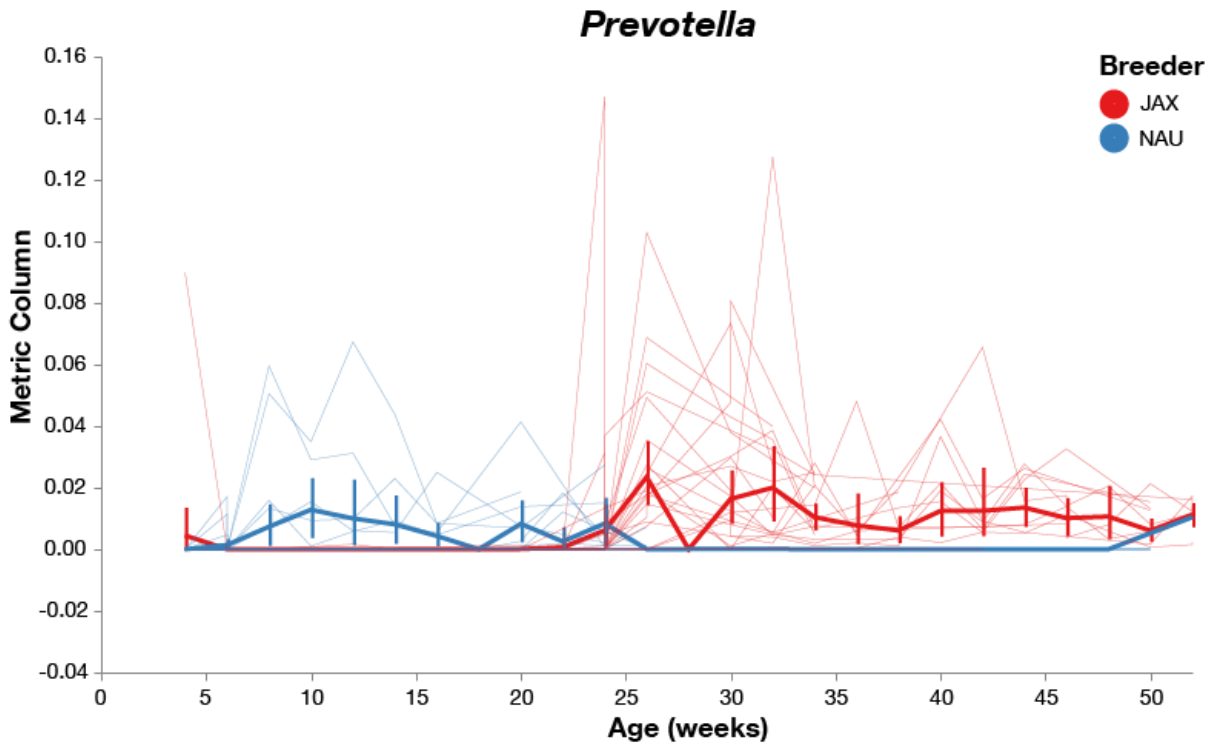

Figure 5. Feature volatility at genus level. Feature volatility chart of *Prevotella* demonstrates increased presence after 24 weeks of age in JAX bred mice while consistently lower abundance in NAU bred mice. Thick lines represent the average change in the gut microbiota on PC1 over time in JAX and NAU bred mice, and thin lines represent changes in the gut microbiota on PC1 over time in individual mice.

DISCUSSION

The mammalian microbiota is composed of a dynamic community of bacteria, viruses, fungi, and archaea, and contributes substantially to host health.[16] Due to the diverse roles the microbiota contributes to, including digestion of dietary fiber,[17] immune modulation,[17,18] and prevention of foreign pathogen colonization,[19] controlling for external gut microbiota alterations is essential for reliable and reproducible microbiome studies.[20] The gut microbiota is sensitive to environmental stress, such as circadian disruption, altitude change, temperature shifts, noise, and diet.[21] This study, and others

like it, provide evidence that the gut microbiota of mouse models vary not only between vendors,[10] but also across breeding sites. Mice purchased from a vendor experience changes in their gut microbiota introduced by transfer and adjustment to a new environment.[22] Diets, bedding, group-housing, and other nuances of animal husbandry are altered, inducing changes in the microbiota.[23] Breeding mice in-house from vendor-bought mice may minimize these confounding factors as offspring will receive milk from mothers on the same diet that they will be on after weaning. Further, the adaptations of the breeders in the breeding facility seem to be passed on to mice bred in house, as they have more stability in their microbial communities overtime.Schedules, bedding, and other external factors also remain consistent for mice bred in house.

To assess compositional shifts in the first year of B6129F2/J bred at NAU compared to bred at JAX, we used unweighted and weighted beta diversity metrics on microbiome composition from 4 to 52 weeks of age. Unweighted metrics (Jaccard and Unweighted Unifrac) showed significant compositional differences between JAX and NAU bred B6129F2/J mice, while weighted metrics (Bray-Curtis and Weighted Unifrac) did not show significant compositional differences over the 48 weeks of sampling. These findings suggest that lower abundance microbial features are responsible for the compositional differences between breeder location. Further, differences between breeder locations are stronger early in life (8 and 24 weeks), than they are later in life (52 weeks). This suggests that microbial features passed on from the maternal microbiome are driving differences early in life between breeder location, as well as potentially transportation stress, housing conditions, and other confounding factors.

To uncover dynamic bacterial features, we ran a volatility analysis using q2-longitudinal. Interestingly, the most dynamic bacterial feature was *Prevotella*, increasing in abundance after 24 weeks of age in JAX bred mice compared to NAU bred mice (Figure 5). *Prevotella sp.* have been linked to higher susceptibility to inflammatory bowel syndrome[24] and mucosal inflammation[25] in humans and mice. While there it is difficult to determine whether *Prevotella* was introduced to the JAX mice after arriving at the NAU facility, or if they were present in low abundances and were able to increase colonization over time, bacterial features that potentially alter inflammatory responses are of concern for many biomedical study designs.

To identify bacterial features that were differentially abundant between breeder locations, ANCOM was applied to JAX and NAU bred mice at 8, 24, and 52 weeks of age. While ANCOM at 8 weeks of age identified the most differentially abundant ASV's when compared to 24 and 52 weeks of age, the same 3 taxonomic group assignments made up the top 9 ASV's. *Lactobacillus sp.*, *Lactobacillus salivarius* and Family *S24-7*, dominated the differentially abundant ASV's. *Lactobacillus salivarius* is passed on from the maternal microbiome through breastfeeding, making *Lactobacillus salivarius* and other *Lactobacillus sp.* unsurprising gut microbial features at 8 weeks of age, when mice are weaned at 3 weeks of age.[26] Interestingly, Family *S24-7* has traditionally been a difficult taxonomic group to classify at the genus and species level using 16S rRNA gene sequencing, also known as *Muribaculaceae,*[27] contain several fermenters and

propionate producers.[28] At 24 weeks of age, *Bacteroides acidifaciens* was increased in NAU bred mice, a member of the *Bacteroides fragilis* group.[29]

In this study, we demonstrated that B6129F2/J mice bred at JAX and raised at NAU compared to bred at NAU demonstrate distinct gut microbiota compositions early in life, and harbor noticeably different bacterial features, particularly early in life. It is becoming clear that early life gut microbial communities impact both short and long term host health.[30] There is potential for subtle changes in microbial communities from animal husbandry, transportation, vendor, or location of breeding to alter the outcomes of biomedical research, not only within, but beyond microbiome studies. With these findings, we recommend that biomedical researchers using mammalian models of disease prioritize either obtaining mice from the same vendor or breeding mice in the same animal facility to reduce confounding factors that shape the communities of microbes that inhabit mammalian models.

Study Limitations: This study is limited by the observational study design that did not investigate mechanistic differences associated with shifts in composition of microbial features of mice bred at JAX and NAU.

CONCLUSIONS

With this information, microbiome experiments need to be carefully constructed to prevent environmental stressors from altering gut microbiota composition to the best of our ability, including using mice from the same vendor, bred in the same facility.

Microbiome adaptations from the breeders will be passed down to mice bred in the same facility, and have more stable microbiome communities over time than those who were bred in a different facility than mice bred at another facility and transported to the experimental site. Furthermore, other experiments, such as immunological studies, should be conducted with the same precautions due to the large role the gut microbiota plays in immune response.

REFERENCES

1. Ursell, L. K., Metcalf, J. L., Parfrey, L. W. & Knight, R. Defining the Human Microbiome. *Nutr. Rev.* **70**, S38 (2012).
2. Young, V. B. The role of the microbiome in human health and disease: an introduction for clinicians. *BMJ* **356**, (2017).
3. Dekaboruah, E., Suryavanshi, M. V., Chettri, D. & Verma, A. K. Human microbiome: an academic update on human body site specific surveillance and its possible role. *Arch. Microbiol.* **202**, 2147–2167 (2020).
4. Berde, C. V., Salvi Sagar, P., Kajarekar Kunal, V., Joshi Suyoj, A. & Berde Vikrant, B. Insight into the Animal Models for Microbiome Studies. *Microbiome in Human Health and Disease* 259–273 (2021) doi:10.1007/978-981-16-3156-6_13.
5. Gurumurthy, C. B. & Lloyd, K. C. K. Generating mouse models for biomedical research: technological advances. *Dis. Model. Mech.* **12**, (2019).
6. Sarkar, S. & Heise, M. T. Mouse Models as Resources for Studying Infectious Diseases. *Clin. Ther.* **41**, 1912 (2019).
7. Wirtz, S. *et al.* Chemically induced mouse models of acute and chronic intestinal

inflammation. https://www.google.com/url?sa=t&rct=j&q=&esrc=s&source=web&cd=&cad=rja&uact=8&ved=2ahUKEwiJxsLmxdX4AhXtEEQIHXbhApwQFnoECAwQAQ&url=https%3A%2F%2Fexperiments.springernature.com%2Farticles%2F10.1038%2Fnprot.2017.044&usg=AOvVaw2jzqZZIYYx6ffQNTesryPY.

8. Miyoshi, J. *et al.* Minimizing confounders and increasing data quality in murine models for studies of the gut microbiome. *PeerJ* **6**, (2018).

9. Analysis of factors contributing to variation in the C57BL/6J fecal microbiota across German animal facilities. *Int. J. Med. Microbiol.* **306**, 343–355 (2016).

10. Ericsson, A. C. *et al.* Effects of Vendor and Genetic Background on the Composition of the Fecal Microbiota of Inbred Mice. *PLoS One* **10**, e0116704 (2015).

11. Wolff, N. S. *et al.* Vendor effects on murine gut microbiota and its influence on lipopolysaccharide-induced lung inflammation and Gram-negative pneumonia. *Intensive Care Medicine Experimental* **8**, 1–13 (2020).

12. Callahan, B. J. *et al.* DADA2: High-resolution sample inference from Illumina amplicon data. *Nat. Methods* **13**, 581–583 (2016).

13. Janssen, S. *et al.* Phylogenetic Placement of Exact Amplicon Sequences Improves Associations with Clinical Information. *mSystems* **3**, (2018).

14. Bokulich, N. A. *et al.* Optimizing taxonomic classification of marker-gene amplicon sequences with QIIME 2's q2-feature-classifier plugin. *Microbiome* vol. 6 (2018).

15. Bokulich, N. A. *et al.* q2-longitudinal: Longitudinal and Paired-Sample

Analyses of Microbiome Data. *mSystems* **3**, (2018).

16. Bleich, A. & Fox, J. G. The Mammalian Microbiome and Its Importance in Laboratory Animal Research. *ILAR Journal* vol. 56 153–158 (2015).

17. Jaramillo, S. A. *et al.* Soluble corn fiber reduces ovalbumin-induced sinonasal inflammation via the gut microbiota-airway axis. doi:10.1101/2020.07.23.216754.

18. Liu, X., Chen, Y., Zhang, S. & Dong, L. Gut microbiota-mediated immunomodulation in tumor. *J. Exp. Clin. Cancer Res.* **40**, 221 (2021).

19. Panwar, R. B., Sequeira, R. P. & Clarke, T. B. Microbiota-mediated protection against antibiotic-resistant pathogens. *Genes Immun.* **22**, 255–267 (2021).

20. Hansen, A. K., Hansen, C. H. F., Krych, L. & Nielsen, D. S. Impact of the gut microbiota on rodent models of human disease. *World Journal of Gastroenterology* vol. 20 17727–17736 (2014).

21. Karl, J. P. *et al.* Effects of Psychological, Environmental and Physical Stressors on the Gut Microbiota. *Front. Microbiol.* **0**, (2018).

22. Montonye, D. R. *et al.* Acclimation and Institutionalization of the Mouse Microbiota Following Transportation. *Frontiers in Microbiology* vol. 9 (2018).

23. Ericsson, A. C. *et al.* The influence of caging, bedding, and diet on the composition of the microbiota in different regions of the mouse gut. *Sci. Rep.* **8**, 4065 (2018).

24. Su, T. *et al.* Altered Intestinal Microbiota with Increased Abundance of Is Associated with High Risk of Diarrhea-Predominant Irritable Bowel Syndrome.

Gastroenterol. Res. Pract. **2018**, 6961783 (2018).

25. Iljazovic, A. *et al.* Perturbation of the gut microbiome by Prevotella spp. enhances host susceptibility to mucosal inflammation. *Mucosal Immunol.* **14**, 113–124 (2021).

26. Martín, R. *et al.* Lactobacillus salivarius CECT 5713, a potential probiotic strain isolated from infant feces and breast milk of a mother-child pair. *Int. J. Food Microbiol.* **112**, 35–43 (2006).

27. Lagkouvardos, I. *et al.* Sequence and cultivation study of Muribaculaceae reveals novel species, host preference, and functional potential of this yet undescribed family. *Microbiome* **7**, 28 (2019).

28. Smith, B. J., Miller, R. A. & Schmidt, T. M. Genomes Assembled from Metagenomes Suggest Genetic Drivers of Differential Response to Acarbose Treatment in Mice. *mSphere* **6**, e0085121 (2021).

29. Wexler, H. M. Bacteroides: the good, the bad, and the nitty-gritty. *Clin. Microbiol. Rev.* **20**, 593–621 (2007).

30. Sarkar, A., Yoo, J. Y., Valeria Ozorio Dutra, S., Morgan, K. H. & Groer, M. The Association between Early-Life Gut Microbiota and Long-Term Health and Diseases. *J. Clin. Med. Res.* **10**, (2021).

CHAPTER 6: Conclusions